DE-FG22-93PC93222--99

NO Decomposition in Non-Reducing Atmospheres

Final Report
September 1993 - February 1997

Work Performed Under Contract No.: DE-FG22-93PC93222

For
U.S. Department of Energy
Office of Fossil Energy
Federal Energy Technology Center
P.O. Box 880
Morgantown, West Virginia 26507-0880

By
Zettlemoyer Center for Surface Studies
and Department of Chemistry
Lehigh University
Bethlehem, Pennsylvania 18015

Disclaimer

NO DECOMPOSITION IN NON-REDUCING ATMOSPHERES

TABLE OF CONTENTS

LIST OF FIGURES

LIST OF TABLES

EXECUTIVE SUMMARY

Co(II)NH_4-erionite zeolites with cobalt contents varying from 0.002 to 8.2 wt% of Co(II) were prepared, and the samples were studied *via* diffuse reflectance spectroscopy in the UV-VIS-NIR region and measurement of magnetic moments of the Co ions. Co(II) ions in different sites were distinguished by optical spectra of the dehydrated Co-erionite samples. Co(II) cations occupy three different sites in dehydrated erionite, which are in the plane of the regular six-ring window (site C), in the plane of the irregular six-ring of the ε-cage (site H), and in the center of the ε-cage (site B). These cation sites exhibit approximately D_{3h}, C_{2v} or C_{1h}, and O_h symmetry, respectively. Sites centered in the deformed six-ring are occupied preferentially, while sites in the regular six-ring are occupied in the zeolite dehydrated at 525°C and sites in the ε-cage are occupied only at high Co loading. Co(II) ions located in the ε-cage (site B) exhibit a closed coordination shell and do not create complexes with guest molecules. Ions located in the six-rings have open coordination shells and form complexes with CO and ethylene. Co(II) complexes with CO or ethylene located in the regular six-ring windows exhibit different spectral features than those located in the deformed six-rings.

Samples of Co(II)-ZSM-5 zeolites were also prepared and studied *via* diffuse reflectance spectroscopy after being dehydrated at 350 and 525°C and after adsorption of carbon monoxide, water, and ethylene. In general, Co-ZSM-5 contains three different Co sites. However, Co-ZSM-5 prepared at acidic conditions contained only two different sites. One of these sites is probably identical with the Co site in Co-erionite. After dehydration

at 500°C, Co siting in these zeolites was changed. In erionite at this same condition, Co ions were located in the plane of the single regular six-ring. Only strong ligands such as water could be adsorbed on Co ions in ZSM-5 zeolite dehydrated at 350°C, but Co ions in zeolites dehydrated at 525°C were also affected by weak ligands.

NO adsorption/desorption studies were carried out, and diffuse reflectance spectroscopy was utilized to monitor the spectral changes that occurred during adsorption of NO on the Co(II) cations, which was observed to occur after dehydration treatments at 350°C and 525°C. Absorption bands in the charge transfer spectral region of NO-Co intrazeolitic complexes depended mainly on Co siting in the zeolites. In selective catalytic reduction of NO by methane, it was observed that Co-mordenite and Co-ferrierite exhibited the highest %NO converted to products and selectivity toward N_2 formation, but Co-A zeolite and Co-erionite yielded the highest selectivities to NO_2 formation. Co-ZSM-5 zeolite exhibited an intermediate behavior.

X-Ray photoelectron spectroscopy and Auger analysis demonstrated that the Auger line intensities of the O K $L_{2,3}$ $L_{2,3}$ and Na K $L_{2,3}$ $L_{2,3}$ line and the binding energy, E_b, of the O 1s photoelectron line of zeolites A, X, Y, and mordenite correlate with structure induced charge transfer effects. Changes in the oxygen Auger spectrum also occur upon replacement of the Na^+ by Co(II) cations.

PROJECT OBJECTIVES

The principal objective was to obtain the fundamental knowledge for technological advancement of selectively converting pollutant NO to N_2 and O_2 under oxidizing or neutral environments that exist in exhaust gases and emissions of sources such as power stations. These studies involve the preparation, testing, and characterization of transition metal exchanged zeolite catalysts. The principal reactions of interest include the following:

$$2NO \Rightarrow N_2 + O_2$$

$$2NO + CH_4 + O_2 \Rightarrow N_2 + CO_2 + 2H_2O.$$

The first reaction is a highly desirable decomposition reaction. However, selectively catalytic reduction of NO by reductants, such as ammonia or hydrocarbons that include methane, is also of interest in this research. Current technology uses ammonia as a reductant, and development of a catalyst that would provide for replacement of the ammonia by methane or other hydrocarbons would be a significant advancement in the selective catalytic reduction of NO.

INTRODUCTION

Conversion of NO (or NO_x in general) to benign products is one of the most important goals of environmental catalysis today. Among the prospective catalysts for resolving this problem by selective catalytic reduction (SCR) of NO to N_2 are Co(II)-containing zeolites. Since it is highly desirable to replace the currently utilized ammonia reductant by a more environmentally acceptable reductant, SCR of NO by methane over transition metal exchanged zeolites has been recently studied (1-5). It has been shown that Co(II) ions, as well as some other transition metal cations, implanted into the zeolite matrix exhibit high catalytic activity in SCR of NO by using hydrocarbons instead of ammonia as the reductant under some reaction conditions (4,5). Although the mechanistic features of the catalytic activity of Co(II) ions incorporated to the zeolite matrix have not been fully elucidated, it is known that the catalytic activity of Co(II) ions for NO SCR by methane differs in different zeolites and also depends on Co loading (1,2) in the zeolite matrix. This indicates the important role of siting of the Co ions on their catalytic activity.

To explain the effects of Co(II) siting and to elucidate the mechanism of SCR of NO, the identification of the individual Co(II) sites in various zeolite matrices and estimation of their population in these sites under various conditions is of a great importance. Co(II) ion sitings in Type A, X, and Y zeolites were studied using X-ray diffraction (6,7) and using UV-VIS-NIR diffuse reflectance spectroscopy (DRS) (8-15), but information on the Co siting in other zeolites is lacking. In particular, there appears to be no available information about Co(II) cation sites in zeolites such as erionite, ferrierite, and ZSM-5. The main source

of information on the location of cations siting in zeolites is usually single crystal X-ray diffraction. However, the use of this method for the identification of cation sites in the high-silica zeolites encounters difficulties because of the low cation concentrations in these matrices. Moreover, high-silica zeolites also often exhibit low crystal symmetry, which complicates identification of cation sites. In addition, preparation of single crystals suitable for X-ray determination of the cation siting in zeolites is unsuccessful for some zeolite structural types (16). For dehydrated zeolites other than synthesized A, X, and Y zeolites, siting of various cations in dehydrated zeolite was successfully determined (17-20) in dehydrated mordenite. In the case of erionite, only sites of potassium and calcium in natural erionite were identified (21).

Metal cations in zeolites can be maintained in different coordination environments and can adsorb gaseous molecules. For example, Co(II) ions in zeolites are known to assume a variety of coordination numbers and symmetries, with distinctly different chemical and physical properties (8,22). In particular, open coordination sites in Type A zeolite has led to the formation of specific complexes with gas molecules that can enter the zeolite cage structure. Such surface complexes are of interest in conversions of the guest molecules, of which the high activity for SCR of NO by hydrocarbons is an example (1-5). Earlier research centered on cobalt exchanged zeolites dealt with catalytic oxidation of CO (23) and Fischer-Tropsch synthesis (24). In each of these cases, the cation siting, the metal cation oxidation state, and the state of agglomeration have not been characterized.

Erionite is taken here as an example of a zeolite with known framework structure, but for which there is a lack of knowledge of the local geometry of the Co(II) cations, as well

as their accessibility to selected molecules. The erionite framework structure is well-known (25), but there is considerable uncertainly in regard to the location of transition metal cations. In natural erionite, the native calcium is located in an inaccessible position hidden in the ϵ-cage, while sodium, magnesium, and potassium occupy open coordination sites (21). The behavior and distribution of Co(II) is expected to be different from the closed shell divalent cations such as Ca(II) and Mg(II) because of the extraordinarily high crystal field stabilization of Co(II) in near-planar geometries (10). Thus, erionite presents the next degree of complexity compared to zeolite A, in which all Co(II) ions are in planar coordination.

EXPERIMENTAL RESULTS

- **Identification of Co(II) Ion Sites in Dehydrated Co-Erionite and Their Adsorption Properties: an UV-VIS-NIR Spectroscopy Study**

In the present work, we have investigated the location, accessibility, and relative populations of the Co(II) sites with the use of DRS in the UV-VIS-NIR region complemented by magnetic susceptibility measurements and by adsorption of probe molecules CO, ethylene, and water. In zeolites, the DRS of the $d \rightarrow d^*$ optical transitions in open shell ions has been shown to both reflect their electronic structure and provide a signature of local geometry (8). In particular, trigonally coordinated Co(II) ions in the oxygen six-ring windows of zeolite A displayed a characteristic optical spectrum that was distinctly different from those of Co(II) in tetrahedral and octahedral coordinations in complexes and solids (13). The trigonal Co(II) spectrum is of special interest in zeolite chemistry as it signals an open coordination site accessible to incoming molecules that has no analogue in the

coordination chemistry of cobalt elsewhere. Even in zeolites, this open coordination Co(II) structure has been rare.

Although the evidence presented here is spectroscopic rather than based on diffraction methods, it can be combined with the knowledge of the erionite framework structure to arrive at a consistent picture of the site accessibility and distribution, which should make it possible to correlate these properties with the catalytic function and activity of Co(II) erionite.

Experimental Methods

Preparation of Co(II) Exchanged Zeolites. NH_4Na-erionite was ion exchanged under different conditions to obtain zeolites with different contents of Co(II) ions. NH_4Na-erionite (74.83% SiO_2, 18.36% Al_2O_3, 0.72% Na_2O, 0.05% CaO, 6.04% NH_4^+) was first prepared from Na-erionite (84.27% SiO_2, 11.09% Al_2O_3, 4.57% Na_2O, 0.07% CaO, <0.01% H_2O), provided by the Institute of Oil and Hydrocarbon Gases, Bratislava, Slovak Republic, by four equilibriations with 0.5 M NH_4NO_3 for 4 h at room temperature. With each 25 g batch of zeolite, 1600 ml of solution was utilized for each exchange step. After filtering, the zeolite was washed three times with 2000 ml of hot distilled water and air-dried. Analyses by XRD was used to confirm that a pure crystalline material was maintained.

Co-erionite samples with Co(II) concentrations of 0.002-8.2 wt% of Co were prepared at room temperature by ion exchange of 5 g portions of zeolite with 0.0001-0.02 M aqueous solutions of $Co(NO_3)_2$ or 0.1 M aqueous $Co(CH_3COO)_2$ solution. Preparations of the Co-erionite samples with high Co contents were carried out by three-step exchange procedures. Exchanged solids were filtered, washed three times with hot distilled water, and air dried.

The resulting Co concentrations and corresponding parameters of the ion exchange of samples No. 1-9 are given in Table 1. The concentration of Na in sample No. 9 with Co content of 8.2 wt% was lower than 0.01 wt%. Reverse exchange of Co from Co-erionite (sample No. 10) was carried out at room temperature by ion exchange of 1 g zeolite with 0.2 M aqueous solution of $NaNO_3$. The resulting Co concentration was 0.14 wt% of Co. The chemical composition of zeolites was determined after their dissolution by atomic absorption spectroscopy at the Institute of Inorganic Chemistry of the Czech Academy of Sciences.

Dehydration of Zeolites. The erionite samples were dehydrated at two different final temperatures of 350°C and 525°C. Dehydration at 350°C was carried out under dynamic vacuum (approximately 7×10^{-3} Torr) in a silica optical cell (26) (or in a silica flask in the case of magnetic measurements) in three steps: 100°C for 1 h, 220°C for 30 min., and 350°C for 3 h. The heating ramp between these temperatures was 5°C/min. The optical cell was then sealed by a stopcock and cooled to room temperature. Sealing of the cell by the stopcock was adequate over several days, as verified by UV-VIS-NIR DRS (in 14 days after sealing, no changes of spectra were observed). For samples dehydrated at 525°C, dehydration at 350°C was first carried out, followed by heating using a ramp of 10° C/min to 525°C, and then holding constant at 525°C for 8 h. After dehydration, samples were pale blue or white, and the color depended on the dehydration temperature and on the Co(II) concentration of the sample.

Adsorption of Carbon Monoxide, Ethylene, and Water. After the Co(II) erionite samples (*ca* 0.8 g) were dehydrated and cooled to room temperature as described earlier, carbon monoxide (99.0+%, Aldrich Chemical Company, Inc.) and ethylene (CP grade,

TABLE 1. Co(II) contents of Co(II)-erionite samples and conditions used for their preparation (type of Co(II) salt, concentration and volume of equilibration solution, initial pH, and time of exchange).

Sample No.	Co(II) (wt.%)	Aqueous Solution	[Co(II)] in Solution (M)	Time of Exchange (h)	Initial pH	Volume of Solution (ml/g)
1	0.002	$Co(NO_3)_2$	0.0001	3	5.8	4
2	0.12	$Co(NO_3)_2$	0.001	3	5.4	20
3	0.15	$Co(NO_3)_2$	0.005	4	6.1	1.7
4	0.30	$Co(NO_3)_2$	0.001	3	5.3	50
5	1.30	$Co(NO_3)_2$	0.01	3	5.1	40
6	1.50	$Co(NO_3)_2$	0.01	3	5.0	8.5
7	3.20	$Co(Ac)_2$	0.1 0.1	4 9	7.0 7.0	17 17
8	7.90	$Co(NO_3)_2$	0.02 0.02 0.02	4 4 14	5.9 5.7 5.5	133 133 180
9	8.20	$Co(NO_3)_2$	0.02 0.02 0.02	2 2 18	5.0 5.0 4.9	180 180 400
10	0.14	$Co(NO_3)_2$ $Co(NO_3)_2$ $Co(NO_3)_2$ $NaNO_3$	0.02 0.02 0.02 0.2	2 2 18 10	5.0 5.0 4.9	180 180 400 500

Linde) at pressures from 0.5 to 700 Torr and water at a pressure of 22 Torr were adsorbed at room temperature. The amount of gas adsorbed was monitored by adsorption at various pressures from volumes of 40, 180, or 1400 ml. Pressures of gases before and during adsorption were measured using a Pirani gauge. Adsorption was considered complete when no decrease in the pressure of adsorbing gas was observed during a time interval 15 min. CO was dried before adsorption by passing through a freezing trap containing liquid nitrogen. Water was degassed by freezing in a flask and evacuating.

Optical Spectroscopy. The diffuse reflectance spectra (DRS) in the UV-VIS-NIR region were acquired with a Varian-Carry 2300 spectrometer with a MgO-coated integrating sphere, and data were collected by a Zenith 386 computer utilizing Spectracalc software. The silica cell containing 0.6-1 g of zeolite was equipped with an Infrasil window (5 mm thick and 24 mm in diameter). The spectra were recorded separately in the UV-VIS region (200-850 nm, 1 nm scanning step, and 1 nm/s scan in the case of samples with Co(II) content higher than 2 wt% or 0.2 nm/s for samples with lower Co concentrations, using a photomultiplier detector, and using hydrated MgO as a standard). In the NIR region (750-2200 nm, 2 nm scanning step, and 0.2 or 0.05 nm/s scan), a PbS detector was employed and a Teflon standard was used. This method of spectral recording allowed an efficient and accurate data collection and removed problems with absorption of dehydrated MgO or Teflon in the UV region and with water absorption bands of hydrated MgO in the NIR region.

The absorption intensities were evaluated by the Schuster-Kubelka-Munk theory ($F(R_\infty) = (1-R_\infty)^2 / 2R_\infty$), where R_∞ is diffuse reflectance from a semi-infinite layer and $F(R_\infty)$

is proportional to the absorption coefficient. Final data processing was carried out using the Microcal Origin 3.78 software (Microcal Software, Inc., U.S.A.). The UV-VIS spectrum of the parent zeolite, dehydrated under the same conditions as utilized for the investigated Co(II) exchanged samples, was subtracted from the recorded spectra. In the case of second derivative mode analysis, no background subtraction was carried out.

Magnetic Susceptibility Measurements. The paramagnetic moments of the bare Co(II) ions in Co-erionite (8.2 wt% Co) dehydrated at 350 and 525°C were determined using the Gouy method (27). The magnetic field was 4200 Gauss, the internal diameter of the sample tube was 6 mm, the sample tube length was 12 cm, and the sample weight was 1.1 g. Pure $HgCo(NCS)_4$ was used for calibration. The measurements were carried out at room temperature, with measurements for each sample being repeated 5 to 10 times to obtain an error of measurement smaller than ±5%.

The magnetic susceptibility of each hydrated sample was measured using a 11 cm high column of zeolite in the sample tube. The sample tube was attached to a flask that was also connected to a silica cell for DRS measurements. After DRS measurements, the zeolite was transferred to the sample tube, which was then sealed off and the magnetic susceptibility of dehydrated sample was measured. The sample tube was then opened, sealed again to the flask and dehydrated at 525°C. Spectroscopic and magnetic measurements were again carried out. The magnetic susceptibility of the parent erionite was also measured using the same procedure. Magnetic susceptibility of Co(II) was taken as a difference between susceptibility of Co-erionite and the parent zeolite. The molar magnetic moment and paramagnetic moment of the Co(II) ions were calculated according to the Curie law (28).

RESULTS

Magnetic Properties. The paramagnetic moments (given in Bohr Magnetons) of Co(II) in erionite dehydrated at 350 and 525°C are summarized in Table 2 and are compared with data from the literature. The value of the paramagnetic moment of cobalt in the hydrated zeolite was in good agreement with the magnetic moment of Co(II) in $[Co(H_2O)_6]^{2+}$ (29), and the high value of the magnetic moment of Co(II) in erionite dehydrated at 525°C was close to the value characteristic of Co(II) in dehydrated A zeolite (8).

TABLE 2. The paramagnetic moments of Co(II) ions in erionite and comparisons with literature.

Co(II) Ion Environment	Paramagnetic Moment of Co(II) (BM)
Co-erionite hydrated	5.0
Co-erionite dehydrated at 350°C	5.2
Co-erionite dehydrated at 525°C	5.7
dehydrated Co-A zeolite (Ref. 8)	5.65
$[Co(H_2O)_6]^{2+}$ (Ref. 28)	5.1
tetrahedral Co (Ref. 28)	4.7 - 4.9

Spectrum of Co-Erionite Dehydrated at 350°C. The UV-VIS-NIR spectrum of the 3.2 % Co(II)-erionite dehydrated at 350°C is shown in Figure 1 and the effect of Co concentration on the VIS-NIR spectra of the Co(II) ions located in the erionite matrix is shown in Figure 2. The details of the normalized VIS spectrum with the asymmetric absorption band centered at 17,000 cm^{-1} characteristic of optical adsorption of the Co(II) ions

and the effect of Co concentration on this normalized VIS band are given in Figure 3. The difference between the spectra of Co(II)-erionite with low (<0.3 % Co) and high (>3% Co)

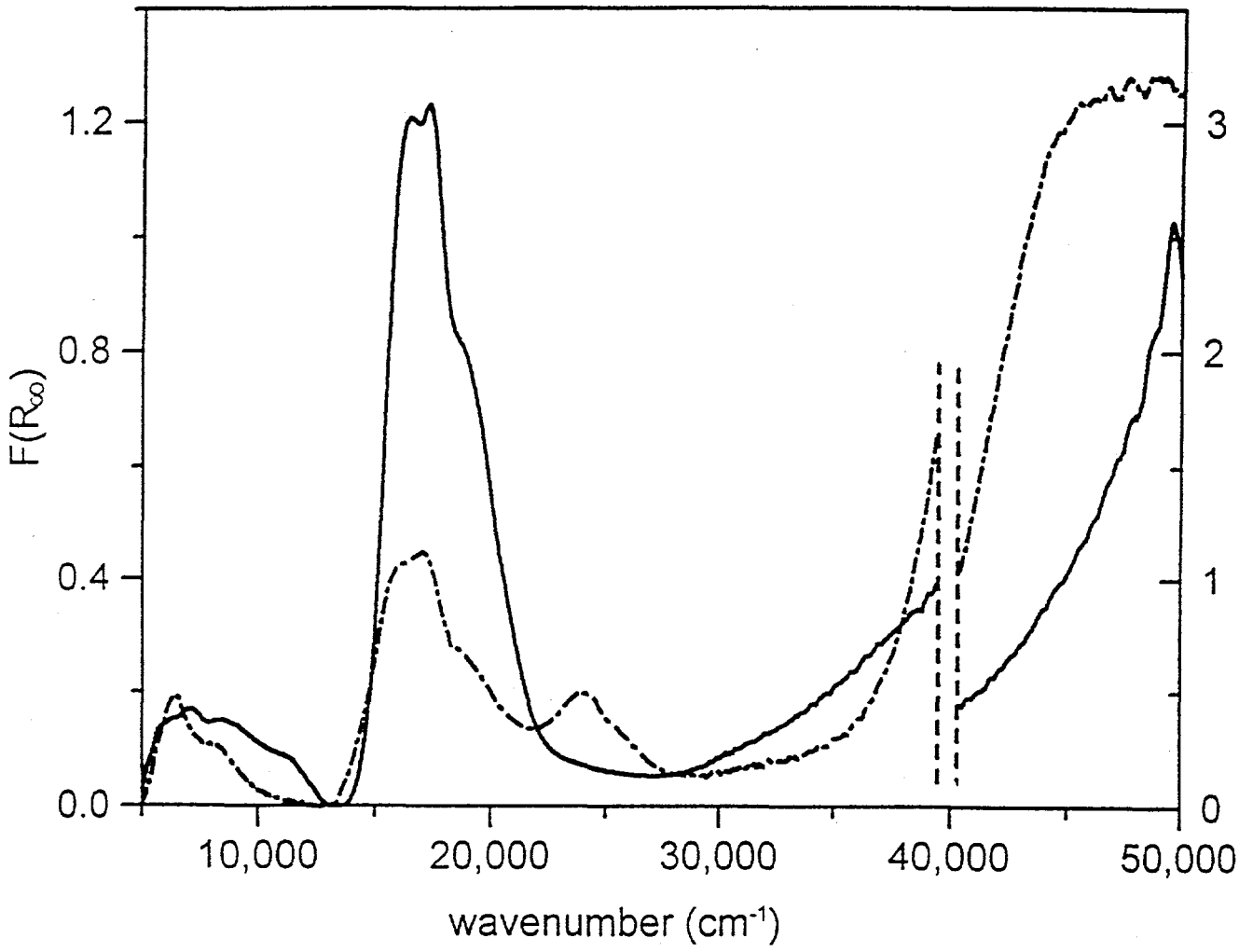

FIGURE 1. UV-VIS-NIR spectra of Co(II)NH_4-erionite (3.2 wt% Co) dehydrated at 350°C (—) and 525 °C (— • —).

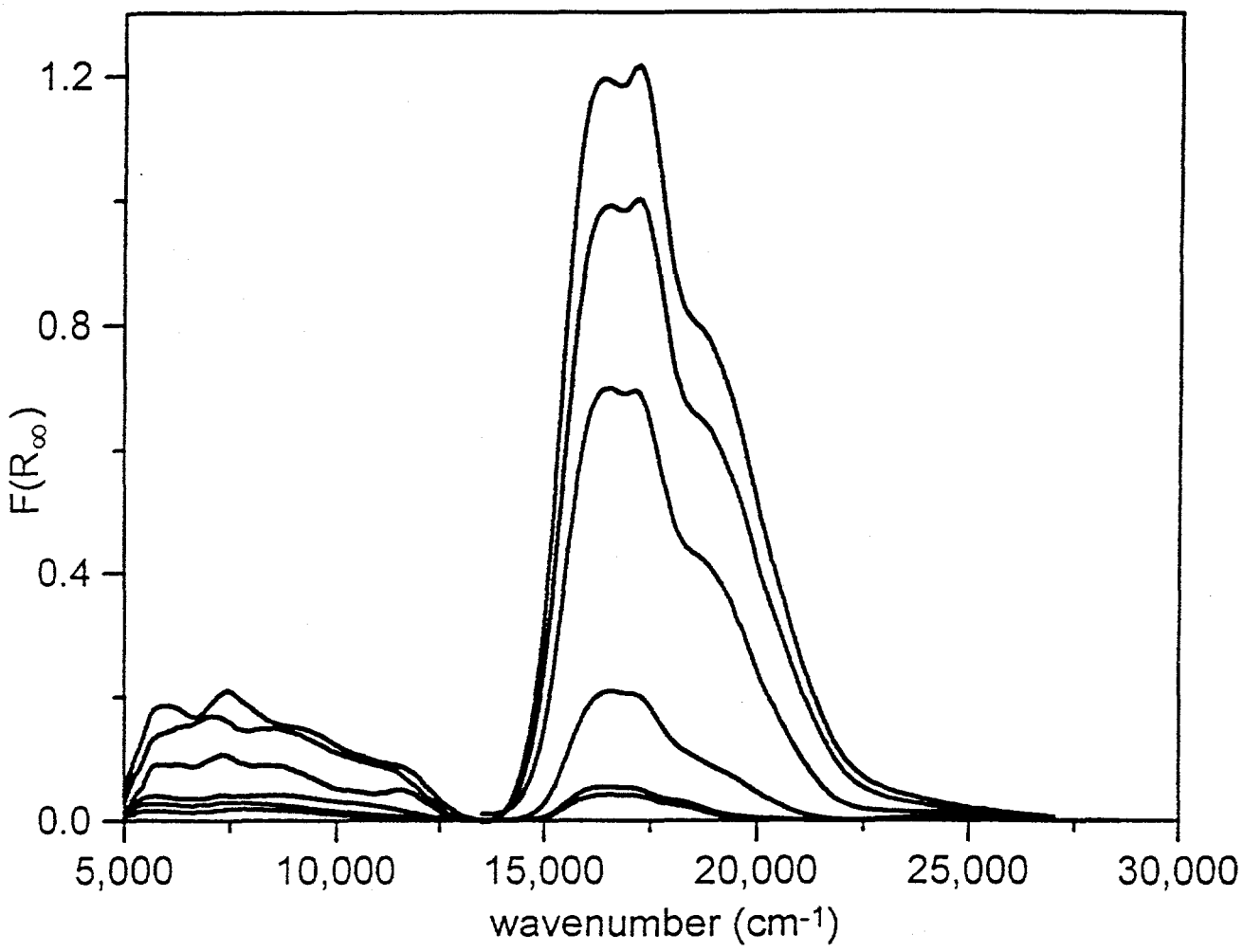

FIGURE 2. The effect of Co(II) concentration on VIS-NIR spectra of Co(II)-erionite samples dehydrated at 350°C. The spectrum of the parent zeolite was subtracted from the spectra shown here. Spectral intensity increases with increasing Co(II) concentration in the series of 0.15, 0.30, 1.3, 3.2, 7.9, and 8.2 wt% Co in erionite.

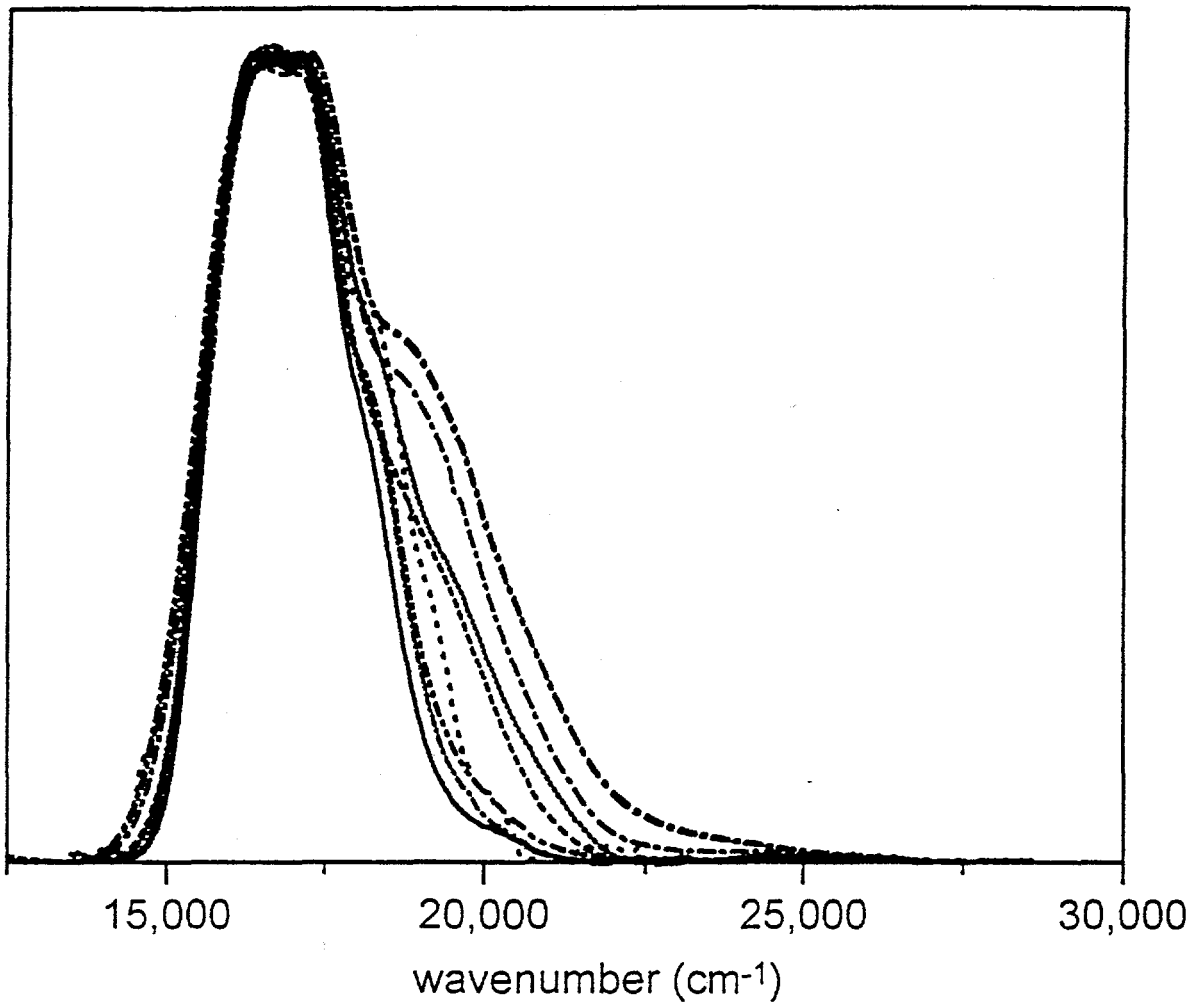

FIGURE 3. The effect of Co(II) concentration on normalized VIS spectra of Co(II)-erionite samples dehydrated at 350°C. The spectrum of the parent zeolite was subtracted. Spectra were separately normalized to 1 at maximum intensity. Co(II) concentrations in the erionite were 0.002 (• • •), 0.12 (—), 0.15 (— •• —), 0.30 (— • —), 1.3 (•••••), 1.5 (- - -), 3.2 (----), 6.2 (-•-•-), and 8.2 (-•-•-) wt% Co.

Co content indicates the presence of two components in the spectrum. Component α has bands centered approximately at 17,000 cm^{-1} and component β at 20,000 cm^{-1}. Spectral features of both components (two maxima and a shoulder in the case of the component α and shoulder at higher wavenumbers in the case of the component β) indicate their complex structure. This fine structure was further analyzed using the second derivative mode analysis (Figures 4 and 5). A minimum in the second derivative mode is localized close to the maximum of the absorption band. Wavenumbers corresponding to the optical transitions were taken as maxima of Gaussian curves to which the spectrum was deconvoluted. The component α is composed of three bands with maxima at 16,050, 17,080, and 18,040 cm^{-1}, while the component β is composed of two bands with maxima at 19,250 and 20,600 cm^{-1}. Areas of the bands at 16,050, 17,080, and 18,040 cm^{-1} were in the ratio 1.9/1.0/1.5 for the whole concentration range, and areas of the bands 19,250 and 20,600 cm^{-1} were in the ratio 1.8/1.0. This suggest an assignment of these bands to two distinct spectroscopic species α and β. The second derivative mode indicates that species β consists of doublets at 19,000 and 19,600 cm^{-1} and 20,600 and 21,300 cm^{-1}. The total intensities of the bands associated with the species α and β do not evolve in a parallel fashion with increasing degree of ion exchange. At low degrees of exchange, species α dominates, followed by evolution of species β that becomes discernible at high than 1 wt% Co(II) concentrations.

The VIS spectrum of Co-erionite (0.14 wt% Co) prepared by reverse exchange of Co-erionite with high Co loading (8.2 wt% Co) with $Na(NO_3)_2$ solution and subsequently dehydrated at 350°C is shown in Figure 6. This spectrum dramatically differs from that of

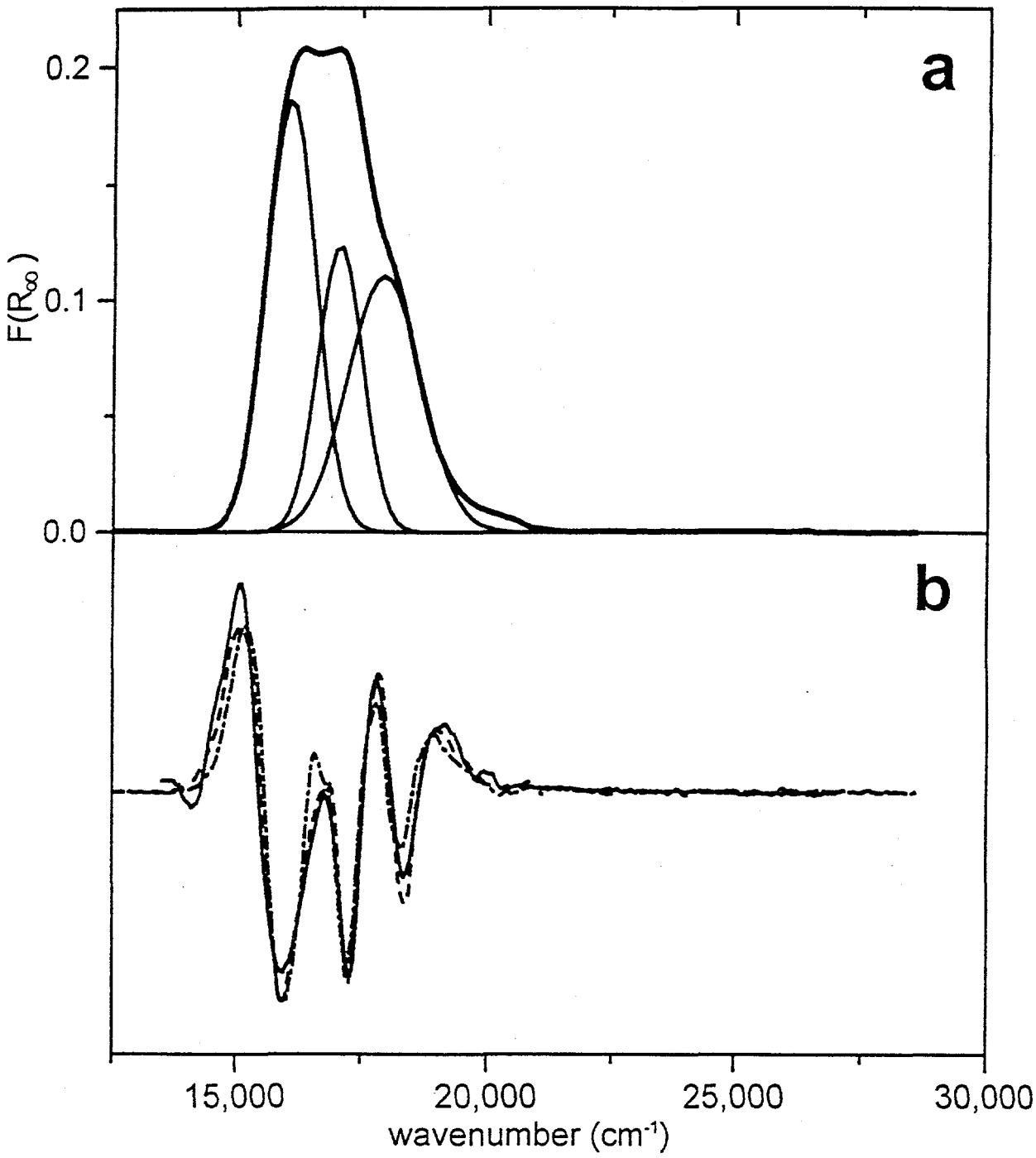

FIGURE 4. VIS spectrum of Co(II)-erionite samples with low Co concentrations dehydrated at 350°C. The spectrum of the parent zeolite was subtracted. (**a**) VIS spectrum of the zeolite with 0.12 wt% Co (—) and Gaussian bands composing the spectrum (—). (**b**) Second derivative mode of VIS spectra of Co(II)-erionite with 0.10 (—), 0.12 (- - -), and 0.30 (-•-•-) wt% Co.

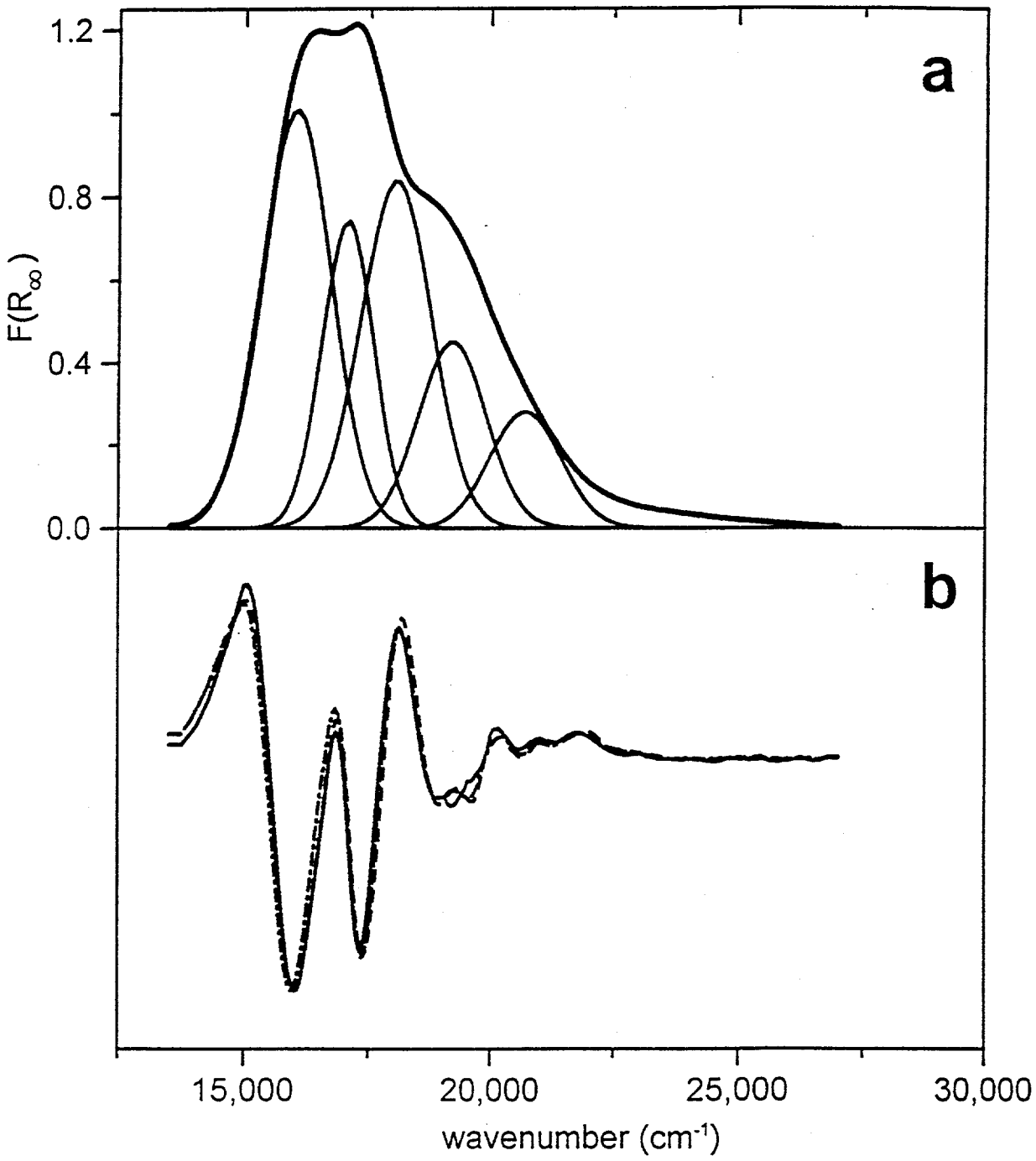

FIGURE 5. VIS spectrum of Co(II)-erionite samples with high Co concentrations dehydrated at 350°C. The spectrum of the parent zeolite was subtracted. (**a**) VIS spectrum of the zeolite with 6.2 wt% Co (—) and Gaussian bands composing spectrum (—). (**b**) Second derivative mode of VIS spectra of Co(II)-erionite with 3.2 (—), 6.2 (- - -), and 8.2 (-•-•-) wt% Co.

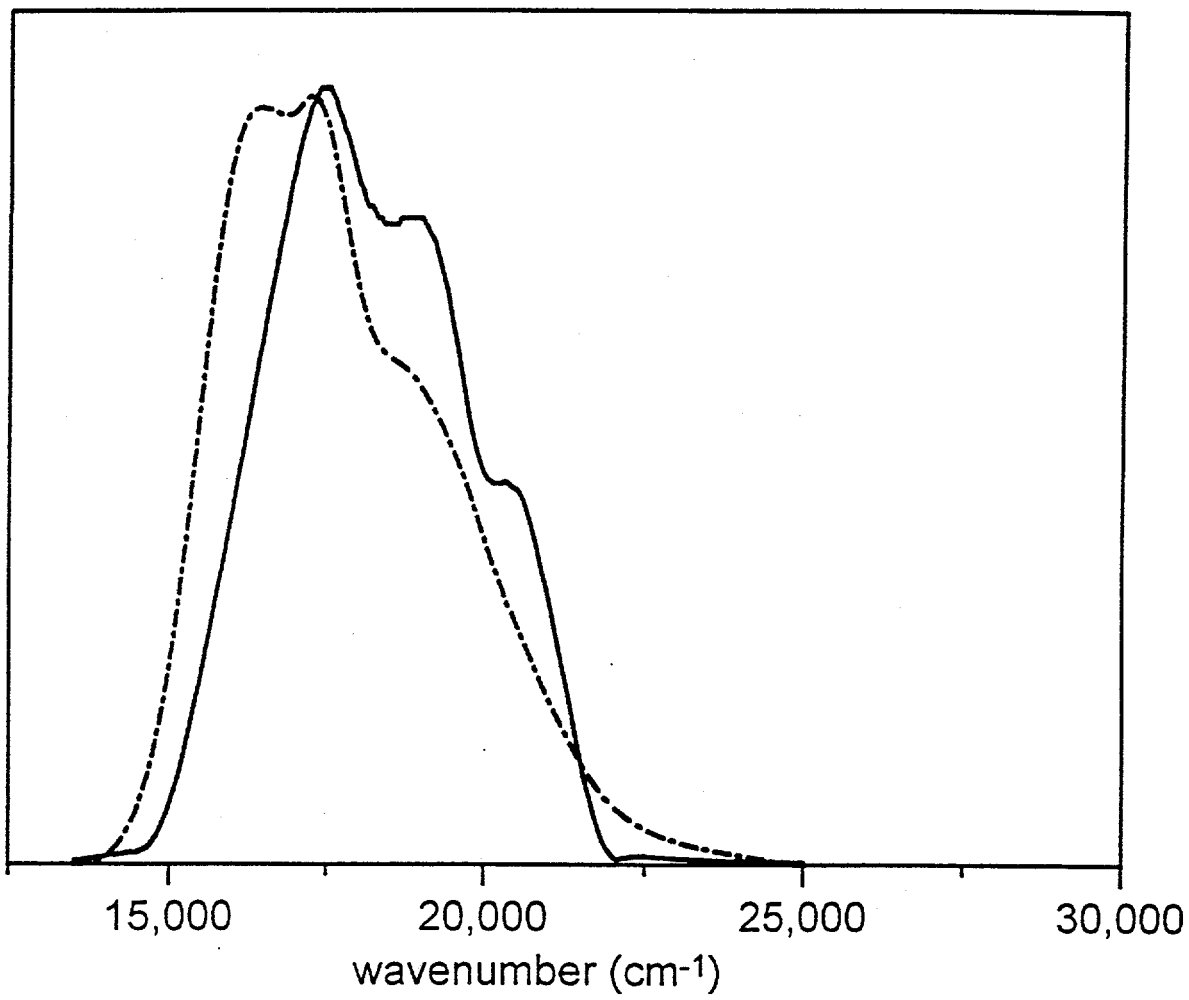

FIGURE 6. The effect of reverse exchange of Co(II) by Na on the normalized VIS spectrum of Co-erionite dehydrated at 350°C. The spectrum of highly exchanged Co(II)-erionite (8.2 wt% Co) (-•-•-) is compared with the spectrum of Co(II)-erionite originally containing 8.2 wt% Co after exchange by Na to reduce the Co(II) content to 0.14 wt% of residual Co(II) (—).

the forward-exchanged Co-erionite with similar Co content (0.12 wt% Co). The VIS bands at 19,250 and 20,600 cm^{-1} dominate the spectrum. Thus, species β corresponds to Co(II) ions in sites that are occupied only at high Co concentration in zeolite and from which it is difficult to exchange the Co ions back out of the cation sites.

The absence of the vibrational combination bands of water at 5,300 cm^{-1} (ν + δ) and 7,150 cm^{-1} (2ν) (30-32) in the NIR DRS spectrum of Co(II) in Co-erionite dehydrated at 350°C (cf. Figure 2) is an evidence for complete dehydration of Co-erionite at 350°C. The NIR bands at 5,800 cm^{-1} and 7,500 cm^{-1} that are attributed to electronic transitions of the Co(II) species α dominate in the spectra of samples with low Co concentrations. The NIR spectra of erionite with high Co content are dominated by bands at 8,500 and 11,500 cm^{-1}, which correspond to electronic transitions in the species β.

Spectrum of Co-erionite dehydrated at 525 °C. The UV-VIS-NIR spectrum of Co-erionite dehydrated at 525°C was shown in Figure 1. The details of the VIS and NIR bands of Co(II) ions of Co-erionite samples dehydrated at 525°C and the dependence of the spectra on Co concentration are given in Figure 7. A new asymmetric band between 22,000 and 27,000 cm^{-1} appeared as a result of dehydration at 525°C. The absorption band centered at 17,000 cm^{-1} was shifted to lower wavenumbers and exhibited a complex structure different from the absorption spectra of the corresponding Co-erionite samples dehydrated at 350 °C. The increasing relative intensity of the band at 17,000 cm^{-1} compared to the band at 25,000 cm^{-1} with increasing Co(II) concentration (Figure 8) indicates that the spectrum is composed of at least two components representing different spectroscopic species.

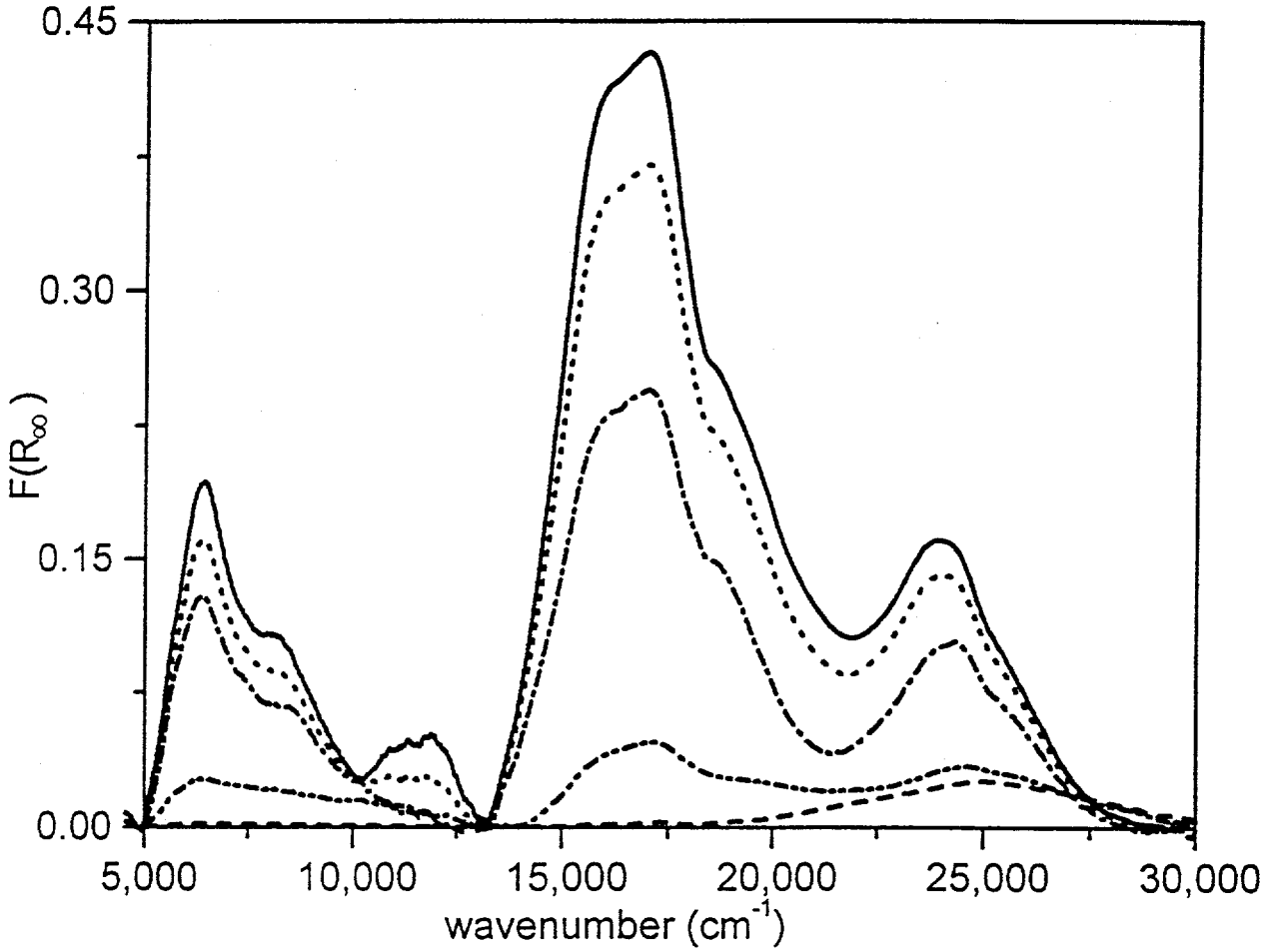

FIGURE 7. The effect of Co(II) concentrations on the VIS-NIR spectra of Co(II)-erionite samples dehydrated at 525°C. The spectrum of the parent zeolite was subtracted. The spectral intensity increases with increasing Co(II) concentration in the series 0.3 (- - -) 1.5 (-••-••-), 3.2 (-•-•-), 7.9 (••••), and 8.2 (—) wt% Co.

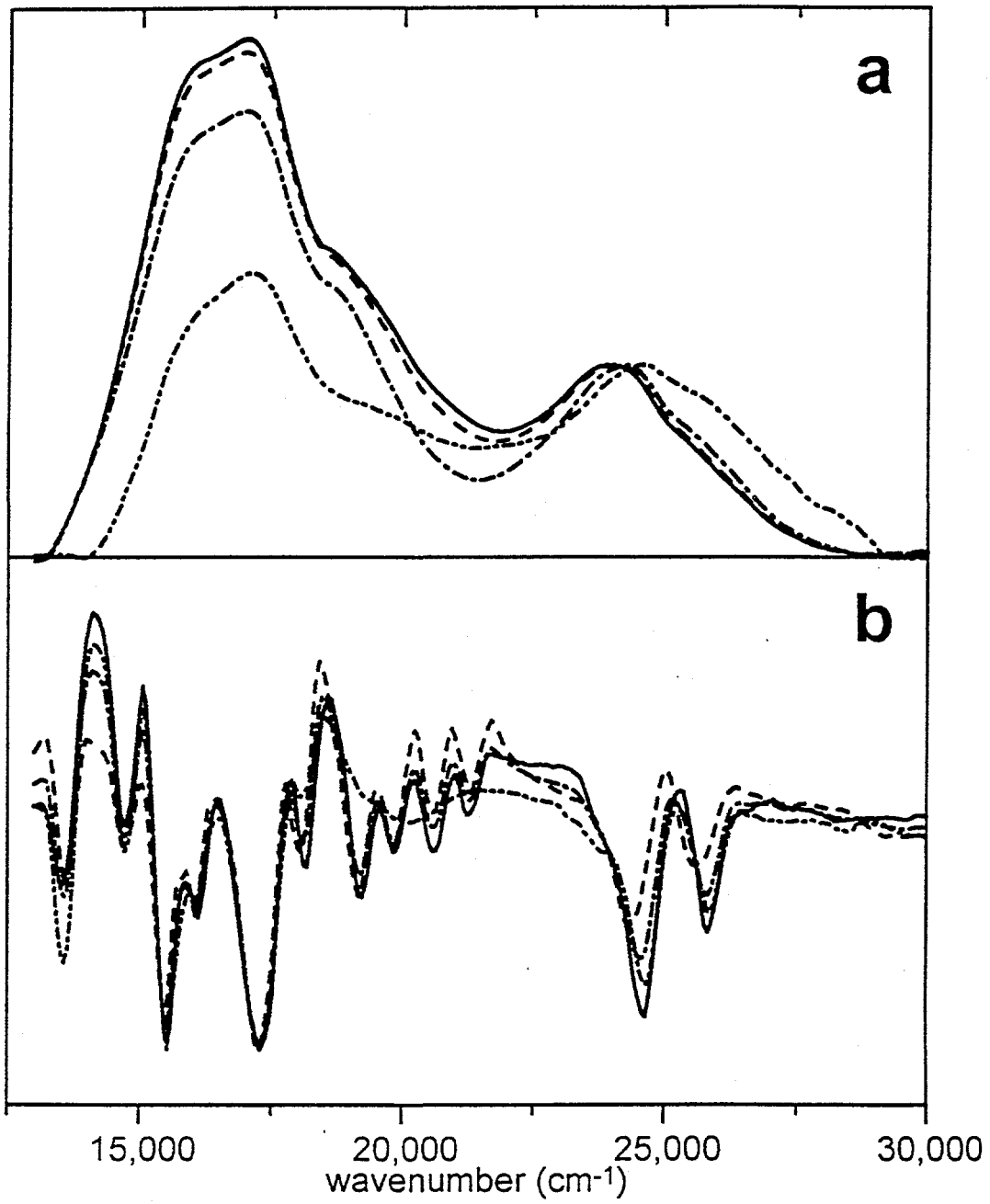

FIGURE 8. The effect of Co(II) concentration on the normalized VIS spectra of Co(II)-erionite samples dehydrated at 525°C. (**a**) The VIS spectra for 1.2 (-••-••-), 3.2 (-•-•-), 7.9 (- - -), and 8.2 (—) wt% Co samples were separately normalized to 1 at the intensity maxima of the bands at 25,000 cm^{-1}. The spectrum of the parent zeolite was subtracted. (**b**) Second derivative mode analysis of VIS spectra of the Co(II)-erionites with 1.3 (-••-••-), 3.2 (-•-•-), 7.9 (- - -), and 8.2 (—) wt% Co(II).

The second derivative mode of the spectra shown in Figure 8 exhibits more complex structure than second derivative mode in the case of samples dehydrated at 350°C (Figures 4 and 5). To the new asymmetric band at 25,000 cm^{-1} correspond bands with maxima located at 24,600 and 25,800 cm^{-1}. In the band at 17,000 cm^{-1}, new peaks appear (in the second derivative mode) at 14,700, 15,500, 17,250 and probably 13,600 cm^{-1}, but peaks at 16,000 and 18,100 cm^{-1} corresponding to the species α and the doublet at 19,200 and 20,300 cm^{-1} characteristic of species β are also observable. The peak at 17,400 cm^{-1} is probably overlapped by a peak at 17,250 cm^{-1}. It is concluded that the VIS spectrum of Co-erionite dehydrated at 525 °C is composed of species α and β, consisting of the VIS spectrum of Co-erionite dehydrated at 350°C, and of one or more new species γ characterized by the doublet at 25,000 cm^{-1} and by bands near 15,000 cm^{-1}. The bands corresponding to the species γ prevails at low Co concentrations and the role of species α and β in the VIS DR spectra increases with increasing Co content in the zeolite. The low content of species β in the spectrum of Co-erionite with 1.3 wt% Co can explain the shift of the maximum of the band at 25,000 cm^{-1} to higher wavenumbers. In the case of the spectra of samples with higher Co(II) loadings, the band at 25,000 cm^{-1} represents the sum of absorption of the bands corresponding to species β and γ.

The NIR spectrum of Co-erionite (cf. Figure 7) contains bands at 5,600, 6,400, 8,500, and 11,500 cm^{-1}. Bands at 8,000 and 11,500 cm^{-1} are characteristic of high Co(II) loading levels and correspond to the species β, while the band at 6,400 cm^{-1} is characteristic of species γ. The band at 5,600 cm^{-1} probably corresponds to the species α. The presence of

the band at 7,500 cm^{-1} of the species α in the spectrum of Co-erionite dehydrated at 525°C cannot be confirmed or excluded.

Adsorption of CO and Ethylene on Co-Erionite Dehydrated at 350°C. Accessibility of the Co(II) ions in erionite to guest molecules (CO, ethylene) and the effect of formation of complexes on the electronic spectra of Co(II) ions were investigated. The molecules of CO and ethylene were adsorbed at room temperature at a final pressure of 30 Torr on Co-erionite dehydrated at 350°C, and the DR spectrum of Co ions was affected by this adsorption.

The spectrum of the CO-Co-erionite (0.12 wt% Co) containing spectroscopic species α is compared in Figure 9a with the spectrum of bare Co(II) in the same sample. It is evident that Co(II) ions in this site are accessible to CO and form a CO-Co complex with new characteristic bands. The resulting spectrum after CO adsorption onto the Co(II) species α is composed of bands at 15,000, 15,400, 16,300, 17,300, 18,100, and 19,700 cm^{-1} (in second derivative mode). Second derivative mode analysis of the spectra of CO-Co-erionite (3.2 wt% Co) containing both species α and β (Figure 9b) indicated the superposition of the CO-$Co(II)_{\alpha}$ and CO-$Co(II)_{\beta}$ species and no minima corresponding to new species appeared in the spectrum.

The absorption spectrum of the ethylene-Co complex in erionite is shown in Figure 10. Ethylene adsorbed on bare Co(II) cations and formed the ethylene-Co complex with characteristic bands at 14,700, 16,300, 17,000, and 18,600 cm^{-1}. Comparison of the spectra of ethylene-Co-erionite with different Co concentrations (i.e. only with spectroscopic species

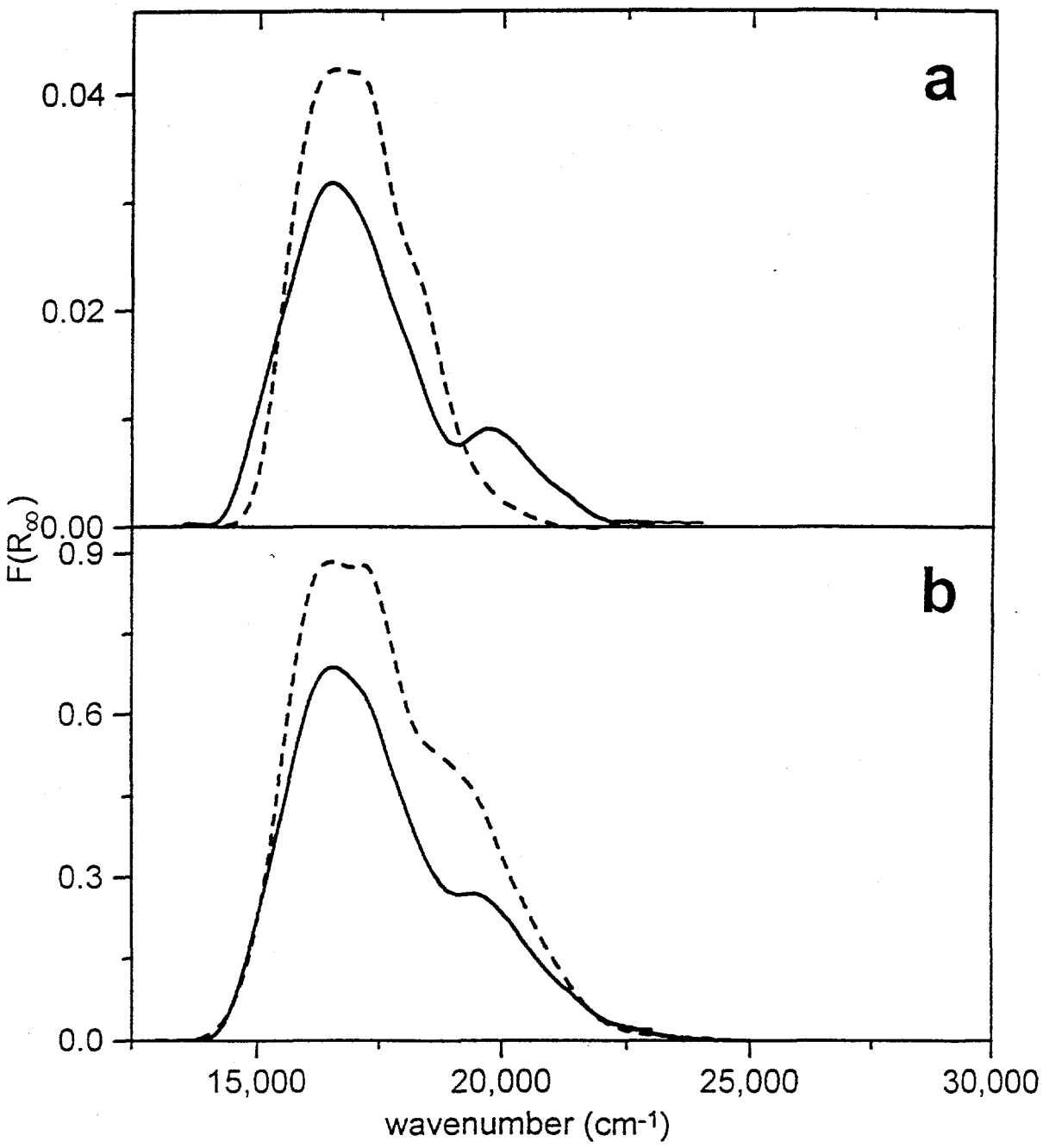

FIGURE 9. The effect of CO adsorption on the VIS spectrum of Co(II)-erionite dehydrated at 350°C. The spectrum of the parent zeolite was subtracted. (**a**) VIS spectrum of Co(II)-erionite with 0.12 wt% Co(II) after dehydration (- - -) and after adsorption of CO (—). (**b**) VIS spectrum of Co(II)-erionite with 3.2 wt% Co(II) after dehydration (- - -) and after adsorption of CO (—).

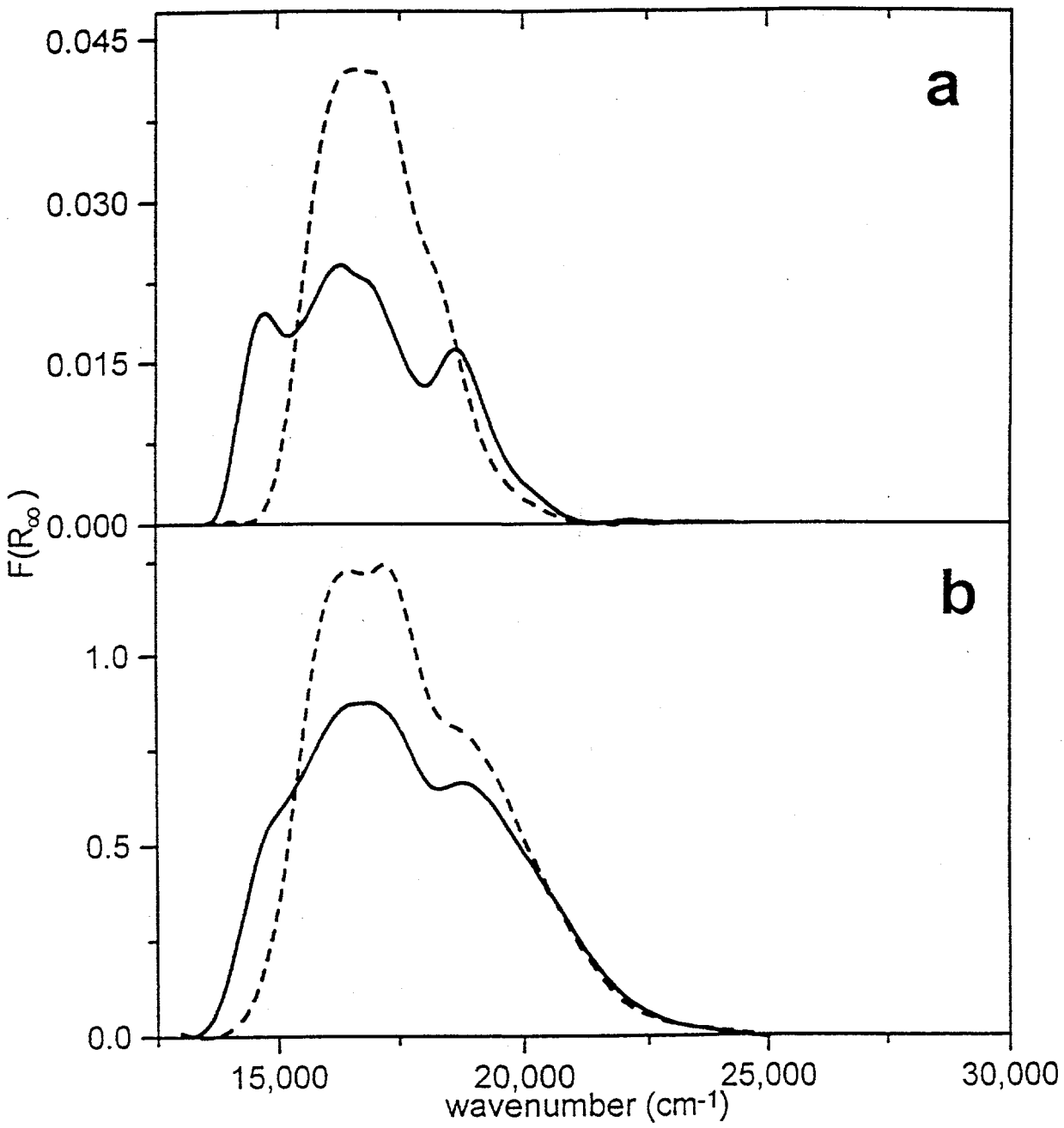

FIGURE 10. The effect of ethylene adsorption on the VIS spectrum of Co(II)-erionite dehydrated at 350°C. The spectrum of the parent zeolite was subtracted. (**a**) VIS spectrum of Co(II)-erionite with 0.12 wt% Co(II) after dehydration (- - -) and after adsorption of ethylene (—). (**b**) VIS spectrum of Co(II)-erionite with 8.2 wt% Co(II) after dehydration (- - -) and after adsorption of ethylene (—).

α (Figure 10a) and with spectroscopic species α and β (Figure 10b)) showed that ethylene did not affect the spectrum of species β. The ethylene-Co complex of the sample with high Co(II) content (with species α and β) exhibits absorption at wavenumbers higher than 20,500 cm^{-1}, where the ethylene-Co complex of species α does not absorb. Moreover, only bands corresponding to the species β and to the ethylene-Co complex of species α are present in the second derivative mode of the ethylene-Co complex of samples with high Co content.

Adsorption of CO, Ethylene, and Water on Co-Erionite Dehydrated at 525°C. At room temperature, carbon monoxide and ethylene were adsorbed onto Co(II) cations in Co-erionite samples dehydrated at 525°C. The spectrum of Co-erionite containing 3.2 wt% Co(II) after CO adsorption is given in Figure 11. This spectrum is composed of multiple bands centered at 16,100 cm^{-1} and of two bands centered at 21,000 cm^{-1} (19,950 and 21,300 cm^{-1}). The spectrum of the ethylene-Co complex formed in a 1.2 wt% Co(II) erionite sample is shown in Figure 12. It is seen that the spectrum of the ethylene-Co complex in Co-erionite dehydrated at 525°C is composed of bands with maxima at 15,100, 16,900, 18,800 and 20,500 cm^{-1}.

The effect of water adsorption on Co(II) spectra in Co-erionite dehydrated at 525 °C and also the effect of equilibration time of water adsorption was studied in the following experiment. A small amount of water (1.5 mol/g of zeolite) was adsorbed on Co-erionite containing 3.2 wt% Co dehydrated at 525°C. After this water adsorption, the doublet at 25,000 cm^{-1} characteristic of accessible Co sites disappeared. After one h of equilibration, the zeolite was dehydrated at 350°C and its spectrum was recorded. The band at 25,000 cm^{-1}

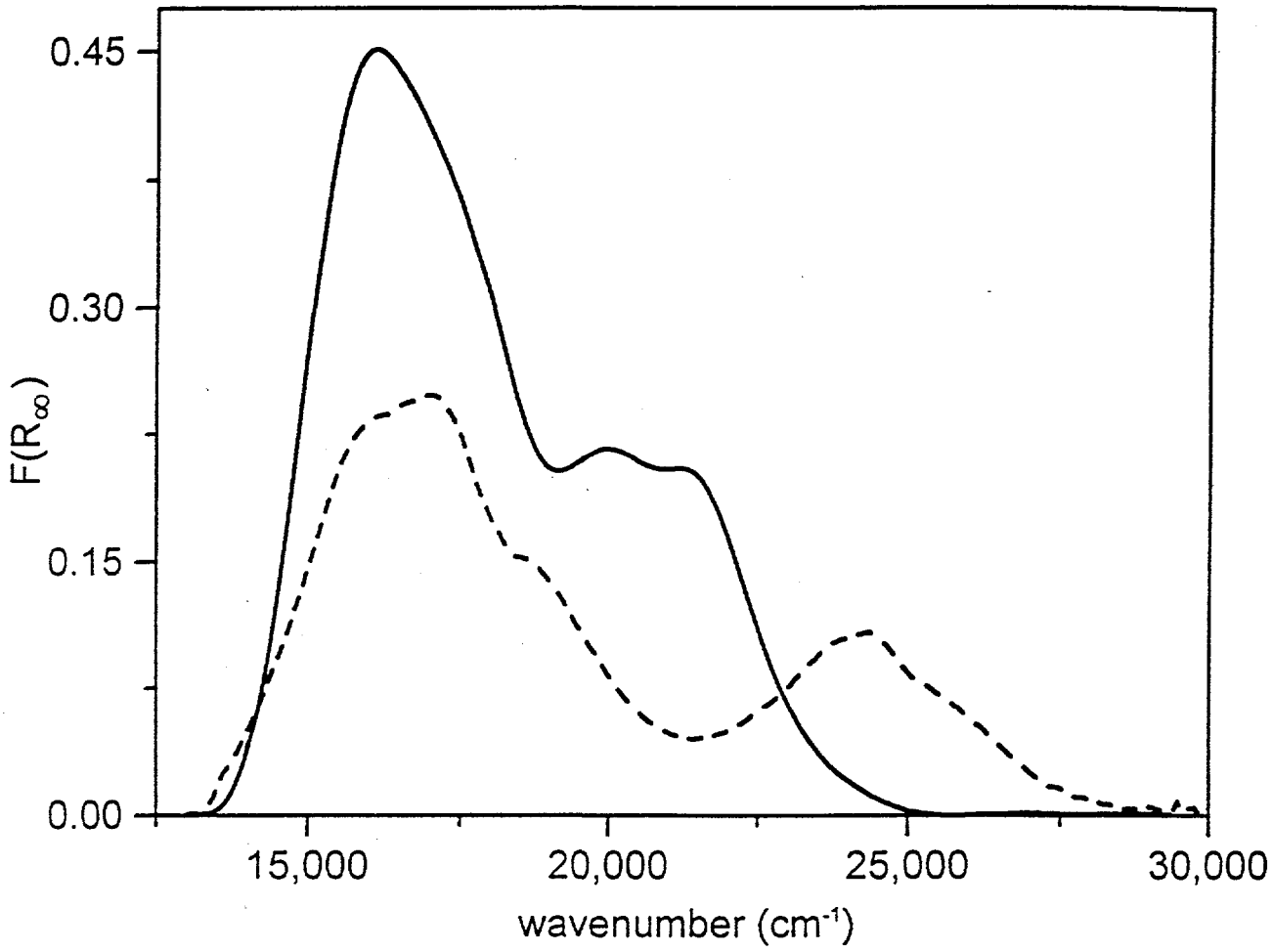

FIGURE 11. The effect on the VIS spectrum of Co(II)-erionite (3.2 wt% Co) dehydrated at 525°C of CO adsorption at room temperature. The spectrum of the parent zeolite was subtracted. The spectra correspond to dehydrated Co(II)-erionite (- - -) and Co(II)-erionite with adsorbed CO (—).

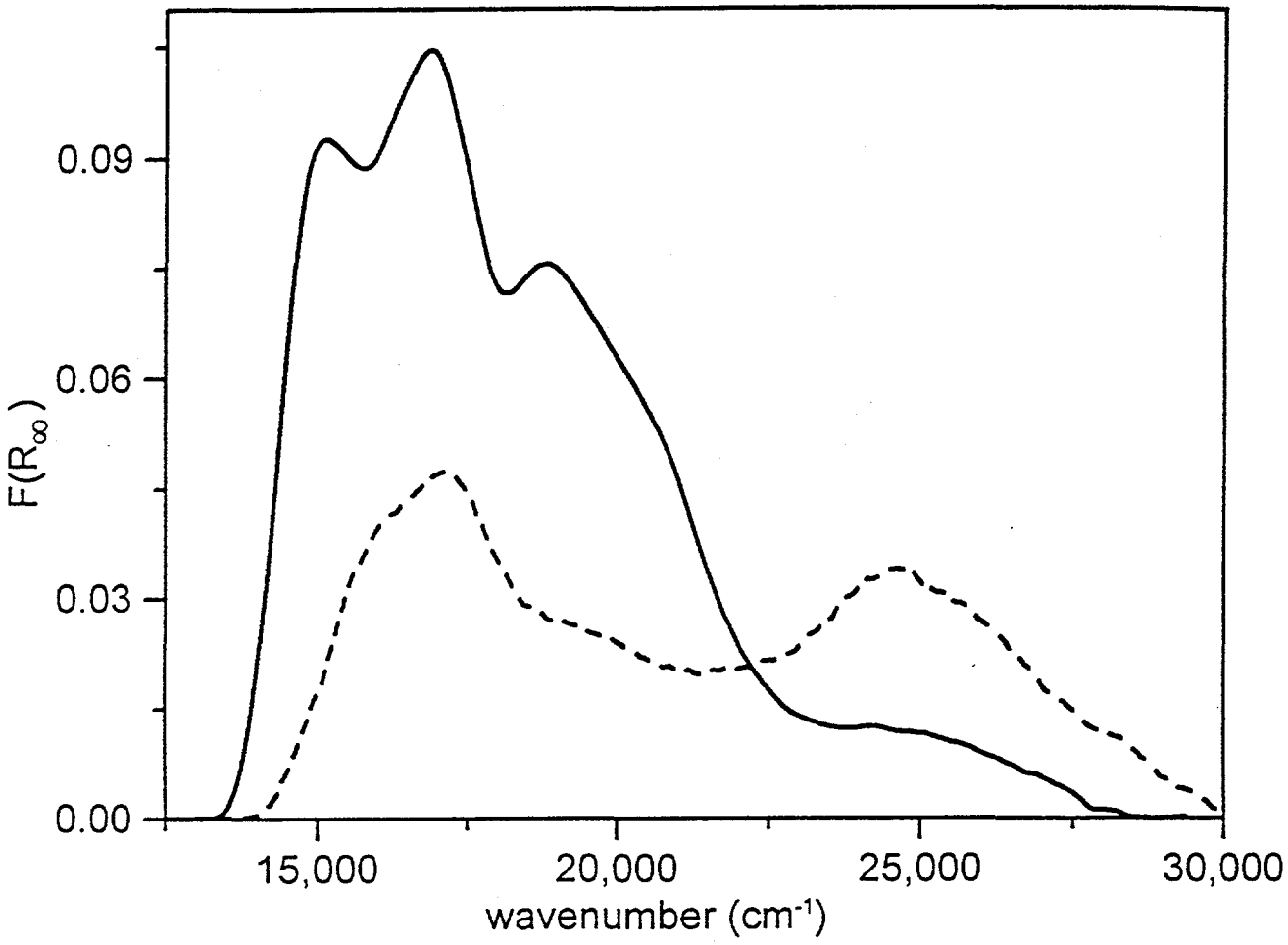

FIGURE 12. The effect of ethylene adsorption at room temperature on the VIS spectrum of Co(II)-erionite (1.5 wt% Co) dehydrated at 525°C. The spectrum of the parent zeolite was subtracted. The spectra correspond to dehydrated Co(II)-erionite (- - -) and to Co(II)-erionite with adsorbed ethylene (—).

reappeared in the VIS spectrum, but its intensity was *ca* 50% of the intensity of the initial sample dehydrated at 525°C. After 22 days of equilibration with adsorbed water and dehydration at 350°C the intensity of the 25,000 cm^{-1} doublet was *ca* 40 % of the intensity of the sample dehydrated at 525°C. The original 25,000 cm^{-1} band was fully recovered after dehydration at 525°C.

Quantification of the Spectroscopically Distinct Species. Estimates of the occupancy of individual cation sites corresponding to spectroscopic species *via* comparison of visible bands corresponding to individual species can be made. Assuming that the area of the species α is proportional to the content of Co(II) ions located in the site characterized by this species, the concentration of Co(II) cations corresponding to the species α or β can be approximately estimated. At low Co(II) concentrations, only species α is present in the spectrum, and the areas of bands corresponding to species α exhibit linear a dependence on Co concentration in zeolite. Spectra at higher Co loading levels were decomposed into Gaussian components, e.g. see Figure 5, and the sums of the total areas of the first three Gaussian components at 16,050, 17,080, and 18,040 cm^{-1} were plotted to represent species α, as shown in Figure 13. The sums of the two Gaussian components at 19,250 and 20,600 cm^{-1}, representing species β, were also plotted in Figure 13. At low Co loadings only species α appeared, while at higher loadings (>1.2 wt%) species β began to evove. The difference between the measured area of species α and its area predicted from the extended initial slope gives, in principle, the content of Co(II) species β. Because of experimental errors involved, only at the higher levels of ion exchange was it possible to estimate the concentration of

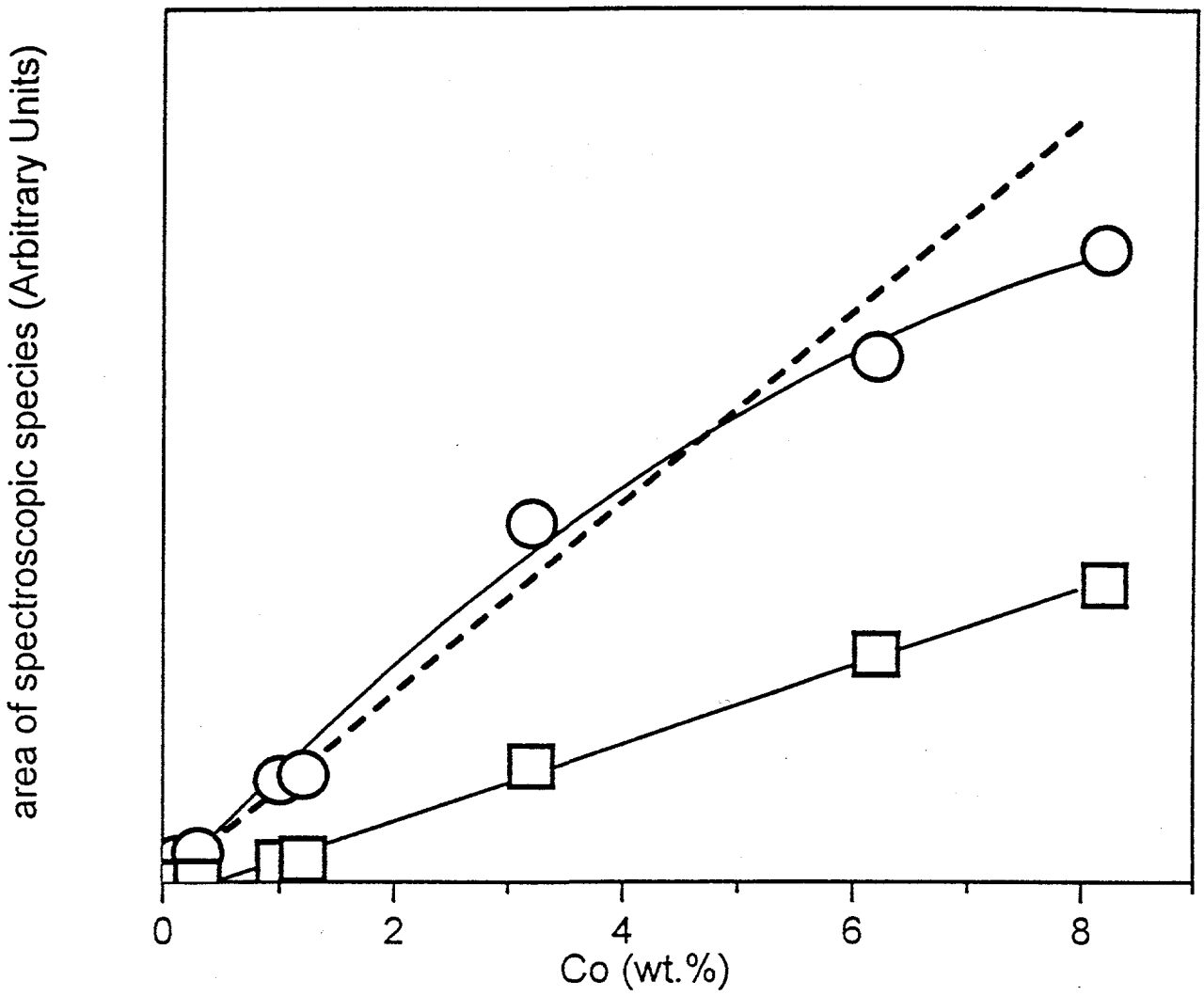

FIGURE 13. Dependence of the spectral areas corresponding to spectroscopic species α and β in Co(II)-erionite dehydrated at 350°C as a function of the Co(II) concentration. Species α (—○—), species β (—□—), and extrapolation of the linear dependence of the area of species α at low Co(II) loading levels (- - -).

species β by this method. For the 8.2 wt% Co(II) -erionite sample, the distribution of species is estimated to be 82 ± 7% species α and 18 ± 7% species β. A comparison of the measured areas of spectral signals of species α and β gives the ratio of 68/32. This indicates that the specific absorption of species β is 2.1 times higher than that of species α. Using this ratio of absorption coefficients, the concentrations of species β could be estimated from the measured areas, as summarized in Table 3.

TABLE 3. Concentration of $Co(II)_{\alpha}$ and $Co(II)_{\beta}$ in erionite dehydrated at 350°C.

Total Co(II) Content (wt%)	$Co(II)_{\alpha}$		$Co(II)_{\beta}$	
	Co(II) Content (wt%)	Relative Population (%)	Co(II) Content (wt%)	Relative Population (%)
0.002	0.002	100	0.00	0
0.10	0.10	100	0.00	0
0.12	0.12	100	0.00	0
0.30	0.29	90	0.03	10
1.0	0.92	92	0.08	8
1.2	1.09	91	0.11	9
3.2	2.77	87	0.43	13
6.2	5.14	84	1.06	16
8.2	6.70	82	1.50	18

A similar approach was used to estimate the population of Co(II) ions corresponding to the species γ characteristic for some of the Co(II) cations in Co-erionite dehydrated at 525°C. The area of the doublet at 25,000 cm^{-1} was plotted in Figure 14 to represent species

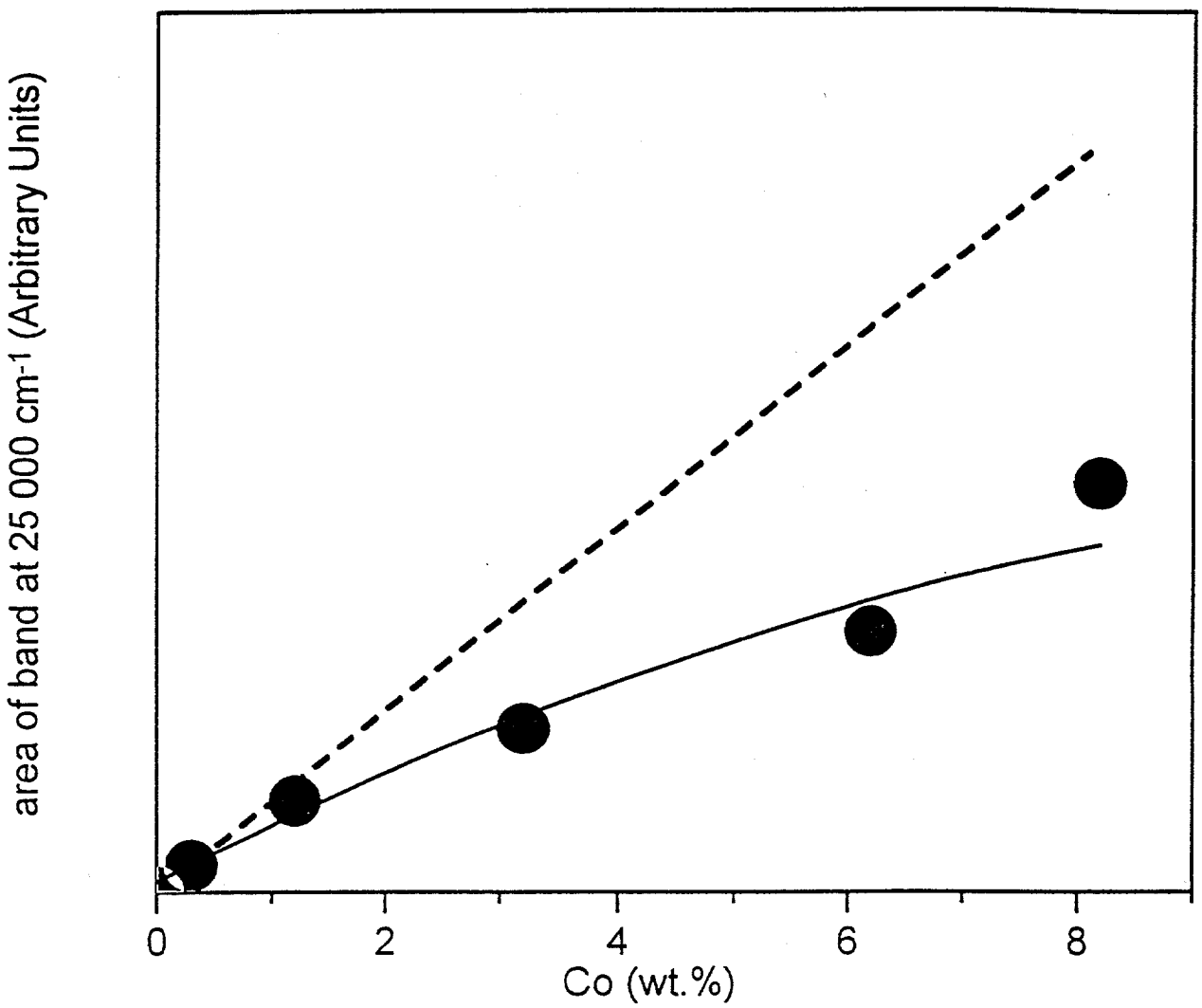

FIGURE 14. Dependence of the spectral area of spectroscopic species γ in the Co(II)-erionite dehydrated at 525°C as a function of the Co(II) concentration in the zeolite. Species γ (—●—) and extrapolation of the linear dependence of the spectrtal area corresponding to the species γ at low Co(II) loading (- - -).

γ. At low Co(II) contents (<1.2 wt% Co), a linear dependence of the $Co(II)_\gamma$ species on total Co(II) concentration was observed. Thus, the absorption coefficient of species γ was estimated from the initial slope of the area of species γ. Using this absorption coefficient and the assumption that the content of species β did not change during the dehydration process (as will be discussed below), the concentration of the $Co(II)_\gamma$ species at high Co loading levels was estimated as summarized in Table 4. At low Co(II) levels (<1.2 wt%), more than 90% of species γ was present in erionite dehydrated at 525°C. At high Co(II) concentrations (>6 wt%), only *ca* 60% of species γ was present, while the rest corresponded to species α (28-16%) or β (16-18%).

TABLE 4. Concentrations of species $Co(II)_\alpha$, $Co(II)_\beta$, and $Co(II)_\gamma$ in erionite dehydrated at 525°C.

Total Co Content (wt%)	$Co(II)_\alpha$		$Co(II)_\beta$		$Co(II)_\gamma$	
	Co(II) Content (wt%)	Relative Population (%)	Co(II) Content (wt%)	Relative Population (%)	Co(II) Content (wt%)	Relative Population (%)
0.3	0.0	0	0.03	10	0.27	90
1.2	0.0	0	0.11	9	1.1	91
3.2	0.6	19	0.40	13	2.2	68
6.2	1.6	28	1.1	16	3.5	56
8.2	1.3	16	1.5	18	5.4	66

Discussion

Magnetic Moments of Co(II) Ions in Erionite. The agreement of the experimental value of the magnetic moment of hydrated Co-erionite with the literature value for the $Co(H_2O)_6^{2+}$ complex, compared in Table 2, confirms the validity of the method used. The values of magnetic moment of Co(II) in dehydrated erionite (5.2-5.7 BM) are significantly higher than the spin-only value (3.87 BM) of the high-spin Co(II) $3d^7$ configuration, indicating a low symmetry coordination with little, if any, quenching of the orbital contribution to the magnetic moment. These values are also significantly higher than the values of magnetic moments of tetrahedral and octahedral cobalt (29) and approximately correspond to the value obtained earlier (8) for Co(II) in dehydrated A zeolite.

Different values of the magnetic moment of Co(II) at the various dehydration temperatures provide evidence of different environments for the Co(II) cation in the zeolite treated at the different conditions. The magnetic moment of Co(II) in erionite dehydrated at 525°C, with a value that is very closed to that for dehydrated Co-A zeolite, indicates a site with trigonal near-planar symmetry. The lower magnetic moment of Co(II) in erionite dehydrated at 350°C could be explained: (i) by a lower orbital contribution to the magnetic moment connected with a different type of planar symmetry, (ii) by cobalt located slightly out of the planar environment, or (iii) as a superposition of magnetic moments of Co(II) cations in various sites.

Spectrum of Co-Erionite Dehydrated at 525°C: Spectroscopic Species γ. The VIS spectrum of species γ with characteristic bands at 6,400, 17,500, and 25,000 cm^{-1} of Co-

erionite dehydrated at 525°C (Figure 7) exhibited bands similar to the spectrum of Co(II) in dehydrated Co-A zeolite (7-12), which was identified by Klier et al. (10,26) as Co(II) with approximately D_{3h} symmetry in regular six-ring windows of A zeolite. The comparison of spectral bands of species γ of Co-erionite dehydrated at 525°C and spectral bands of dehydrated Co-A zeolite is given in Table 5. Generally good agreement was obtained between these two spectra, and it is concluded that spectroscopic species γ, present in Co-erionite dehydrated at 525°C, corresponds to Co(II) ions in sites with a near-D_{3h} symmetry. This is also confirmed by the nearly identical values of the magnetic moment of Co(II) ions in dehydrated A zeolite and erionite dehydrated at 525°C (cf. Table 2). The slight differences in the fine structure of the bands centered at 17,500 cm^{-1} can be explained by the

TABLE 5. Comparison of spectral transitions of Co(II) species γ in Co-erionite dehydrated at 525°C and of transitions in the spectrum of dehydrated Co-A zeolite.

Wavenumber of Optical Transition (cm^{-1})	
Species γ of Co(II)-erionite	Co(II)-A Zeolite (Ref. 10)
6,400	6,800
	7, 500
14,700	14,000
15,500	16,000
17,250	18,300
24,600	24,400
25,800	25,500

small differences in the geometry of the regular six rings in erionite (where all oxygen atoms are located in the plane of the ring) and A zeolite (where oxygen atoms are located alternating up and down from the ring plane) and by the difference in the aluminum distribution (Si/Al = 1 for A zeolite and Si/Al = 3.5 for erionite).

The VIS spectrum of Co(II) in erionite is strongly affected by the adsorption of CO or ethylene. It indicates that species γ represents low coordinated Co(II) accessible to guest molecules. The spectra of Co-erionite with low Co content (with Co(II) represented by species γ) after CO adsorption (Figure 11) and of the CO-Co complex in regular six-rings in A zeolite with Co(II) in C_{3v} symmetry (14) are compared in Table 6. The close similarity of these spectra indicates an identical geometry of this CO-Co complex in the two zeolites.

TABLE 6. Comparison of transitions in the spectra of the CO-Co(II) and ethylene-Co(II) complexes in erionite dehydrated at 525°C and in dehydrated Co(II)-A zeolite in the range 15,000 - 22,000 cm^{-1}.

Wavenumber of Optical Transition (cm^{-1})			
CO-Co(II) Complex		Ethylene-Co(II) Complex	
Co(II)-Erionite	Co-A(II) Zeolite (Ref. 14)	Co(II)-Erionite	Co-A(II) Zeolite (Ref. 12)
15,500	15,700	15,100	14,750
16,300	16, 500	16,900	15,900
17,400	17,300	18,800	16,800
18,100	18,300	20,500	19,250
19,950	20,100		
21,300	21,400		

The effect of CO adsorption on planar trigonal Co(II) in this site was discussed by Lin (14), who concluded that the bare Co(II) ion with C_{3v} symmetry is pulled out by CO adsorption only slightly from the framework oxygen plane, and CO is only weakly adsorbed as an axial ligand.

The comparison of the spectrum of the ethylene-Co complex in regular six-rings in erionite (Figure 12) and in Type A zeolite (12) is also given in Table 6. Between 15,000 and 22,000 cm^{-1}, both spectra show four bands of very similar lineshape, but the absorption band of the ethylene-Co-erionite complex is shifted by some 500-1,000 cm^{-1} to higher wave-numbers compared to that in A-zeolite. The adsorption of olefins on Co(II) ions located in the regular six-ring window with D_{3h} symmetry of A zeolite was studied experimentally and theoretically by Kellerman and Klier (10). After ethylene adsorption, the Co ions were moved from the plane (D_{3h} symmetry) and formed a digonally distorted nearly tetrahedral complex. The spectral features of this complex were affected by the presence of ethylene π electrons, and the ^4P energy levels between 14,000 and 20,000 cm^{-1} above the ground state were asymmetrically split.

These fine interactions between ethylene, Co(II) ion, and framework oxygen atoms are likely affected by the different Si/Al ratios and by subtle differences in the geometry of the trigonal sites in erionite and A zeolite. The total splitting of the band centered at 17,000 cm^{-1} is larger in Co-erionite (5,400 cm^{-1}) than in CoA zeolite (4,500 cm^{-1}), indicating a more strongly bonded ethylene-Co-erionite complex. Both the tetrahedral component, which primarily affects the ground state, and the digonal component, to which the splitting in the excited state is sensitive (12), contribute to the bonding in the complex. Since the adsorption

heat of ethylene in the 1:1 complex ethylene:Co(II)A zeolite was found to be equal to 68 kJ/mol (12), the present shifts and splittings of *ca.* 1,000 cm^{-1} in Co(II) erionite add 11 kJ/mol to the stability of the ethylene-Co(II) complex.

It is concluded that the Co(II) ions identified as spectroscopic species γ in erionite dehydrated at 525°C are located in D_{3h} sites with an open coordination shell. The adsorption of CO or ethylene create 1:1 CO-Co or ethylene-Co complexes with C_{3v} or C_{3h} symmetry as in Type A zeolite. At high Co concentrations, part of Co(II) cations are located in different sites, creating different spectroscopic species α and β, as discussed below.

Co-Erionite Dehydrated at 350°C: Spectroscopic Species α and β. The optical absorption band near 20,000 cm^{-1} for Co(II) ions is well-known and is characteristic of Co(II) complexes with octahedral symmetry (33). The comparison of the spectrum of species β with the spectrum of Co(II) hexaquocomplex in 0.1 M aqueous $Co(NO_3)_2$ solution is given in Table 5. The main bands in the spectrum of species β are similar to those of the Co(II) hexaquocomplex. The band at ≈19,400 cm^{-1} for the Co(II) hexaquocomplex exhibits fine structure, and peaks were identified using second derivative mode analysis. The two Gaussian curves produced maxima at 19,350 and 21,400 cm^{-1}. The ratio of the areas of these bands was 1.5/1.0, similar to the ratio of the absorption bands of species β (1.8/1.0). The very weak band of the O_h Co(II) complex at 16,000 cm^{-1} could not be detected due to overlapping high intensity bands of species α. It is concluded that the spectroscopic species β correspond to Co(II) ions with octahedral symmetry. The band at 8,000-8,500 cm^{-1} corresponds to the $^4T_{1g}$ (F) → $^4T_{2g}$ (F) transition, while the bands at 19,000-21,300 cm^{-1}

correspond to the $^4T_{1g}$ (F) → $^4T_{1g}$ (P) transition. The fine structure of this transition may be caused by the Jahn-Teller effect or by a slight deviation of the Co(II) site from ideal octahedral symmetry. The band at 11,500 cm^{-1} can be attributed to the shifted $^4T_{1g}$ (F) → $^4T_{2g}$ (F) transition or to the shifted $^4T_{1g}$ (F) → $^4A_{2g}$ (F) transition.

The spectra of Co(II) complexes in various zeolites were studied by Klier et al. (8-13) and by Wichterlová et al. (15). The spectral features characteristic of the spectroscopic species α reported here were not previously observed in the Co(II)-containing A, X, and Y zeolites or for ethylene, CO, N_2O, H_2O, and NH_3 Co(II) complexes in these zeolites. The species α does not correspond to the complexes of Co(II) ions located in regular six rings with C_{3v} or T_d symmetry. Thus, this species could, in principle, correspond to (i) Co complexes with adsorbed H_2O, OH^-, or NH_3 that was incompletely removed, (ii) Co(II) ions affected by defects or intrazeolitic species, or (iii) Co(II) cations in bare sites other than regular six rings locations. The pros and cons regarding (i) - (iii) are discussed below.

Ad (i): The NIR spectra of Co-erionite dehydrated at 350°C indicate a complete absence of molecular water. The spectroscopic species α is accessible to weak ligands such as CO and ethylene. Water, the OH group, and ammonia are stronger ligands than these weak ligands (12) and CO or ethylene cannot replace them. Thus, species α does not correspond to a Co complex with adsorbed molecule. Moreover, the magnetic moment of Co(II) in erionite dehydrated at 350°C corresponds to a bare Co(II) cation with a planar or octahedral symmetry. Thus, species α and β do not represent Co(II) complexed with adsorbed molecules.

Ad (ii): The intensity of the bands corresponding to the species α decreases with increased dehydration temperature. The number of defects usually increases with increase of treatment temperature (34). Both defects and intrazeolitic species cannot be removed by dehydration at high temperature and mild hydration. However, the spectra of Co-erionite samples dehydrated at 350°C and at 525° C and then subsequently slightly hydrated and dehydrated at 350 °C are different. The spectrum of species γ appeared and the intensity of species α decreased as a result of this treatment. Moreover, the intensity of species α depended only on the Co loading and was not affected by the conditions of ion exchange (cobalt nitrate or cobalt acetate solutions used for ion exchange or pH of these solutions). This shows that spectra were not affected by extraframework species or defects created during the ion exchange. The XRD diffraction pattern of the parent zeolite did not indicate the presence of the extraframework species in the parent zeolite. Thus, species α and β do not represent Co(II) ions affected by intrazeolitic species or defects.

Ad (iii): Species α appeared at certain loadings (≤ 1 wt%) as single spectroscopic species and were accessible to weak ligands. The value of the magnetic moment of Co(II) in zeolite dehydrated at 350°C also corresponded to the value of magnetic moment of Co(II) ion. Since it is spectroscopically distinct from the planar γ sites, it is concluded that the species α, present in the spectrum of Co(II) erionite dehydrated at 350°C, are Co(II) ions in the bare sites with symmetry other than trigonal planar.

The CO and ethylene molecules are adsorbed on Co(II) ions located in the erionite matrix and the DR spectrum of Co(II) ions is affected by this adsorption. It was observed

that CO was adsorbed only on Co ions corresponding to the species α and not on Co ions corresponding to the species β (Figure 9). Thus, the Co(II) ions species α exhibit open coordination shell. The inaccessibility of Co cations corresponding to the species β is in agreement with closed coordination shell of Co ions surrounded by six oxygen atoms in a site with O_h symmetry.

Structural Aspects of Co(II) Ion Siting in Dehydrated Erionite. The sites available to cations in dehydrated erionite are schematically shown in Figure 15 with the notation used by Mortier (22). The location of these sites consist of the following:

Site A in the hexagonal prism,

Site B in the center of the ε-cage,

Site C in the center of the the regular six-ring in the plane of oxygen atoms,

Site E on the three-fold axis of the regular six-ring out of oxygen plane,

Site H in the deformed six-ring of ε-cage,

Site I boat-shaped site created by two four-rings in the wall of the main cavity,

Site J in the eight-ring of the main cavity.

Site D in the center of the eight-ring cannot be occupied by small cations such as Co(II) in dehydrated erionite.

Spectroscopic species γ is easily attributed to the Co cations located in site C. After adsorption of a guest molecule, the Co(II) ion is pulled out of the plane to site E with a C_{3v}, C_{2v}, or T_d symmetry. The number of the sites C or E is smaller than the number of the Co(II) ions in highly exchanged Co-erionite. The unit cell of the erionite framework of chemical

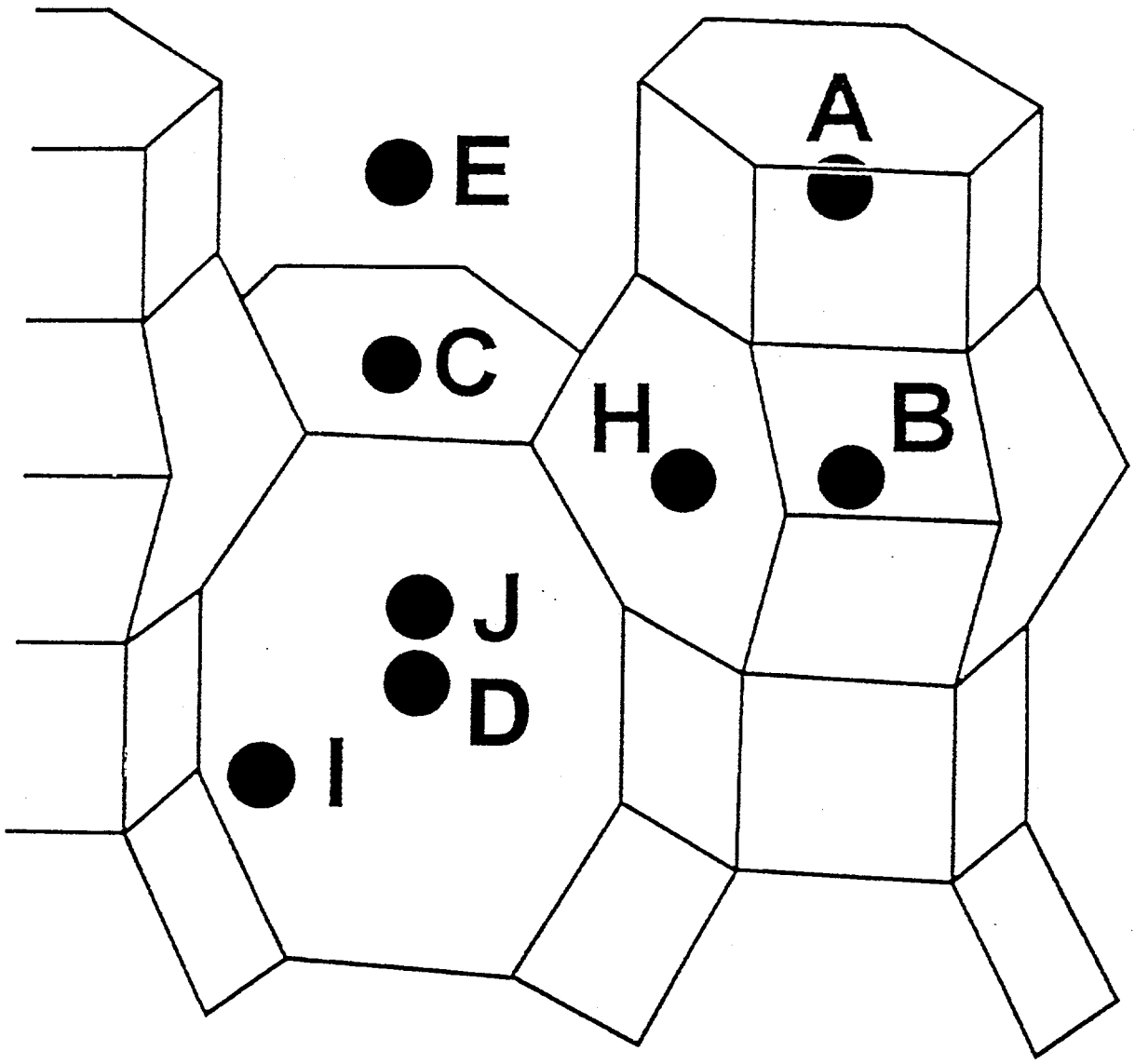

FIGURE 15. Notation of cation sites in erionite according to Ref. 22: A -- hexagonal prism, B -- center of ϵ-cage, C -- plane of regular six-ring, E -- three-fold axis of regular six-ring, H -- deformed six-ring center of ϵ-cage, I -- two four-rings in the wall of the main cavity, and J - eight-ring.

formula $[Al_xSi_{36-x}O_{72}]^{x-}$ contains two oxygen six-rings associated with site C, two ε-cages, one eight-ring, and one hexagonal prism. For Si/Al = 3.5 for this erionite, x = 8 and the unit cell accommodates up to 4 Co(II) cations at full exchange. Only two of the Co(II) ions can fill sites C, i.e. corresponding to 50 % of the ion exchange capacity. Thus, at Co loadings higher than 50% ion exchange, part of the Co(II) ions cannot be located in site C. This is in a good agreement with the observed presence of the species α and β in highly exchanged Co-erionite dehydrated at 525°C. It is concluded that absorption bands at 5,800 and 7,100-7,500, 14,700, 15,500, and 17,250 cm^{-1} and the doublet at 24,600 and 25,800 cm^{-1} of Co-erionite dehydrated at 525°C correspond to the species γ of Co(II) ions with D_{3h} symmetry located in the plane of regular six-ring.

The spectroscopic species β with the spectrum indicating O_h symmetry may be attributed to the sites A in hexagonal prism or B in the ε-cage for the following reasons. First, the erionite sample exchanged with ammonium ion contained residual Na^+, which is likely to be located in sites A or B (21,25,35,36) and whose concentration began to decrease significantly at high Co loading levels. Second, once the Co(II) cations enter sites A or B in the closed cages, they are difficult to back-exchange with excess Na (see Figure 6), showing both kinetic and thermodynamic preference of these sites for Co(II). Both sites A and B can be represented by six neighboring oxygen atoms creating two staggered trigonal bases and arranged in approximately octahedral symmetry. Site A exhibits symmetry only slightly different from that of the site B. The angle between the three-fold symmetry axis and a line between the Co ion and oxygen is 49° in the case of the ε-cage and 51° in the case

of the hexagonal prism, and the oxygen-atom triangles are identical. The Co-O distances are 0.298 nm in the ε-cage and 0.291 nm in the hexagonal prism (the geometric parameters of sites were calculated from XRD data (37)). Thus, optical properties of the Co(II) ions in these sites are expected to be very similar. The only factor discriminating between sites A or B is the fact that in dehydrated erionite, site A is unoccupied by metal cations and only site B is occupied by Ca ions in dehydrated KCa-erionite (21). The ionic radii of Ca(II) (0.09 nm, (25)) and Co(II) (0.069 nm, (29)) are close, thus indicating that site B is more likely to be occupied by the Co ions. It is concluded that species β represented by the doublet at 19,250 and 20,600 cm^{-1} and by the band centered at 8,000-8,500 cm^{-1} corresponds to Co(II) ions with O_h symmetry in the center of ε-cages (site B).

The spectroscopic species α of the Co(II) ions accessible to guest molecules and with symmetry different from D_{3h} and O_h could correspond to Co(II) cations located in sites H, I, or J. The assignment of species α to Co(II) cations in the eight-rings connecting the main cavities (site J), analogous to Ca siting in sites B or D of dehydrated Ca-mordenite (17), is ruled out for the following reasons. The species α are most populated in Co-erionite dehydrated at 350 °C. In the case of highly loaded zeolites, *ca.* 7 wt% of Co(II), i.e. 70 % of Co cations exchangeable to erionite corresponds to this species. There is only one eight-ring (site J) per unit cell, which can accommodate only Co(II) ion, i.e. 25% of full ion exchange. However, 70% of maximum theoretical exchange gave rise to the spectroscopic species α, far in excess of the available J-sites, Therefore, the Co ions must occupy some other sites, of which the so far unassigned ones are sites H or I. The exclusion of the J sites

is also corroborated by the low occupancies of sites with similar geometry in Co chabasite (38) and in Ca-erionite with high Ca loading (17).

The distinction between sites H or I is difficult to make because both have an open coordination for the Co(II) ions and their geometries are quite complex, especially in view of the lack of knowledge of the Co ion elevation above the plane of the nearest oxygens. Tentatively, it is proposed that site H is favored because (i) it is closer to planar hexagonal and would favor high orbital contributions to the Co magnetic moment, in agreement with the measured 5.2 BM (Table 2) and (ii) site I of erionite is similar to the site E in mordenite, where the Co ions exhibit a strong absorption band at 14,800 cm^{-1}, as observed in other studies carried out here, and which is absent in the spectrum of Co(II) species **α**.

Conclusions

Base on the present optical study, the measured magnetic moments, the knowledge of the framework structure of erionite, and reference spectra in earlier investigations of other Co-zeolites, the Co(II) cations in Co(II)NH_4-erionite are proposed to occupy three types of cation sites consisting of:

- Species **α** in the deformed six-ring of the ε-cage (site H). The Co(II) ion is coordinated to oxygen atoms of this ring approximately in the oxygen plane. The symmetry of this site is C_{1h}. For Co(II) in this site, a triplet observed in the VIS spectrum at 16,050, 17,080, and 18,040 cm^{-1} is characteristic.
- Species **γ** in the regular six-ring (site C). The Co(II) cation is coordinated to 6 oxygen atoms of this six-ring and is located approximately in the oxygen plane. Symmetry

of this site is close to D_{3h}. A doublet centered at 25,000 cm^{-1} (24,600 and 25,800 cm^{-1}) is characteristic of Co(II) in this site. This site is similar to the Co(II) site in dehydrated A zeolite.

- Species β in the ε-cage (site B). The Co(II) ion is coordinated to 6 oxygen atoms with approximately octahedral symmetry. Co(II) in this site exhibits weak absorption bands at 19,250 and 20,600 cm^{-1}.

After dehydration at 350°C, the Co(II) species α are located in the deformed six-rings (site H). During dehydration at 525°C, the Co(II) cations migrate to the regular six-rings (site C) -- species γ, but the number of these sites is limited to a maximum concentration of Co ions of *ca* 5 wt%, or 50% of the total ion exchange capacity. Thus, some of the Co(II) ions are forced into sites H.

The Co(II) species β located in the sites B in the ε-cage exhibits a highly coordinated geometry and are not accessible to guests molecules. The Co(II) ions centered in sites C (species γ) and H (species α) in the regular and deformed six rings exhibit open coordination shells. Moreover, both types of the six-rings form walls of the erionite cavity. Thus, all molecules that can enter the internal erionite structure can be adsorbed by the Co(II) ions in these sites and make complexes with Co(II) ions. Complexes of Co(II) with CO and ethylene formed by the Co(II) ions in sites of different types of six-rings exhibit different electronic properties. Thus, the Co(II) ions in regular and in deformed six-rings create two different possible catalytic centers.

• **Optical Study of Co(II) in Dehydrated ZSM-5 Zeolite**

Ever since Iwamoto et al. (39,40) found that Cu-exchanged ZSM-5 zeolites exhibited higher catalytic activity for NO decomposition than any zeolite catalysts studied previously, NO abatement studies with zeolites have tended to be centered on this Cu(II) ion exchanged zeolite. Commercial NO abatement catalytic processes utilize ammonia as the reductant, but there is much interest in replacement of ammonia by a more benigh reductant such as a hydrocarbon. It was observed that the Cu-ZSM-5 catalyst that was active for NO decomposition under model conditions and for NO reduction by methane in the absence of oxygen (1) did not effectively reduce NO with methane in the presence of excess oxygen (2), as would exist under industrial conditions. In contrast, Co-ZSM-5 zeolites, as well as Co-ferrierites, were found to be surprisingly good for NO reduction by methane in the presence of excess oxygen (1,3). Thus, Co-ZSM-5 catalysts have been prepared and investigated here by optical spectroscopy todetermine the locations of the cations and possibly improve the activity and stability of the catalysts.

Experimental Methods

Preparation of Co-ZSM-5 Zeolites. A series of $Co(NH_4)$-ZSM-5 samples with a wide range of Co contents (0.25-2.6 wt%) was prepared under acidic conditions by ion exchange. Samples were prepared from NH_4-ZSM-5 (Si/Al = 10) prepared at Air Products and Chemicals, Inc. by exchange from aqueous $Co(NO_3)_2$ solutions with molarities of 0.01 or 0.02 at room temperature. The detailed conditions of the preparations are described in Table 7. The acid pH = 4.5 of the exchange solution was obtained by addition of 0.02 M

HNO_3 to the mixture of 5 g zeolite with a corresponding amount of Co(II) solution. The pH = 4.5 represents the natural pH of a mixture of 1 g of zeolite with 8.5 ml 0.01 M solution of $Co(NO_3)_2$. Samples 40, 44, and 45 were prepared by double or triple exchange treatments, and values in Table 7 represent the condition of each step of the preparation. At the end of each step of exchange, the zeolite mixture was filtered and new cobalt nitrate solution was added. All samples were filtered, washed with 1000 ml of distilled water, and dried at 110°C.

The Co(II) concentration in each zeolite was estimated *via* diffuse reflectance spectroscopy (DRS). The integrated intensity of the VIS absorption band of fully hydrated Co-ZSM-5 was compared with a calibration curve using previously prepared and well-characterized Co(II) zeolites (Co-ZSM-5: Si/Al = 10, Co 4.4 wt%; Co-ZSM-5: Si/Al = 22.5, Co 0.75 wt%; Co-erionite: Si/Al = 3.5, Co 3.2 wt%) that were obtained from the laboratory of Dr. B. Wichterlova of the Institute of Physical Chemistry in Prague, Czech Republic. This method of estimating the Co(II) content in prepared samples was used due to the small amount of zeolites prepared. Additional Co-ZSM-5 samples were prepared by ion exchange but some of the experimental conditions, e.g. pH, were not as closely monitored as those listed in Table 7. The additional samples are listed in Table 8.

DRS Spectroscopy. Procedures used for the optical measurements at room temperature were described in the previous section of this report. Spectra were evaluated by the Schuster-Kubelka-Munk theory; $F(R_\infty) = (1-R_\infty)^2/(2R_\infty)$. Samples were dehydrated at 350°C as described earlier. Co-erionite, Co-ZSM-5/45, and $Co(NH_4)$-ZSM-5/28 zeolites, where /xx indicates the sample number given in Table 7 or Table 8, were dehydrated at

TABLE 7. Conditions used to prepare Co(II)-ZSM-5 zeolites from (NH_4)-ZSM-5 (with Si/Al = 10) and the resultant Co(II) content of the zeolites achieved by ion exchange under acidic conditions.

Sample Number	Co(II) Content in Zeolite (wt%)	Conditions of Preparation			
		Vol. of exchange solution/g of zeolite	Time of exchange (h)	Initial pH	Co(II) exchange solution (M)
35	1.69	135	2	4.50	0.01
36	0.3	8.5	2	4.51	0.01
37	0.8	25.5	2	4.22	0.01
38	1.7	76.5	2	4.50	0.01
39	2.3	272 272	3 3	4.15 4.42	0.01 0.01
40	2.4	400 400 400	2 3 3	4.50 4.50 4.52	0.01 0.01 0.01
41	0.24	3.6	2	4.33	0.01
42	1.24	36	3	4.40	0.01
43	1.8	16	2	4.47	0.01
44	1.6	76 26	2 2	4.54 4.55	0.01 0.01
45	2.6	76 800 800	2 12 12	4.49 4.52 4.52	0.01 0.02 0.02

TABLE 8. Co-ZSM-5 zeolites prepared at different conditions.

Sample Number	Zeolite	Co Concentration (wt%)	Si/Al Ratio
28	$Co(NH_4)$-ZSM-5	4.4	10
29	$Co(NH_4)$-ZSM-5	4.0	10
30	$Co(NH_4)$-ZSM-5	2.0	10
31	CoNa-ZSM-5	4.0	10
32	$Co(NH_4)$-ZSM-5	0.5	10
33	CoNa-ZSM-5	0.6	10
34	CoNa-ZSM-5	0.6	22.5

temperatures ranging from 400 to 550°C. In these cases, the zeolite was first dehydrated at 350°C, and after this it was dehydrated at higher temperature for 1 to 12 h.

An additional experiment was carried out in which $Co(NH_4)$-ZSM-5/29 was dehydrated for 1 h in a stream of helium at 515°C. The zeolite was first evacuated at room temperature for 30 min, and then under evacuation it was heated at a rate of 5°C/min to 515°C. This treatment corresponds to the procedure of sample calcination before testing catalytic activity.

The UV-VIS spectrum of $Co(NH_4)$-ZSM-5/29 was recorded at low temperature. A quartz cuvette with evacuated double front window and with a through-flow jacket cooled by a flow of liquid nitrogen was used for this measurement. A flow of dry gaseous nitrogen, 20 ℓ/min was maintained through the analysis chamber of the spectrometer in which the temperature of the sample cell was 85K.

Adsorption and Desorption of CO, H_2O, and C_2H_4. Adsorption and desorption of CO and H_2O with $Co(NH_4)$-ZSM-5 samples were studied in detail *via* UV-VIS-NIR DRS spectroscopy. After the zeolite was dehydrated at 350 or 550°C, the amount of gas adsorbed by *ca.* 0.8 g of dry sample was regulated by adsorption of gas at pressures of 0.5-700 (NO, CO) or 0.5-22 Torr from 40, 180, and 1400 ml volumes at atmospheric pressure. Carbon monoxide (99.0+%, Aldrich Chemical Company, Inc.) was purified by freezing liquid nitrogen and then thawing. After adsorption at room temperature, desorption of gas was studied at temperatures ranging from room temperature to 440°C. Samples were evacuated from 30 min to 3 h.

Results

Concentration Dependence of UV-VIS DR Spectra of Co-ZSM-5 Dehydrated at 350°C. Spectra of Co-ZSM-5 samples with Co contents from 0.24 to 2.4 wt% exhibits two maxima in the 12,000-30,000 cm^{-1} spectral region. The first maximum (A) was at about 17,000 and the second maximum (B) was located at approximately 20,000 cm^{-1} (Figures 16 and 17). Upon normalization of the spectra, little difference connected with concentration changes was observed (Figure 18). The dependence of the area of the VIS absorption band of the dehydrated samples as a function of Co(II) concentration is given in Figure 19. This dependence is nonlinear and indicates the presence of at least one more spectroscopic species in the spectra of the more highly exchanged samples of $Co(NH_4)$-ZSM-5. The existence of more components in the spectra is also confirmed by the linear decrease of the position of band B located at ≈20,000 cm^{-1} with increasing Co(II) concentration (Figure 20).

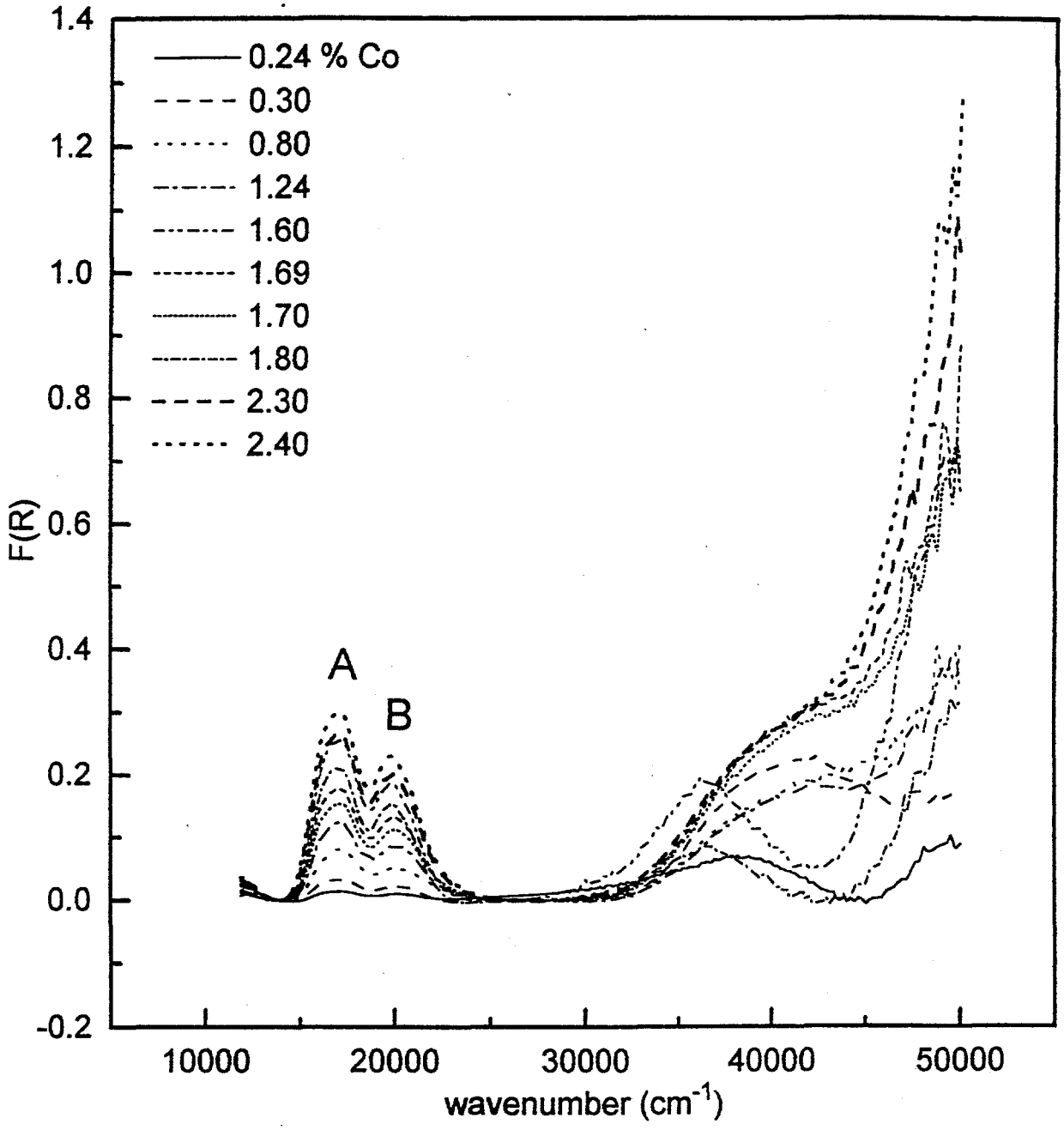

FIGURE 16. The UV-VIS reflectance spectra of Co-ZSM-5 zeolites with different contents of Co(II). The spectra were obtained after dehydration of the samples at 350°C. The spectrum of the parent zeolite was substracted.

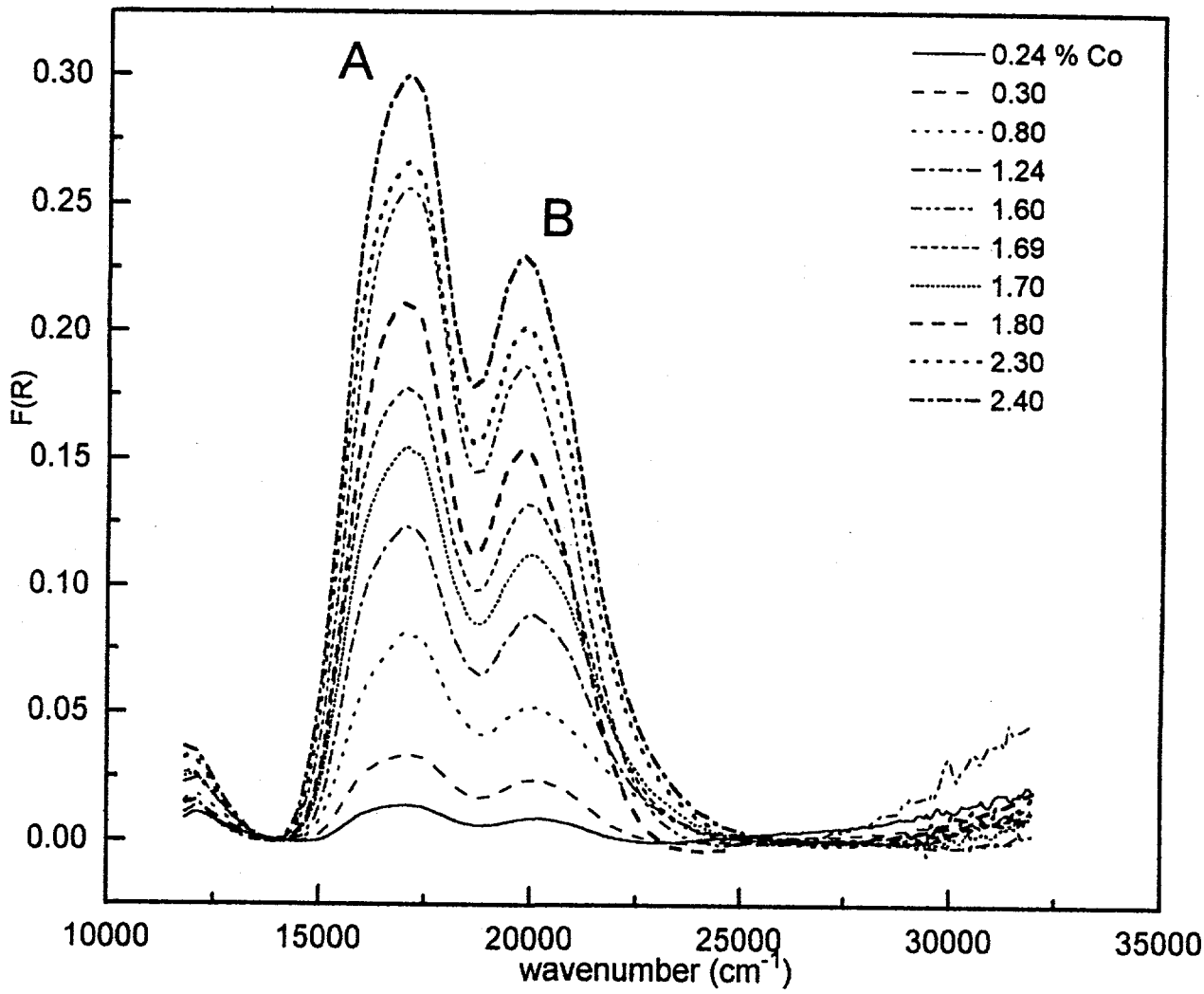

FIGURE 17. The UV-VIS reflectance spectra obtained in the range of 13,000-34,000 cm^{-1} for Co-ZSM-5 zeolites with different contents of Co(II). The spectra were obtained after dehydration of the samples at 350°C. The spectrum of the parent zeolite was substracted.

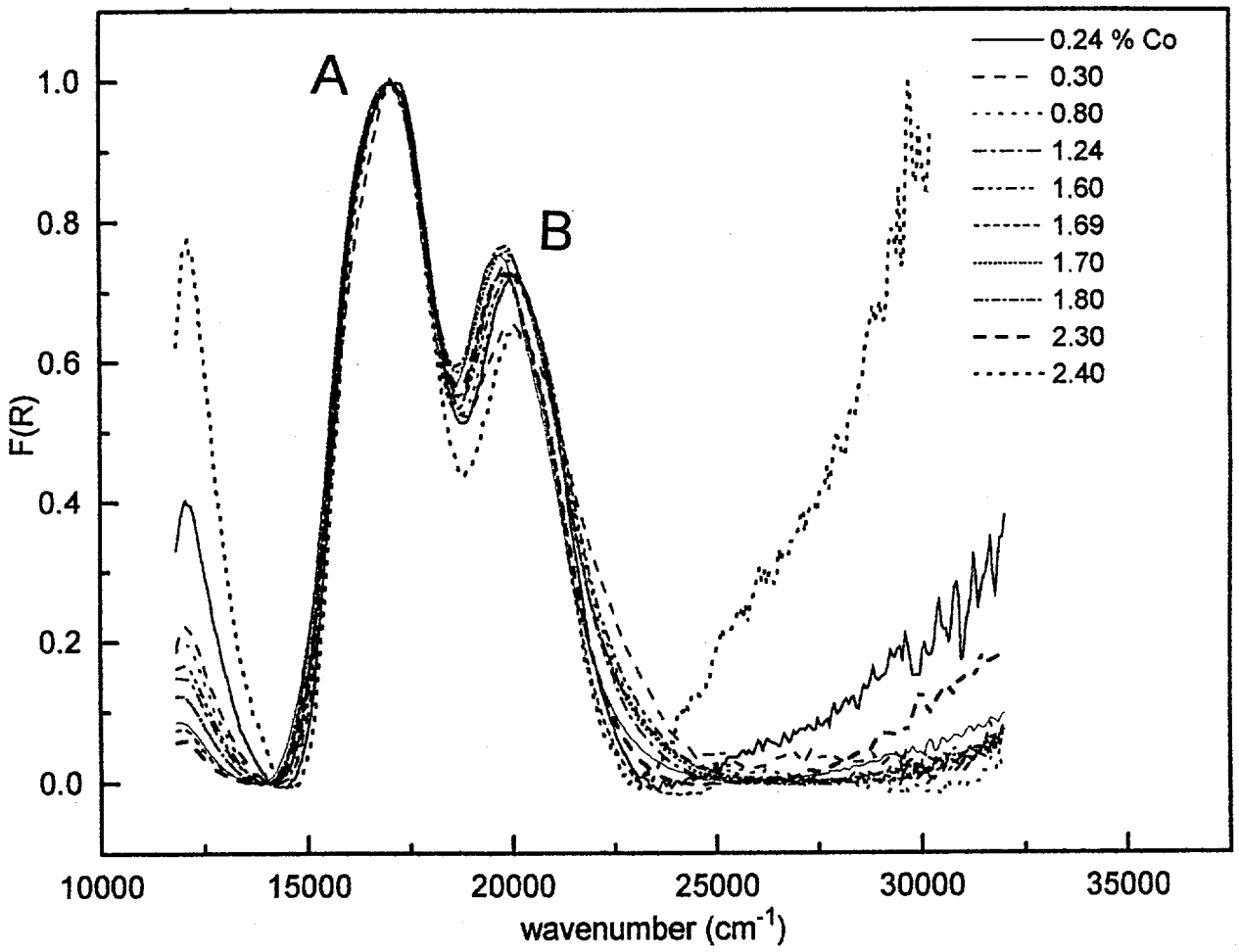

FIGURE 18. The normalized UV-VIS reflectance spectra obtained in the range of 13,000-34,000 cm^{-1} for Co-ZSM-5 zeolites with different contents of Co(II). The spectra were obtained after dehydration of the samples at 350°C. The spectrum of the parent zeolite was substracted.

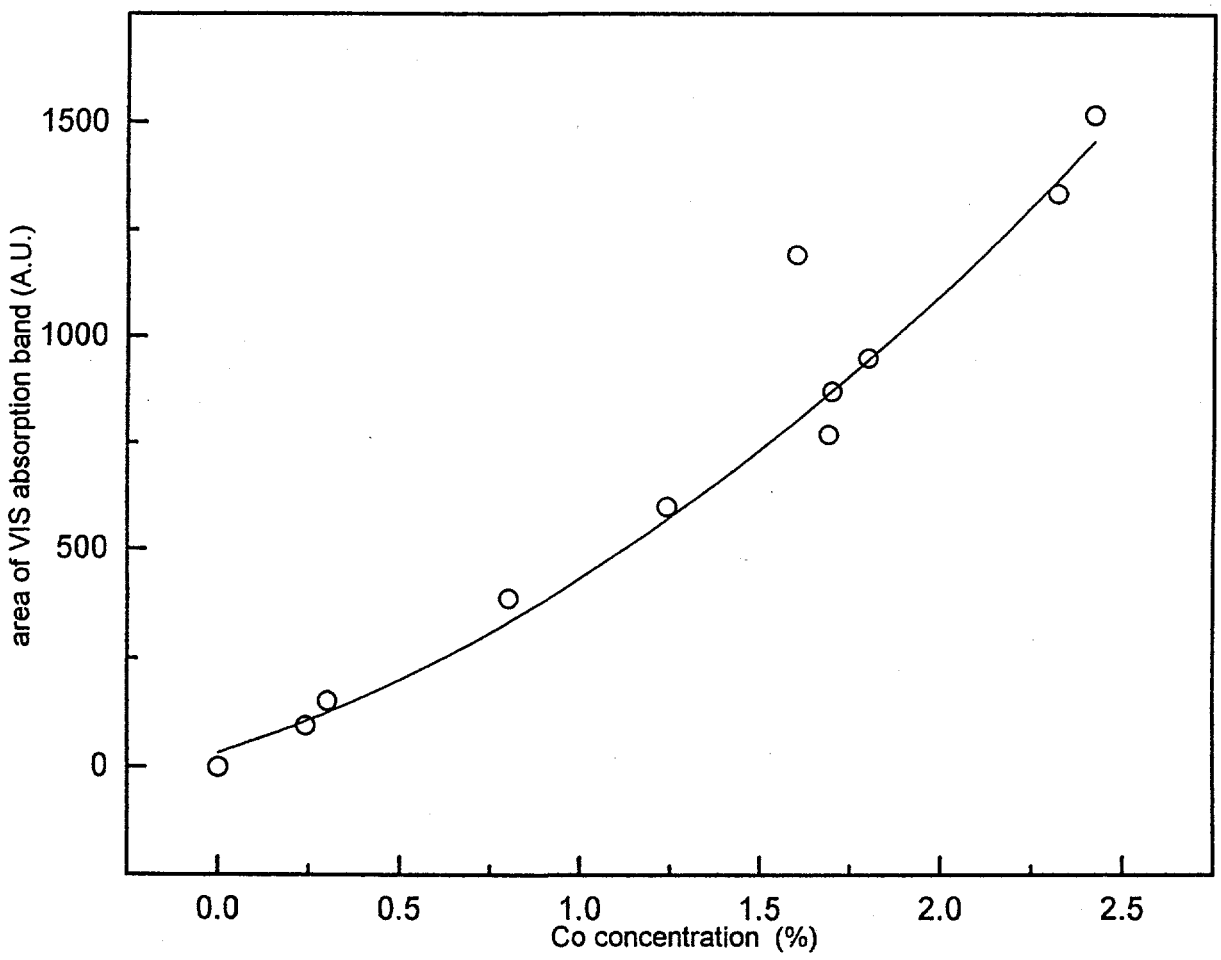

FIGURE 19. The spectral intensity of the VIS absorption band in the reflectance spectra of Co-ZSM-5 zeolites with different contents of Co(II) as a function of the Co(II) concentration. The spectra were obtained after dehydration of the samples at 350°C. The spectrum of the parent zeolite was substracted.

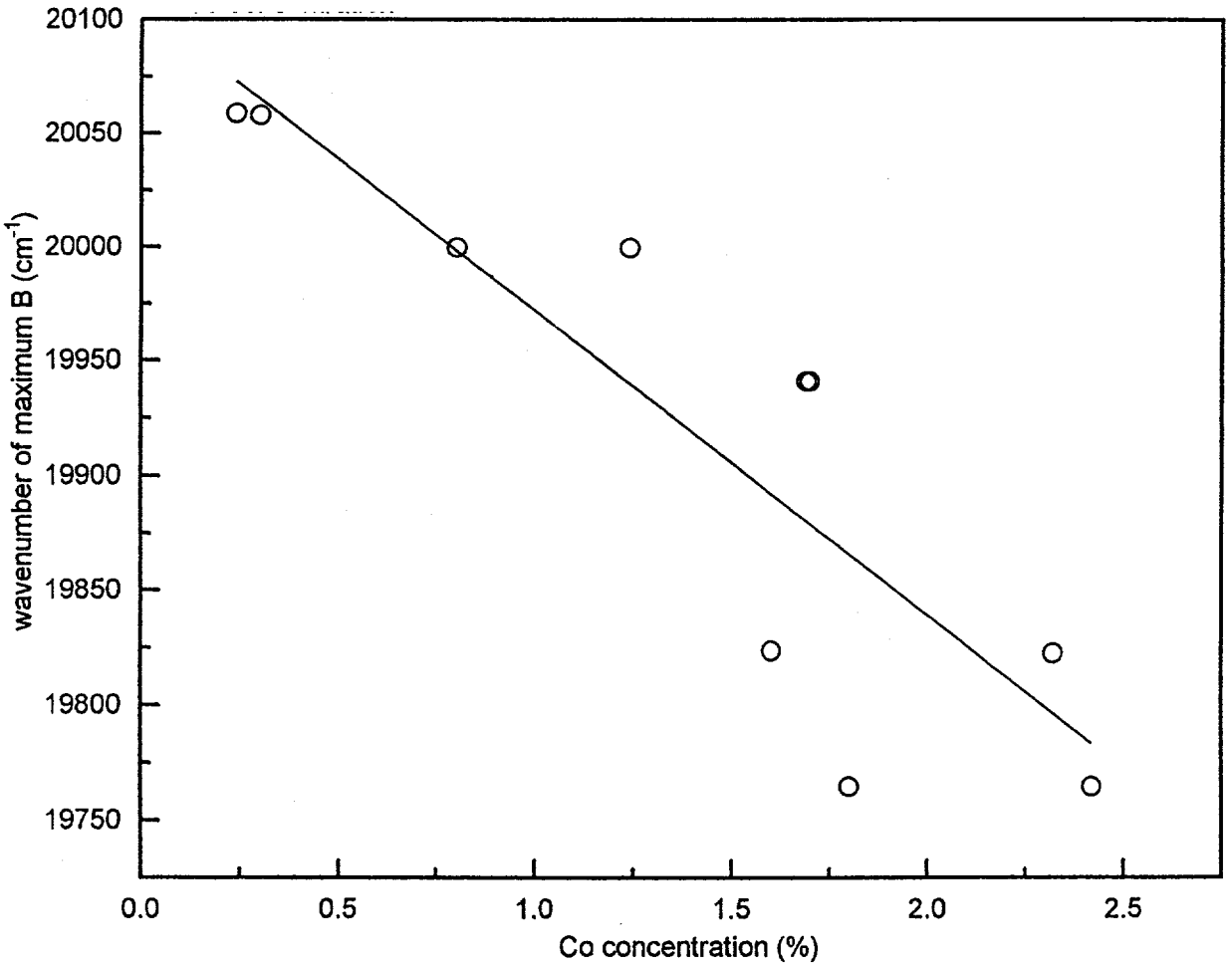

FIGURE 20. The dependence of the position of Band B located at ≈20,000 cm^{-1} on the Co(II) concentration in Co-ZSM-5 zeolites. The spectra were obtained after dehydration of the samples at 350°C. The spectrum of the parent zeolite was substracted.

The dependence of the ratio of maximum intensity of the 20,000 cm^{-1} spectral band (B) to the maximum intensity of the 17,000 cm^{-1} spectral band (A) on the Co(II) concentration in the Co-ZSM-5 zeolites is shown in Figure 21. This concentration dependence exhibiting a linear increase with increasing concentration is characteristic for two different sites, one of which is occupied preferentially at low concentration, but its occupation is saturated at high concentration. It can be concluded that Co(II)-ZSM-5 zeolites prepared from (NH_4)-ZSM-5 contain Co(II) ions in a minimum of two different sites.

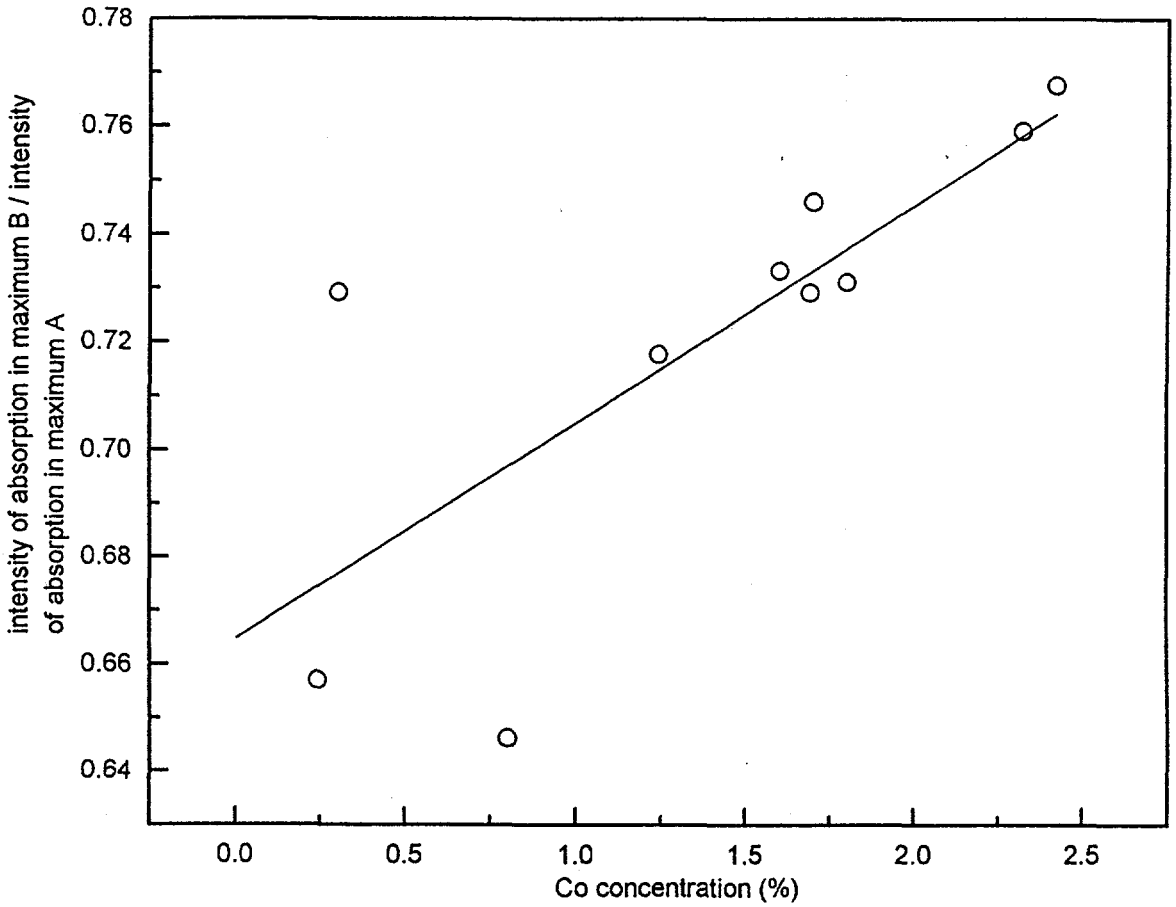

FIGURE 21. The dependence of the ratio of the intensity of Band B located at ≈20,000 cm^{-1} to the intensity of Band A located at ≈17,000 cm^{-1} on the Co(II) cation concentration in Co-ZSM-5 zeolites. The spectra were obtained after dehydration of the samples at 350°C. The spectrum of the parent zeolite was substracted.

Detailed Analysis of the VIS Spectrum of $Co(NH_4)$-ZSM-5. In the VIS spectra of $Co(NH_4)$-ZSM-5 zeolites, two main optical bands were present as described above, but the irregularities in features of these spectra indicate the presence of a number of overlapping bands. To distinguish these individual bands and to approximately determine the location of the maxima of these bands in wavenumbers, the second derivative mode of these spectra was determined. The validity of this method was confirmed by comparison of second derivative mode of fully hydrated Co-ZSM-5 containing 1.69 wt% Co(II) (Figure 22). All bands corresponding to transitions of complexes of octahedral cobalt(II) observed in the VIS spectral region at room temperature (33) were found and no extraneous spectral band was observed here.

Second derivatives plots of the VIS band of $Co(NH_4)$-ZSM-5 zeolites dehydrated to 350°C are shown in Figure 23. It is possible to identify derivative absorption bands with minima around 15,900, 17,000, 17,400, 17,800, 18,350, 19,500, 20,000, and 21,000 cm^{-1}. The presence of this large number of individual spectral features in the spectra of Co-ZSM-5 zeolites was confirmed by recording the spectrum of Co-ZSM-5/38 (1.7 wt% Co(II)) at a temperature of 85K after dehydrating the sample at 350°C. This DRS spectrum is shown in Figure 24, and its second derivative mode with data points and a smoothed curve is shown in Figure 25. Eight bands with minima corresponding approximately to the minima recorded at room temperature (Figure 23) are observed in this spectrum. Moreover, three additional bands are evidenced using this second derivative mode. Bands with minima near 15,500, 16,500, and ≈22,280 cm^{-1} are much more evident in the low temperature spectrum than in the spectra recorded at room temperature. It is evident that this large number of apparent

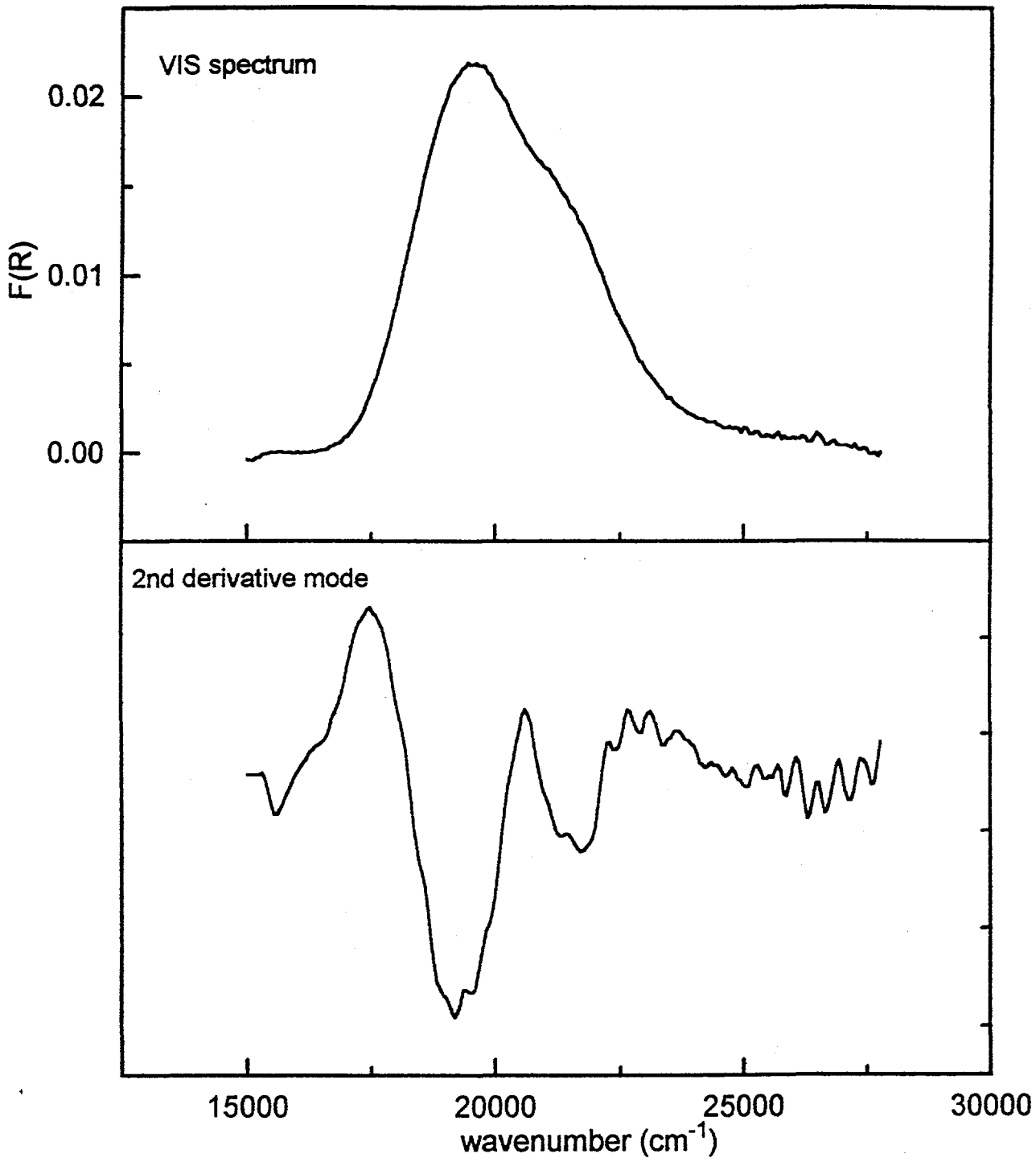

FIGURE 22. The VIS diffuse reflectance spectrum and second derivative mode analysis curve for fully hydrated Co(II)-ZSM-5/35.

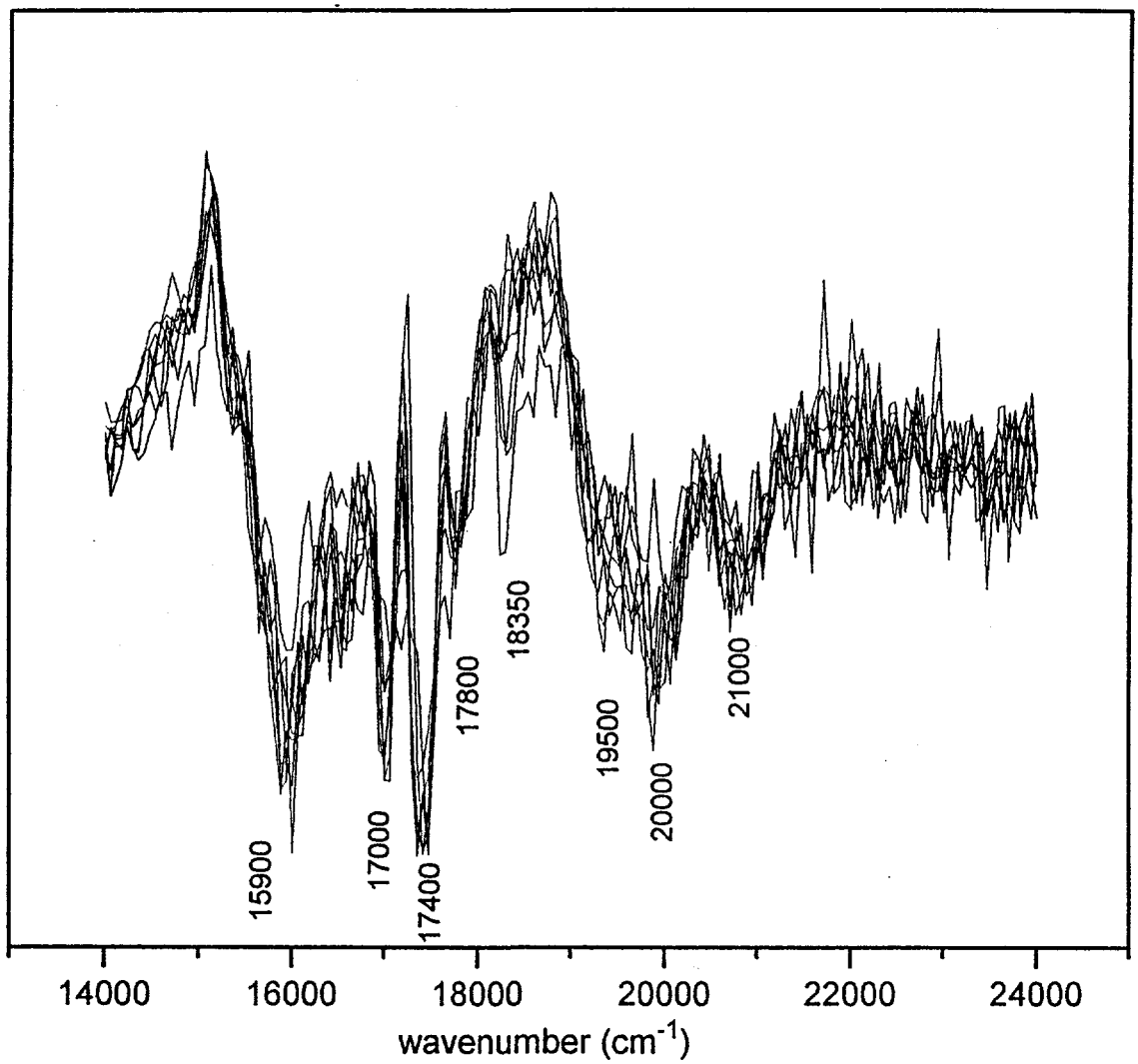

FIGURE 23. The second derivative mode of the VIS diffuse reflectance spectrum of Co(II)-ZSM-5 zeolites with different contents of Co(II), obtained after dehydration at 350°C.

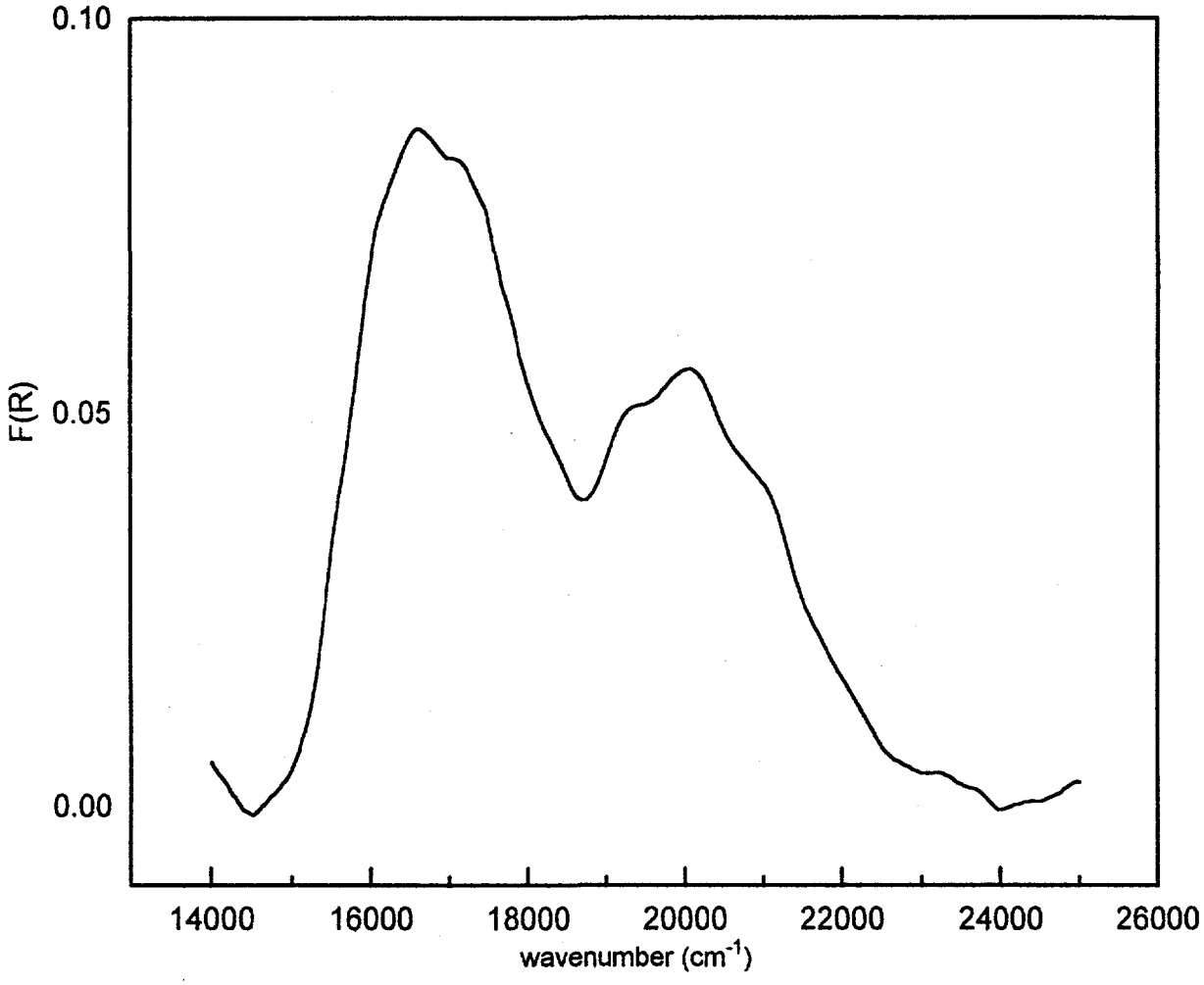

FIGURE 24. The VIS diffuse reflectance spectrum of Co(II)-ZSM-5/38 zeolite recorded at 85K, obtained after dehydration of the zeolite at 350°C.

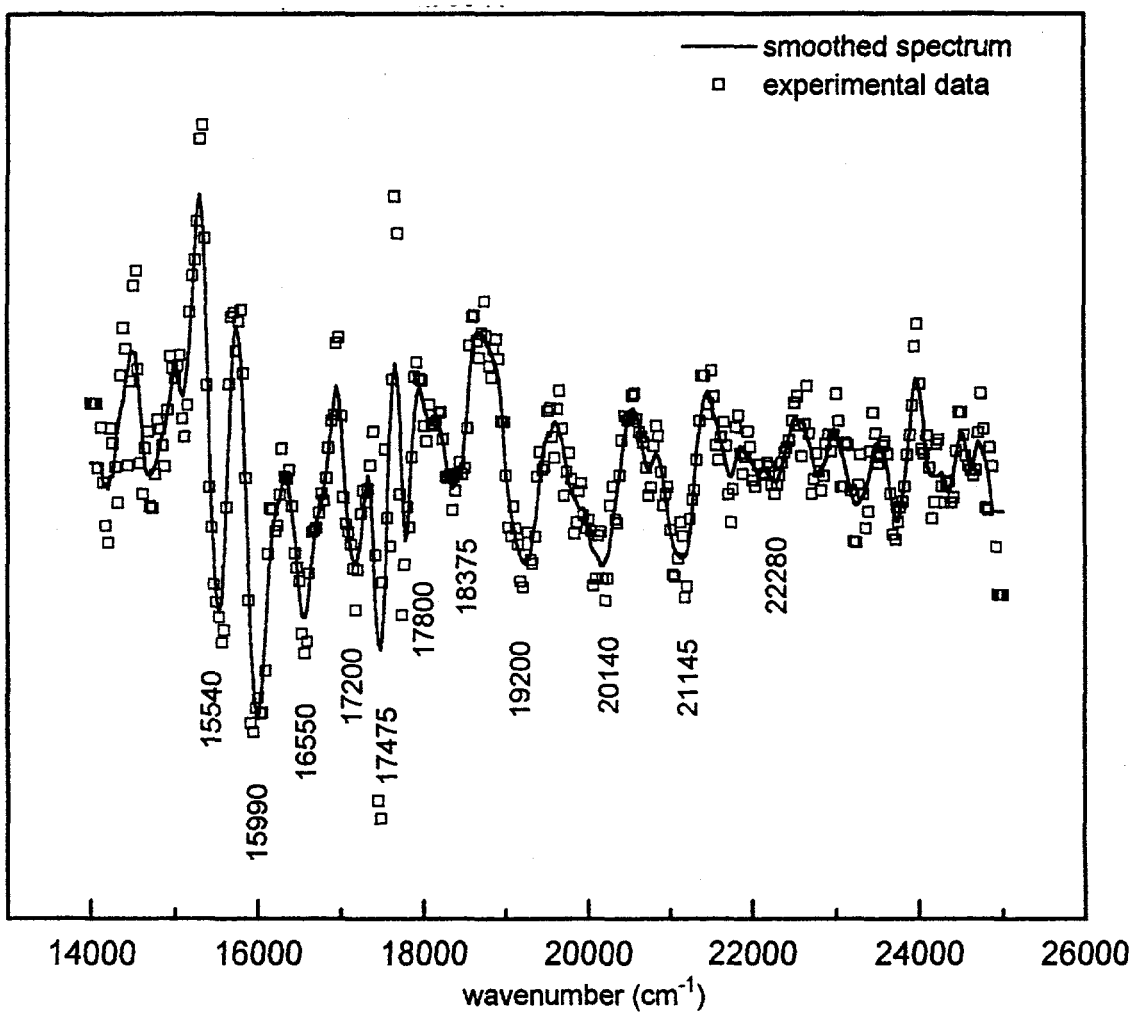

FIGURE 25. The second derivative mode of the VIS diffuse reflectance spectrum of Co(II)-ZSM-5/38 zeolite recorded at 85K, obtained after dehydration of the zeolite at 350°C.

spectral features cannot be attributed to only Co(II) ions located in different lattice sites in the ZSM-5 zeolite without further experiments. Although the VIS spectrum of $Co(NH_4)$-ZSM-5 zeolite dehydrated at 350°C is composed from many overlapping bands (at approximately 15,500, 15,900, 16,500, 17,000, 17,400, 17,800, 18,350, 19,500, 20,000, 21,000, and 22,300 cm^{-1}) these bands probably correspond to Co(II) ions in only two or three different environments.

Adsorption of CO and H_2O. Adsorption studies were carried out using CO at pressures of 20, 100 (180 ml) and 600 Torr (1400 ml) over Co-ZSM-5/45 dehydrated at 350°C. There was no significant effect on the Co(II) spectrum caused by exposure of the sample to a CO environment, as is shown in Figure 26. This result agrees with the observation that the only decrease of pressure of CO corresponded to expansion of CO to the volume of the spectroscopic cell.

In contrast, adsorption of water affected the Co(II) spectrum in the zeolite dehydrated at 350°C, as shown in Figures 27 and 28. The effect was observed for adsorption of a small amount of water (22 Torr, 180 ml), as well as in the presence of a large excess of water. Upon water adsorption, the intensity of the Co(II) absorption bands decreased, and there were also observable changes in the spectrum shape. The decrease in intensity of absorption in the VIS region and the absence of a symmetric triplet centered around 17,000 cm^{-1} indicate that a tetrahedral cobalt(II) complex was not present in the partially hydrated Co-ZSM-5 zeolite. This is in agreement with observations of sample dehydration when the high intensity blue band (typical for tetrahedral coordinated cobalt) was not observed in any stage of sample dehydration.

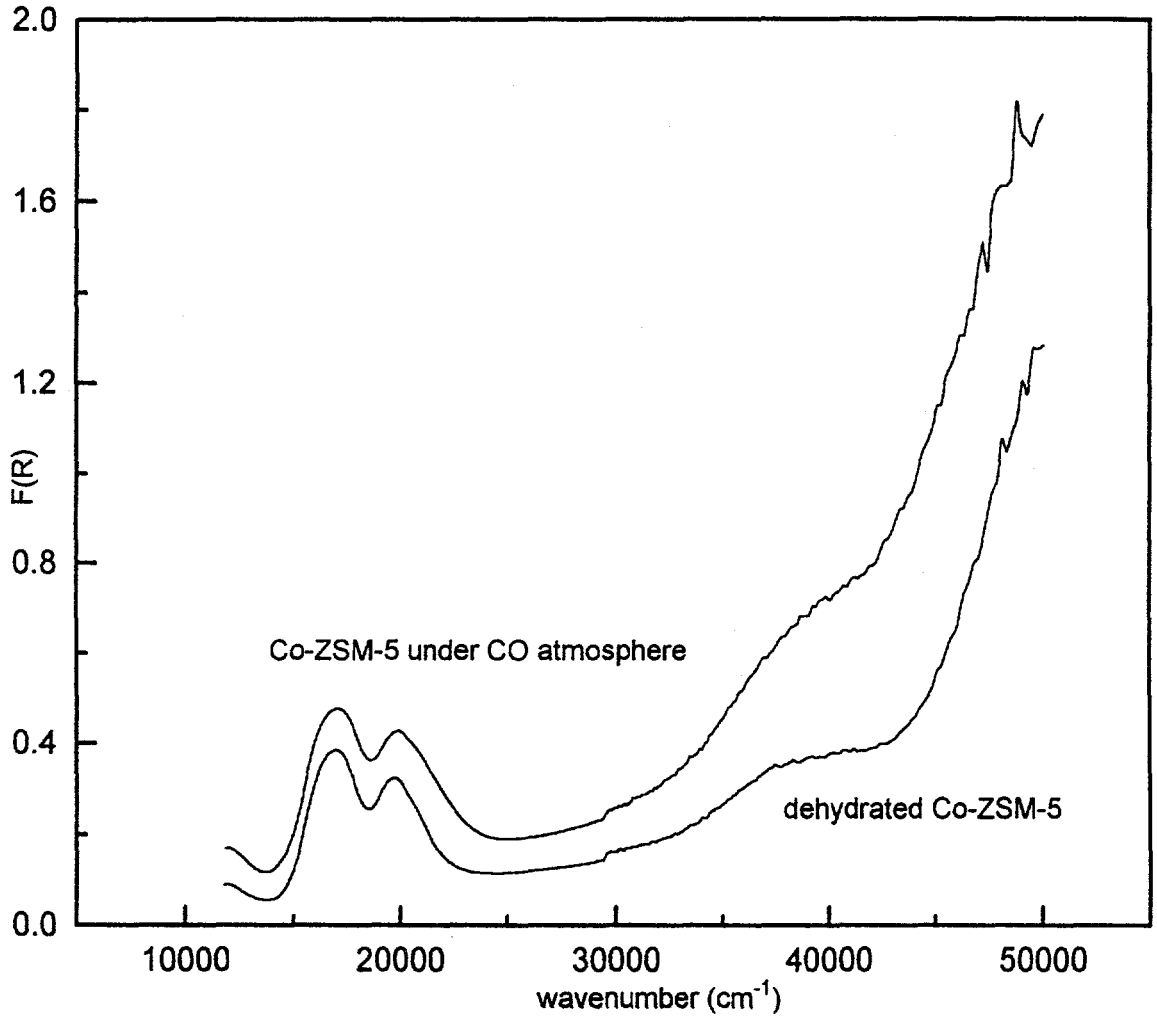

FIGURE 26. Comparison of the UV-VIS diffuse reflectance spectrum of the Co-ZSM-5/38 sample dehydrated at 350°C before and after exposure to CO.

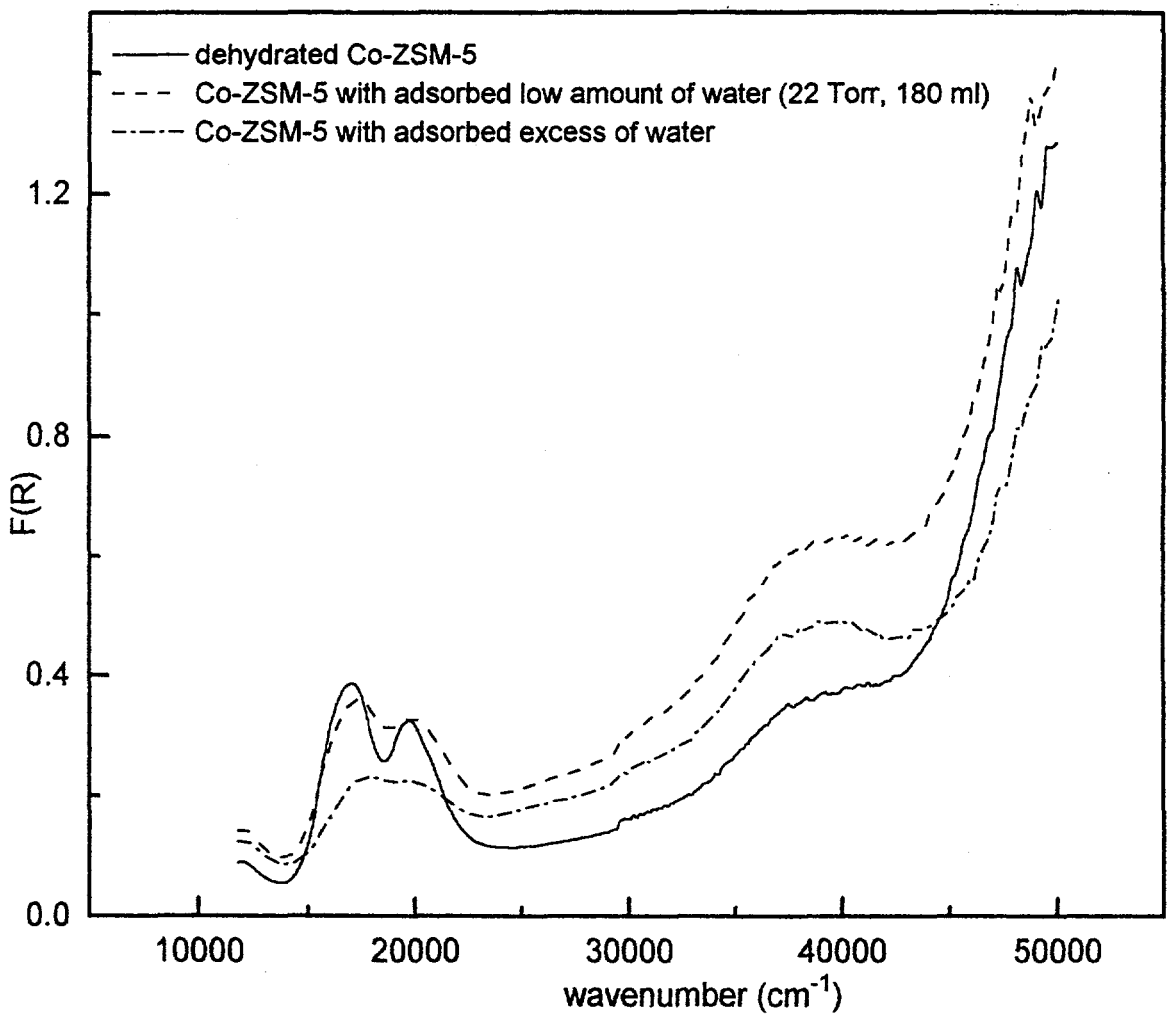

FIGURE 27. Effect of water adsorption on the UV-VIS diffuse reflectance spectrum of the Co-ZSM-5/38 sample that was dehydrated at 350°C. The spectrum of the parent zeolite dehydrated under the same conditions was subtracted from these spectra.

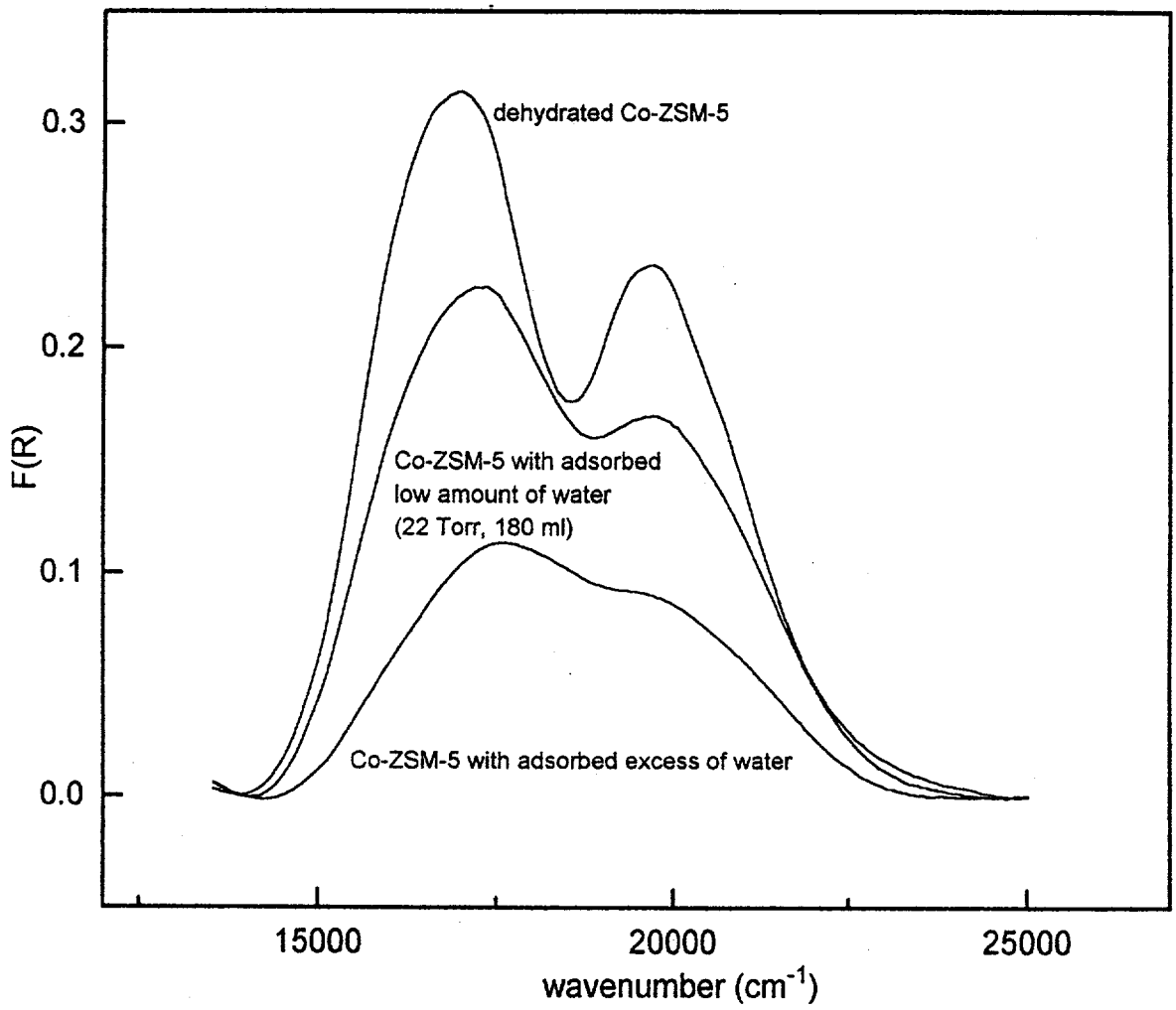

FIGURE 28. Normalized spectra in the 12,000-25,000 cm^{-1} spectral range showing the effect of water adsorption on the UV-VIS diffuse reflectance spectrum of the Co-ZSM-5/38 sample that was dehydrated at 350°C. The spectrum of the parent zeolite dehydrated under the same conditions was subtracted from these spectra.

Adsorption of water, along with the absence of adsorption of CO, on the Co(II) ions indicate that most of the Co(II) ions are located in environments accessible only to strong ligands (i.e. H_2O), but not to weak ligands such as CO. The absence of CO adsorption might be due to Co(II) ions being in inaccessible sites or by blocking of the Co(II) ion by a stronger guest molecule (possibly an OH group).

VIS Spectrum of Dehydrated Co-ZSM-5 at Higher Temperatures. Samples of Co-ZSM-5/30 and Co-ZSM-5/45 were dehydrated for 4 h at 510°C and 12 h at 525°C. Compared with the Co-ZSM-5 zeolites dehydrated at 350°C, the high temperature dehydration induced dramatic changes in the Co(II) spectrum, as is shown in Figures 29 and 30 for Co-ZSM-5/45. Absorption bands characteristic for the low temperature dehydrated Co-ZSM-5 disappeared and new bands with low intensity appeared, consisting of a complex band centered at 17,500 cm^{-1} (composed from bands at 16,000, 17,000 and 19,000-20,000 cm^{-1}), a single weak band at 22,200 cm^{-1}, and a multiple band centered at 24,800 cm^{-1}. The differences in appearance of the two spectra shown in Figure 29 indicate that the spectrum of Co-ZSM-5 dehydrated at 525°C represents Co(II) in more sites. A distinct band at 22,500 cm^{-1} was not observed in these cobalt-containing zeolites. The band at ≈25,000 cm^{-1} might be a doublet that would be similar to the doublet observed for dehydrated Co-A zeolite. This doublet was identified as $^4E'' \rightarrow {}^4E''$ transitions of the Co(II) ion in an environment with D_{3h} symmetry, which arises when the Co(II) cation is localized in the trigonal oxygen plane of the regular six-ring window of A-zeolite (8). There is no evidence for the presence of regular six-ring windows in the ZSM-5 framework. Explanation of this spectrum requires further experiments and computations of term diagrams of cobalt(II) ions in crystal fields

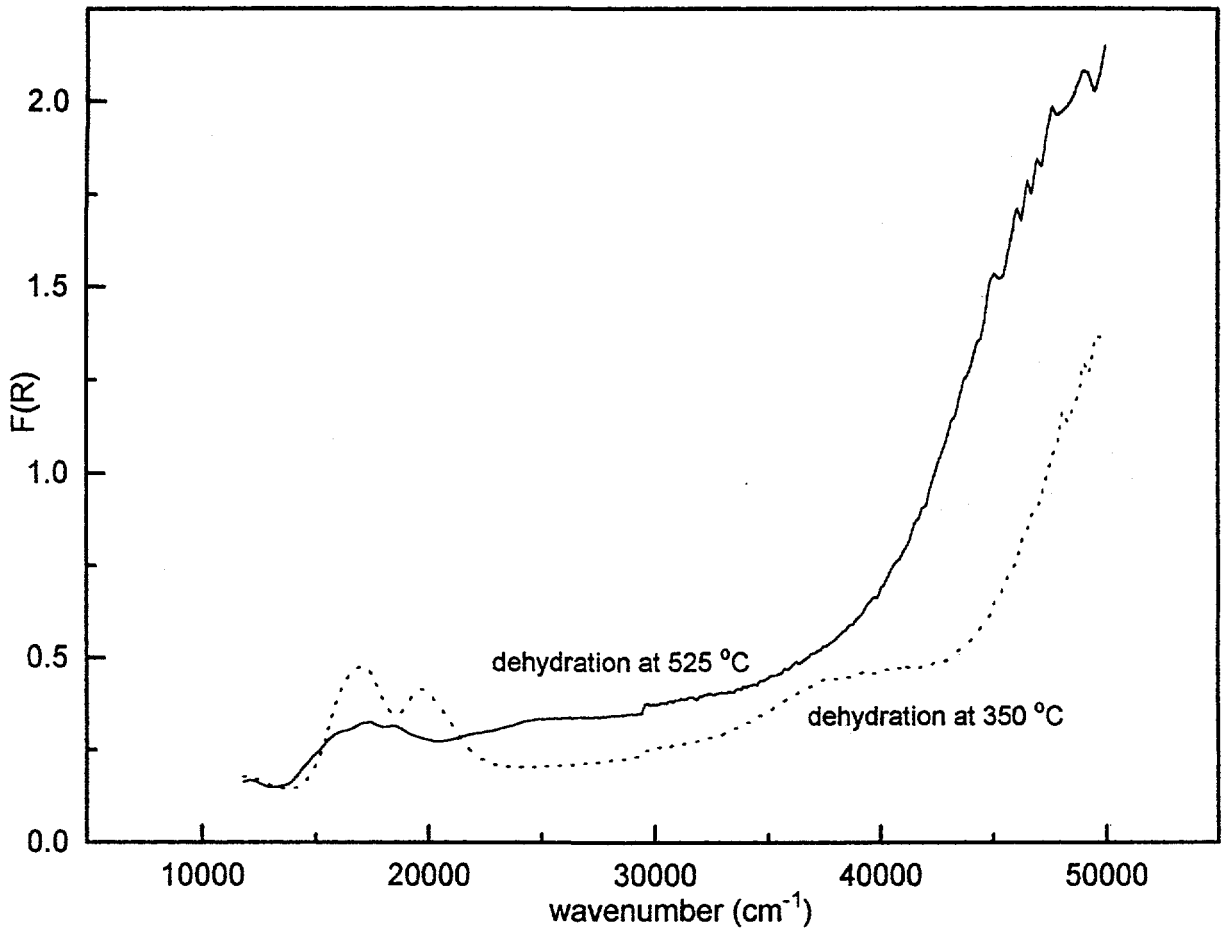

FIGURE 29. Comparison of the UV-VIS diffuse reflectance spectrum of the Co-ZSM-5/45 zeolite sample dehydrated at 525°C with that obtained after dehydration to only 350°C.

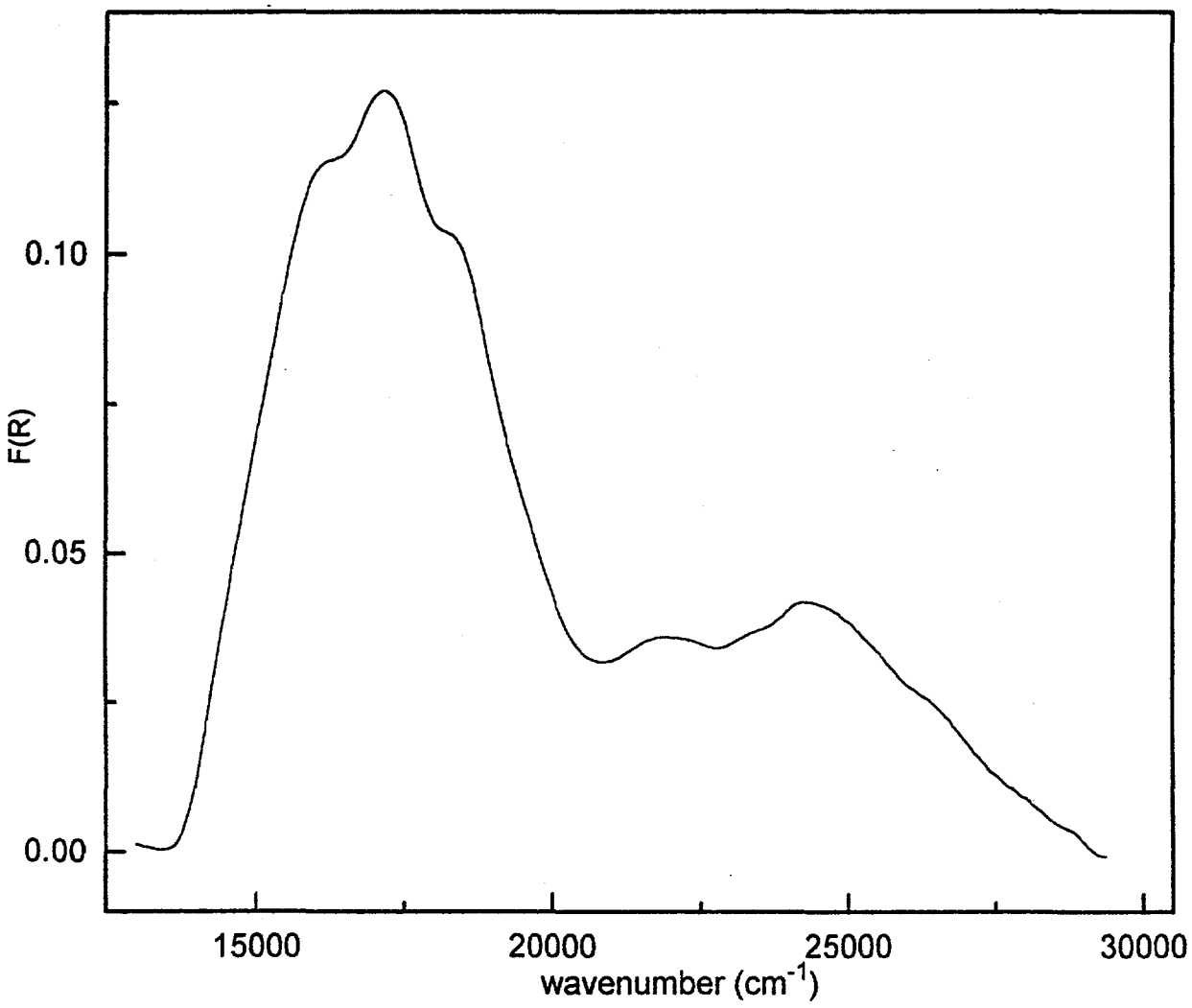

FIGURE 30. The UV-VIS diffuse reflectance spectrum in the range of 11,000-29,000 cm^{-1} for the Co-ZSM-5/450 zeolite sample dehydrated at 525°C. The spectrum of the parent zeolite dehydrated under the same conditions was subtracted.

with various low symmetries.

Adsorption of CO and H_2O on Co-ZSM-5 Dehydrated at 525°C. The effect of exposure of CO to the Co-ZSM-5/45 zeolite dehydrated at 525°C on the spectrum is shown in Figures 31 and 32, and it is seemed that CO strongly affected the cobalt(II) spectrum. Bands at 22,200 and 24,800 cm^{-1} disappeared, and the complex band consisting of at least a triple in the 15,500-18,500 cm^{-1} region was broadened into a more distinct asymmetric triplet (probably quartet) with bands at 16,000, 18,000, (19,500) and 21,000 cm^{-1}. These dramatic changes indicate that the Co(II) cations in the ZSM-5 matrix dehydrated at 525°C were easily accessible to guest molecules such as CO.

The spectrum of Co-ZSM-5/45 with adsorbed water is given in Figure 33. As in the case of CO adsorption, the spectrum of cobalt(II) in dehydrated zeolite was strongly affected by adsorption of water molecules. As shown is Figure 34 in the normalized spectra, bands at 22,200 and 24,800 cm^{-1} disappeared upon water adsorption, and the triplet centered at about 17,000 cm^{-1} was increased in intensity and the higher wavenumber conponent was shifted from ≈18,000 cm^{-1} to ≈19,800 cm^{-1}. The spectrum obtained upon water exposure exhibited features similar to the spectrum of Co-ZSM-5 dehydrated at 350°C, as well as of the band at ≈17,000 cm^{-1} observed with the Co-ZSM-5/45 sample dehydrated at 525°C. It indicates that after adsorption of water, the Co(II) sites corresponding to the zeolite dehydrated at 350°C are restored, but this needs further confirmation.

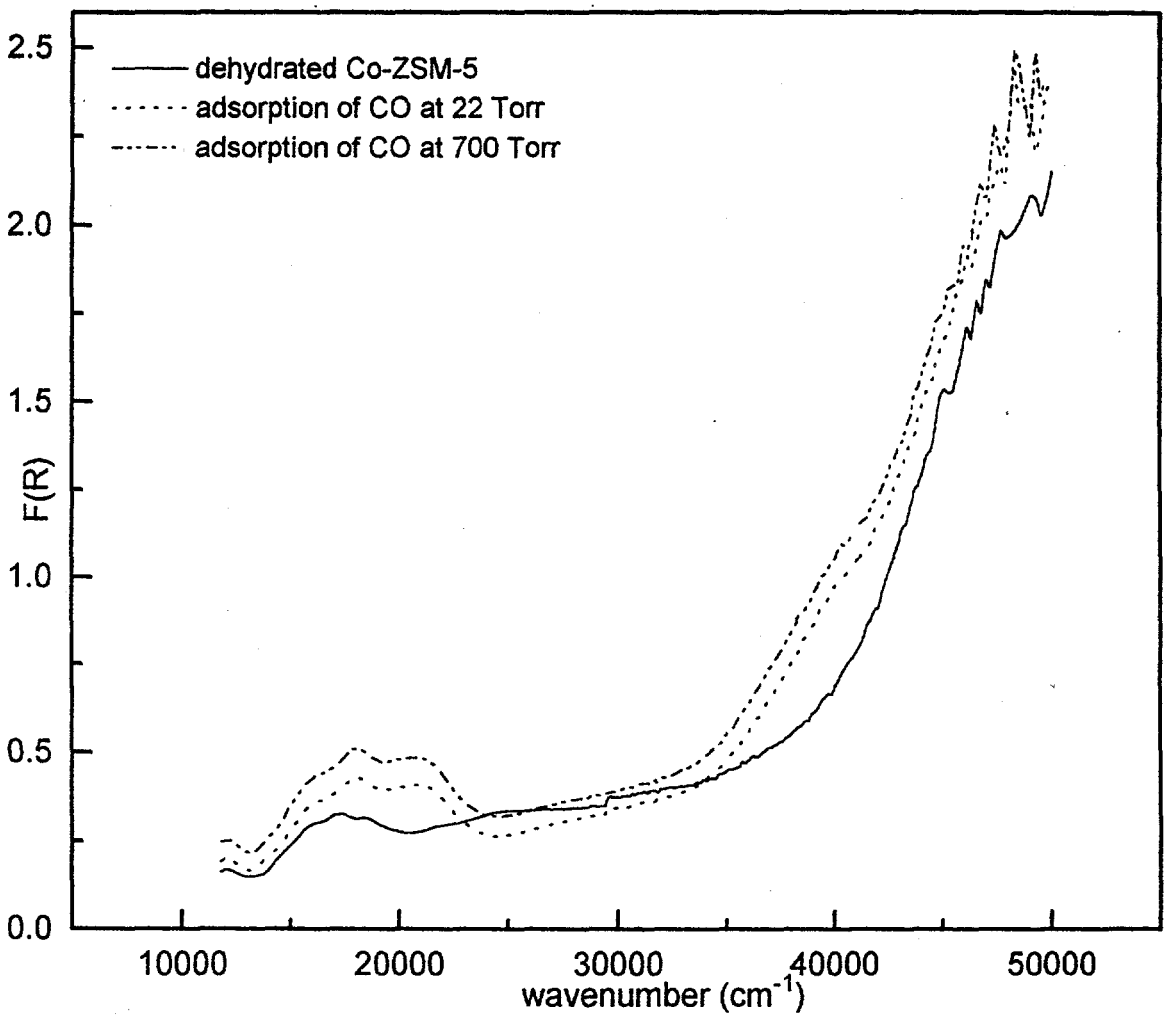

FIGURE 31. Comparison of the UV-VIS diffuse reflectance spectrum of the Co-ZSM-5/45 sample dehydrated at 525°C before and after exposure to CO.

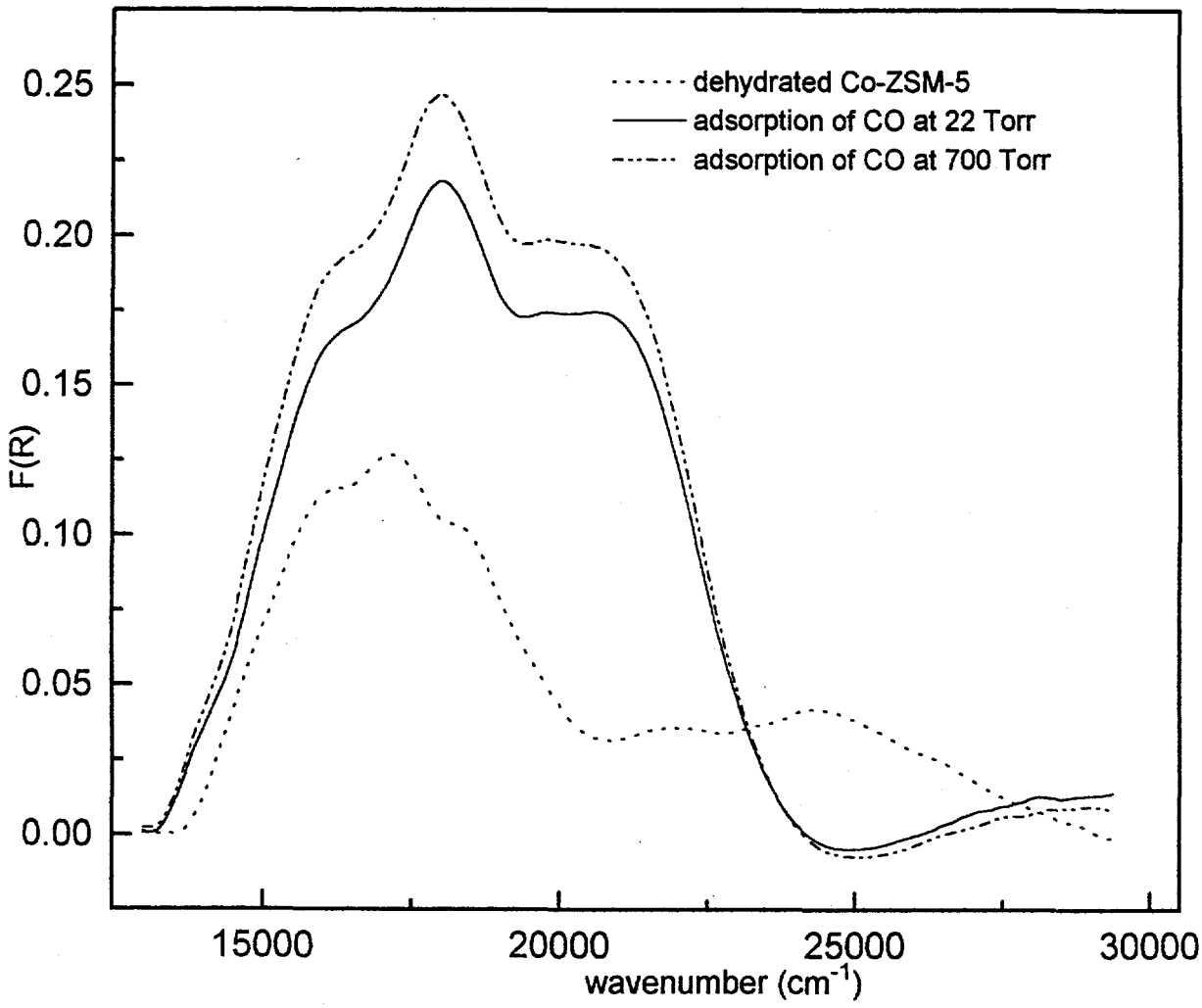

FIGURE 32. Comparison of the normalized UV-VIS diffuse reflectance spectrum in the 13,000-29,000 cm^{-1} spectral range of the Co-ZSM-5/45 sample dehydrated at 525°C before and after exposure to CO. The spectrum of the parent zeolite treated under the same reaction conditions was subtracted.

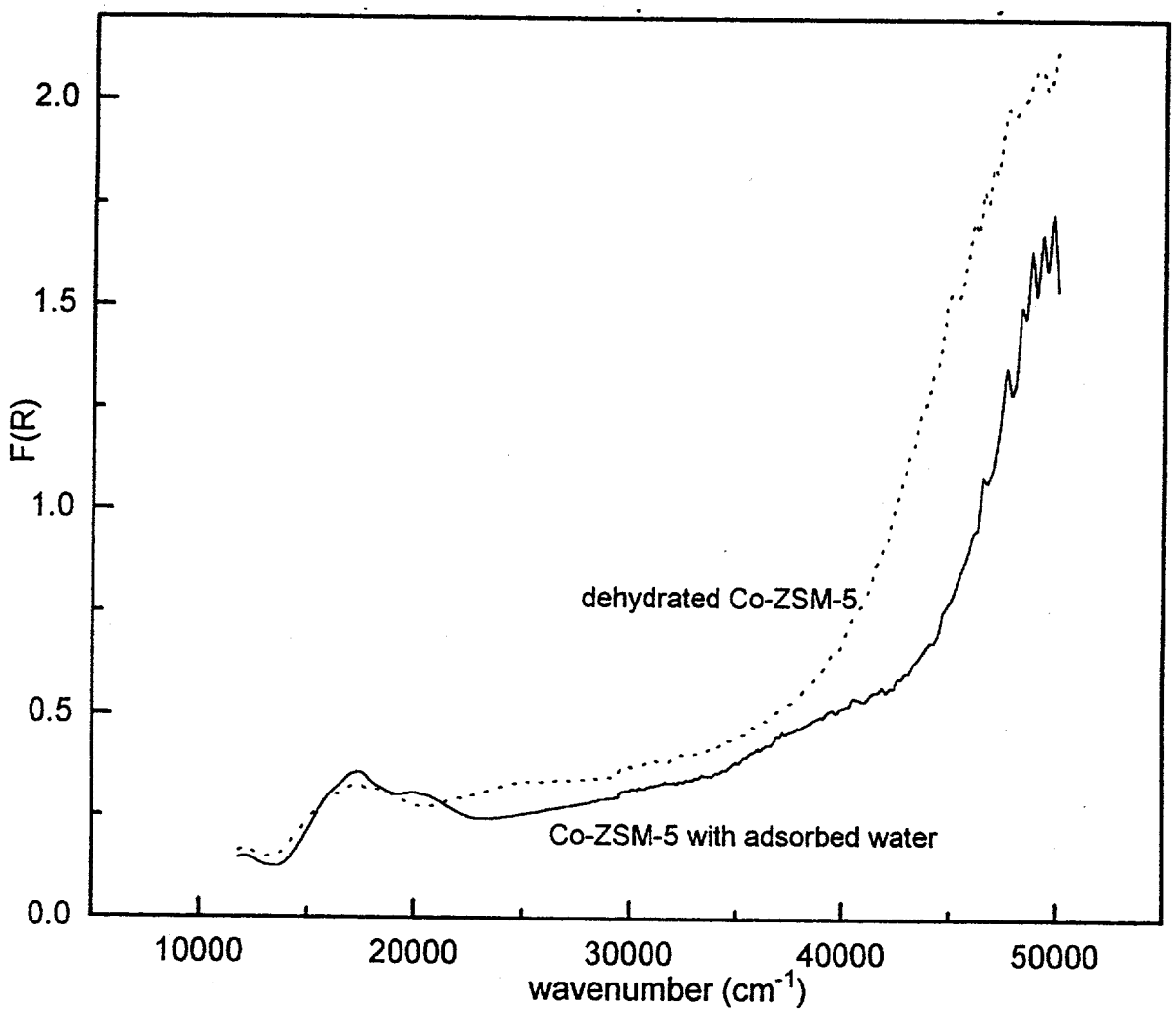

FIGURE 33. Comparison of the UV-VIS diffuse reflectance spectrum of the Co-ZSM-5/45 sample dehydrated at 525°C before and after exposure to water vapor at ambient temperature.

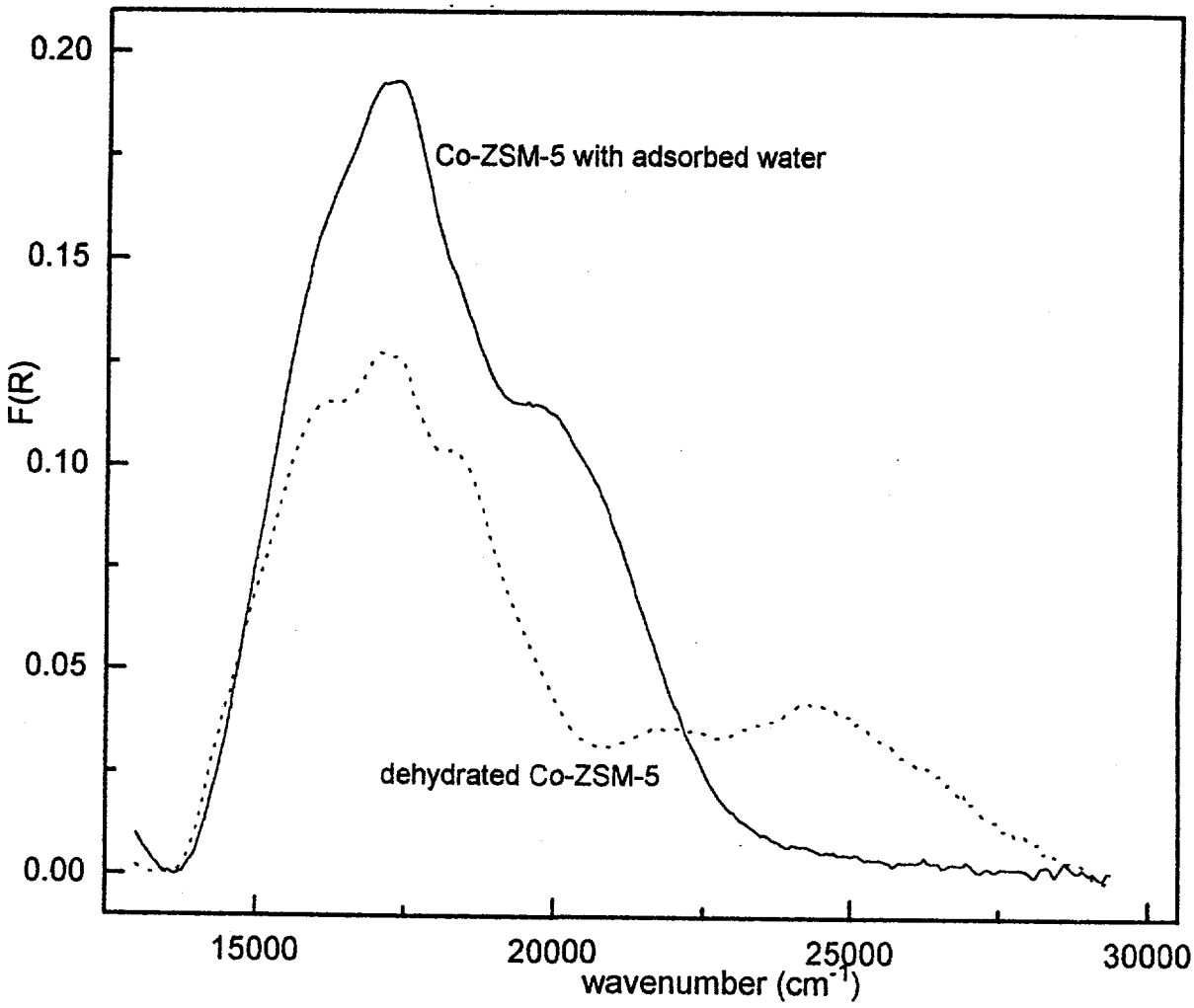

FIGURE 34. Comparison of the normalized UV-VIS diffuse reflectance spectrum in the 13,000-29,000 cm^{-1} spectral range of the Co-ZSM-5/45 sample dehydrated at 525°C before and after exposure to water vapor. The spectrum of the parent zeolite treated under the same reaction conditions was subtracted.

Adsorption of Ethylene. Ethylene at pressures of 0.5 Torr (40 ml), 0.95 Torr (180 ml) and 450 Torr (1400ml) was adsorbed onto Co-ZSM-5/30 after dehydrating the zeolite at 525°C. The resulting spectra are shown in Figures 35 and 36. The band centered at 22,500 cm^{-1} was most sensitive to adsorption of the guest molecule and disappeared at low pressure of ethylene. At the high pressure of 450 Torr of ethylene that was employed, the band at ≈25,000 cm^{-1} also disappeared, and the broad band centered at 17,500 cm^{-1} increased in intensity and split into a distinct symmetric triplet with maxima at 15,100, 16,900, and 18,750 cm^{-1}.

The ethylene-Co(II)A zeolite complex was studied by Klier et al. (12), and an asymmetric triplet was reported to be characteristic for ethylene adsorbed on cobalt(II) in a regular six-ring window. A symmetric triplet for a ethylene-Co-ZSM-5 complex does not correspond to this report. Moreover, the observed spectrum of Co-ZSM-5 with adsorbed ethylene was distinctly different from the spectrum of the ethylene-CoA complex. The symmetrical triplet shown in Figure 36 for this ethylene-Co-ZSM-5 complex indicates that Co(II) ions are not located in regular six-rings and that the absorption band at 25,000 cm^{-1} in the spectrum of dehydrated Co-ZSM-5 corresponds to a symmetry different from D_{3h} symmetry.

Dehydration of Co-ZSM-5 in Helium and in Vacuum. There were no significant differences observed between the spectrum of Co(II)-ZSM-5 zeolites dehydrated at 515°C in flowing helium and the spectrum of the corresponding zeolites dehydrated at 350°C in vacuum. Thus, it appears that the siting of the Co(II) cations in ZSM-5 zeolites is the same for these methods of preparation.

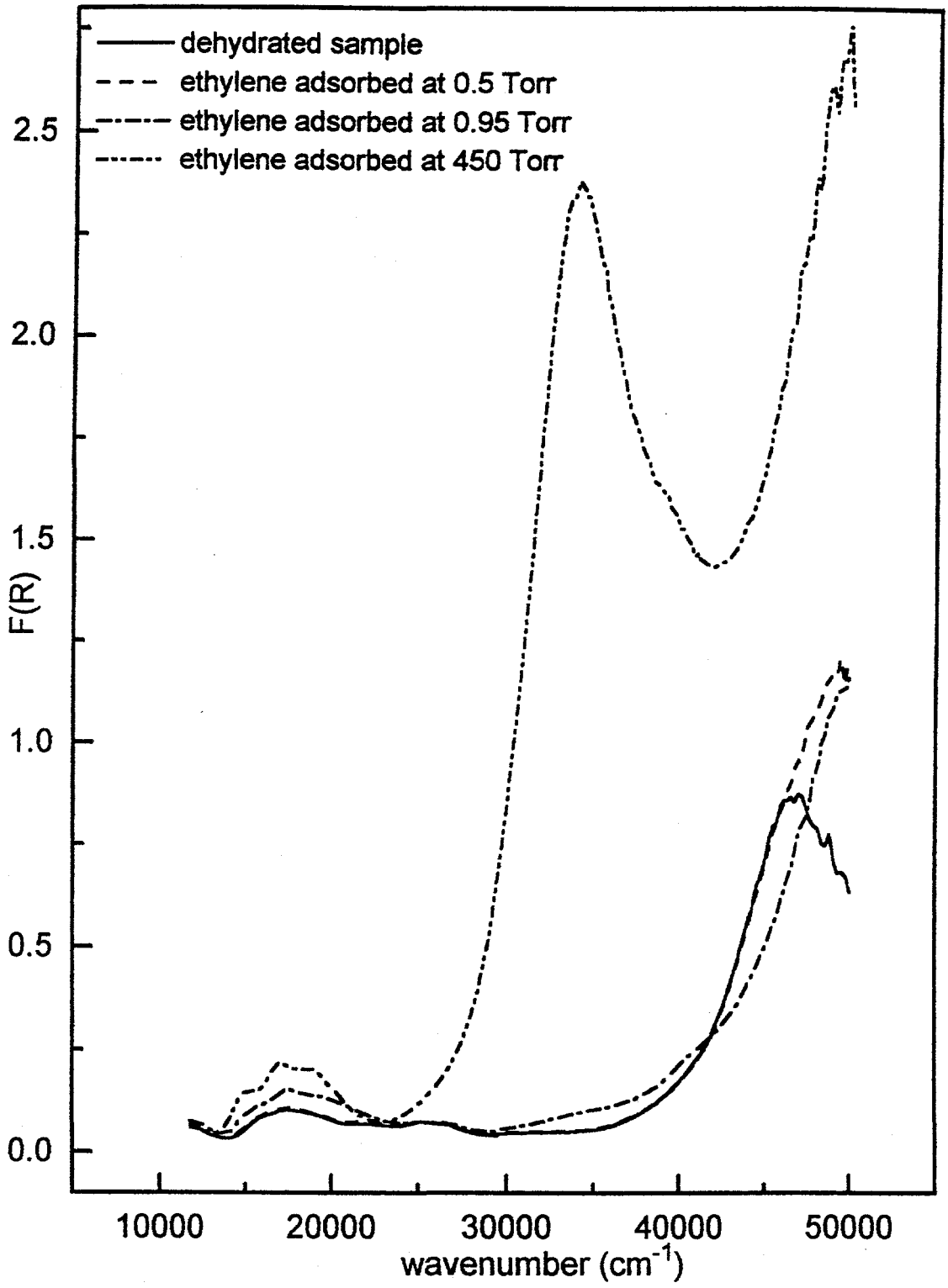

FIGURE 35. The effect of ethylene adsorption on the UV-VIS diffuse reflectance spectra of Co-ZSM-5/30 after dehydration at 525°C.

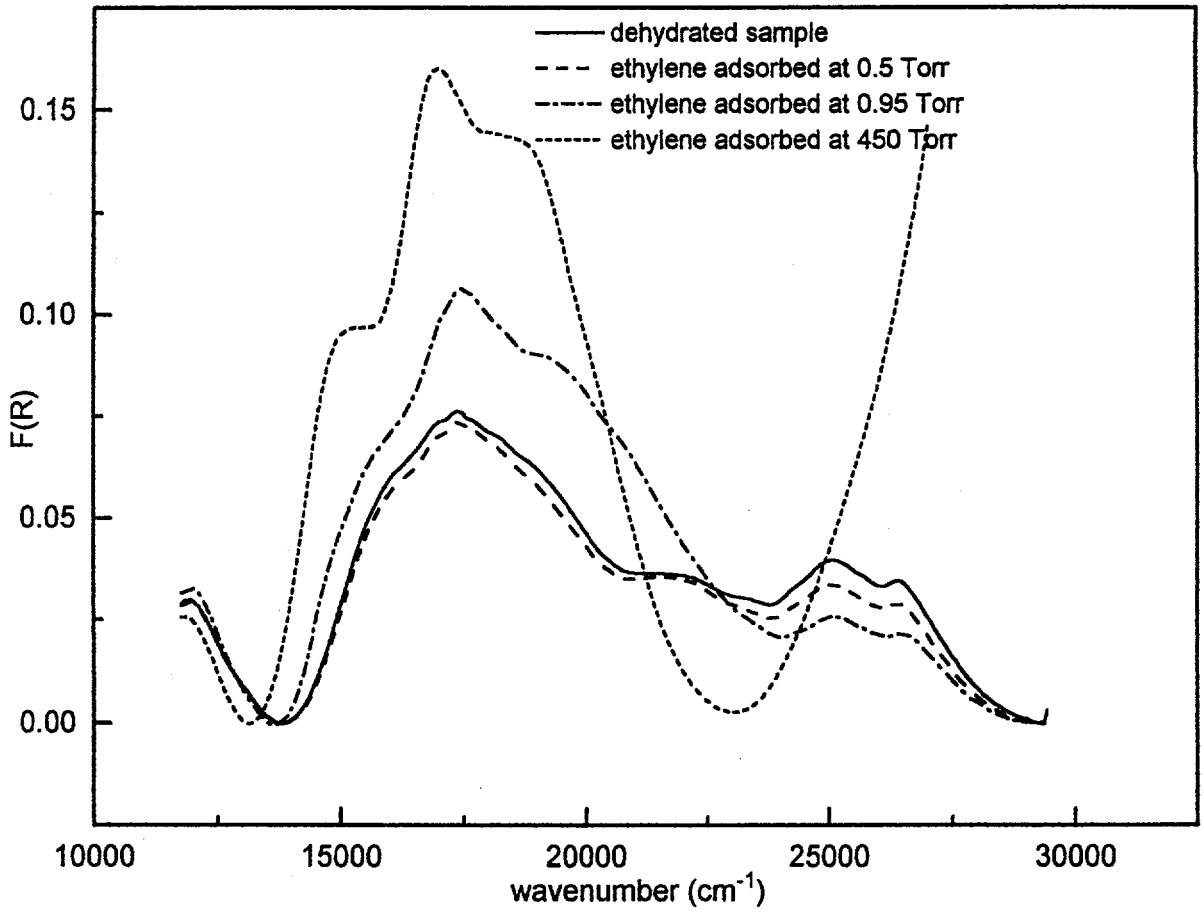

FIGURE 36. The effect of ethylene adsorption on the normalized UV-VIS diffuse reflectance spectra of Co-ZSM-5/30 after dehydration at 525°C. The spectrum of the parent zeolite was subtracted.

The influence of dehydration temperature on the DRS observations was investigated while maintaining the Co(II)-ZSM-5/28 zeolite under a dynamic vacuum. The spectra of the Co-ZSM-5/28 zeolite dehydrated in vacuum at temperatures ranging from 30°C to 540°C are present in Figures 37 and 38. The spectrum for the zeolite evacuated at 30°C (room temperature) corresponded to the spectrum of a hydrated sample with only a low intensity band at 19,500 cm^{-1}. The spectrum of the sample dehydrated at 100°C exhibited features characteristic for hydrated zeolite and of the zeolite dehydrated at 350°C and represents the transition stage of dehydration of Co-ZSM-5 samples. Samples dehydrated at temperatures from 180 to 360°C were similar, and the spectra correspond to that of a sample dehydrated at standard conditions that were previously used (vacuum for 3h at 350°C). Spectra of samples dehydrated at high temperatures (424-540°C) exhibited different fine structure than spectra obtained with a sample dehydrated at the standard condition of 350°C.

It is evident that there are a number of different Co(II) sites in Co-ZSM-5 depending on conditions, particularly the temperature, used for dehydration of the samples. Dehydration at 350°C might not result in complete dehydration of the Co-ZSM-5 zeolite. The DRS results indicate that the spectra of Co-ZSM-5 zeolites are more complex that the Co-erionite spectra. However, some of the bands and second derivative peaks appear to correspond to similar species.

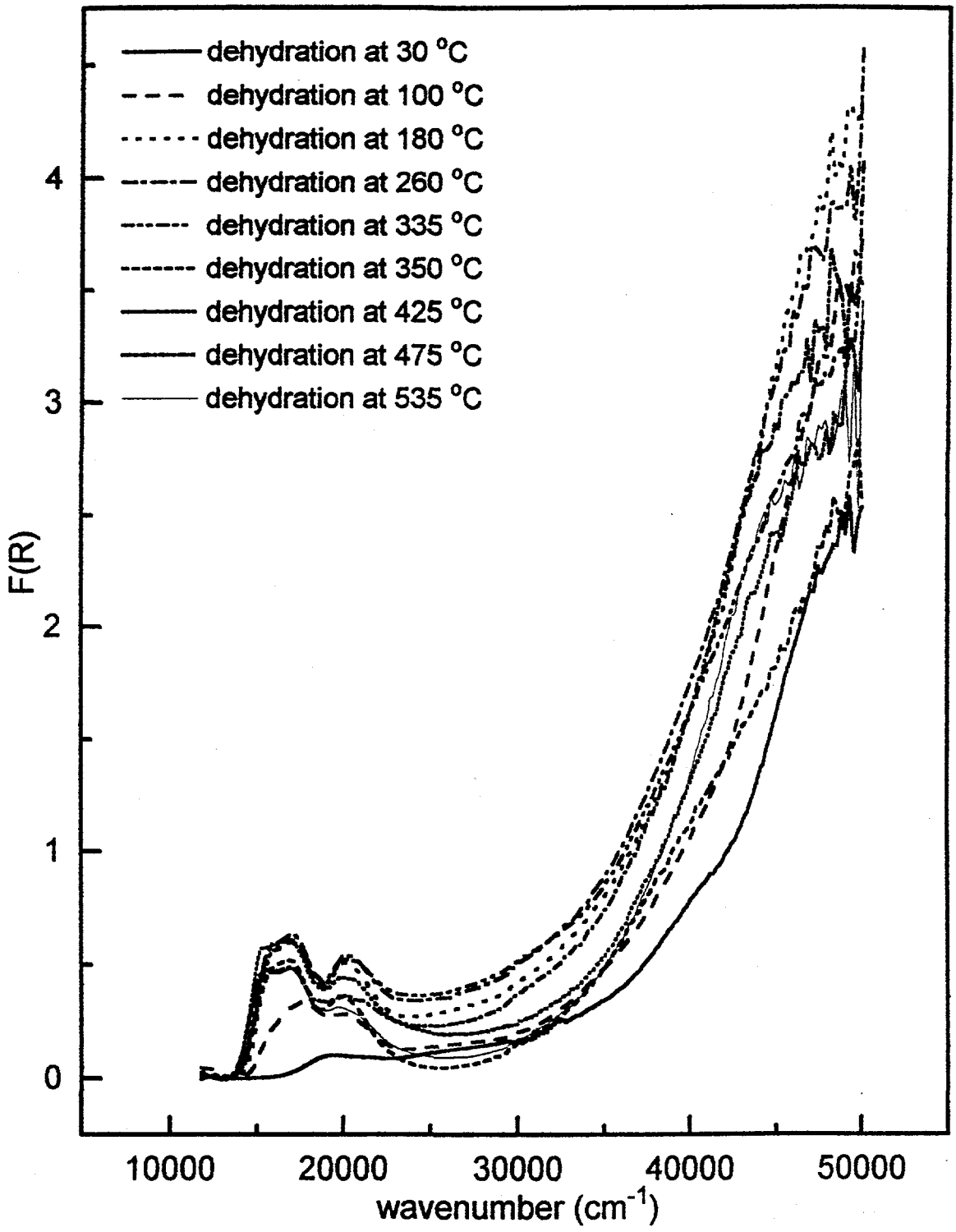

FIGURE 37. The dependence of the UV-VIS diffuse reflectance spectra of Co(II)-ZSM-5/28 on the dehydration temperature employed during evacuation of the samples.

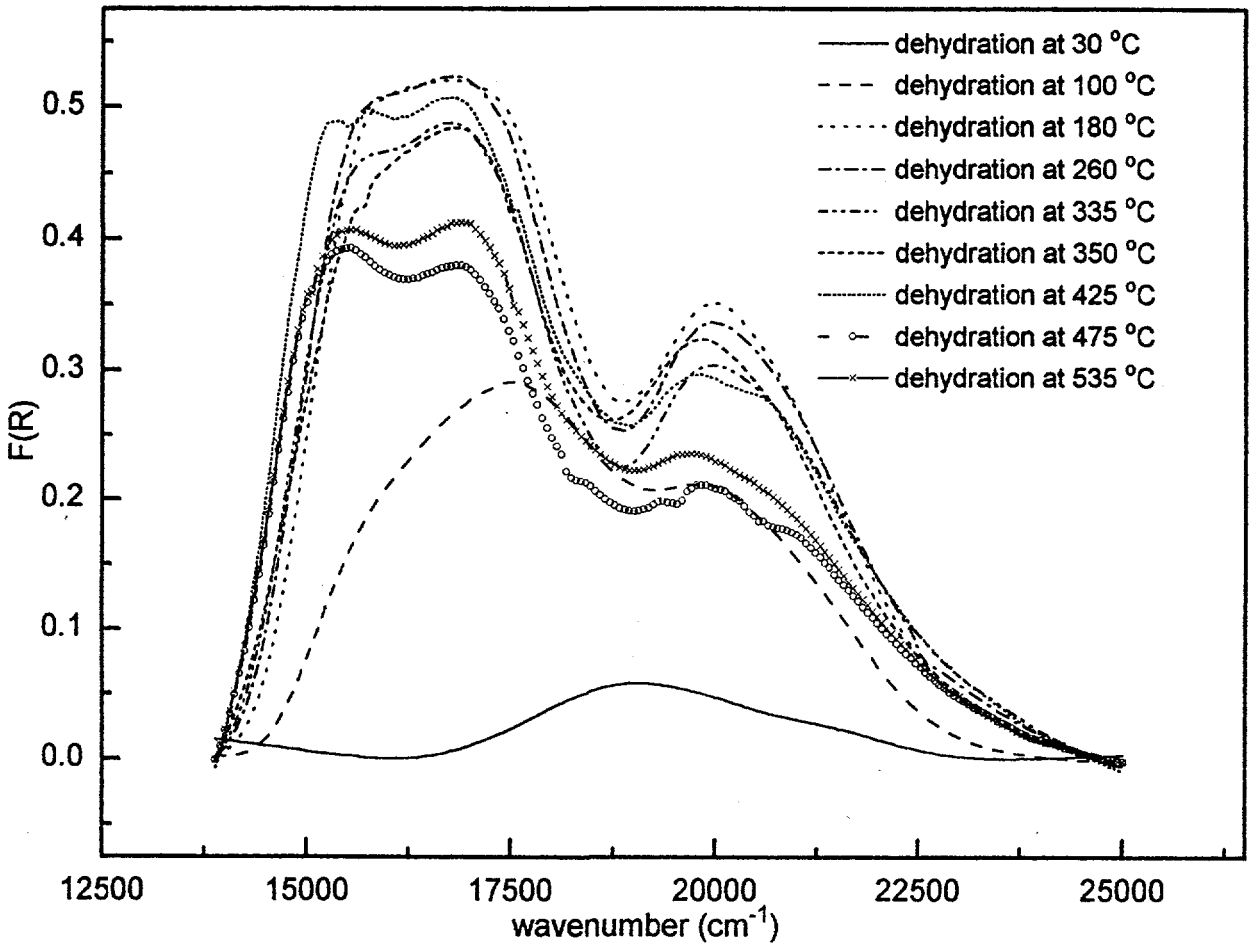

FIGURE 38. The dependence of the normalized UV-VIS diffuse reflectance spectra in the spectral range of 13,750-25,000 cm^{-1} of Co(II)-ZSM-5/28 zeolites on the dehydration temperature employed during evacuation of the samples. The spectrum of the parent zeolite dehydrated under similar conditions was subtracted.

Summary Conclusions

It appears that Co(II)-ZSM-5 after dehydration at 350°C has a minimum of three cobalt sites with different environments. One site is characterized by the presence of a spectral band at 15,000 cm^{-1}, and it is observed with samples prepared under basic conditions of ion exchange, preferentially in high silica ZSM-5. In Co-ZSM-5 samples exchanged at acid pH, there are at least two other cobalt ion sites present with different environments. These sites are characterized by 7-10 absorption bands. Co(II) cations in these sites easily interact with strong guest molecules such as water.

After dehydration at 525°C, cobalt(II) ions in different environments are present in zeolites. These Co ions are also easily accessible to weak guest molecules such as CO and ethylene. Siting of the Co(II) ions in ZSM-5 is different from the siting of Co(II) in A zeolite. Co erionite (dehydrated at 350°C) exhibits a much simpler spectrum than Co-ZSM-5, but some of the spectral bands observed with these zeolites appear to be common for both. Thus, there is at least one type of Co(II) site common for both zeolites. Co(II) ions in this site in ZSM-5 zeolite were accessible only to strong guest molecules. The spectrum of Co-erionite dehydrated at 500°C is similar to the spectrum of Co-A zeolite, and this corresponds to Co(II) ion with D_{3h} symmetry located in the plane of six-ring windows. Cobalt in this site is easily accessible to guests molecules.

These studies provide input into the NO adsorption/desorption studies and NO catalytic decomposition/reduction studies over Co(II) zeolites thatwere carried out.

• **Adsorption and Conversion of NO on Co(II) Zeolites**

This section of the report summarizes our research centered on (i) investigating the adsorption of NO on Co(II) zeolites, (ii) determining the effect of NO adsorption on the diffuse reflectance spectral (DRS) features of Co(II) in zeolite sites, and (iii) examining the catalytic activity of the Co(II) zeolites for NO reduction by methane in the presence of excess O_2 in a flowing gas stream. In particular, the catalytic activity of Co-ZSM-5, Co-erionite, Co-mordenite, and Co-ferrierite was investigated for NO decomposition and for the selective reduction of NO by methane.

In general, the spectral features of the Co(II) zeolites were presented in the previous sections of this report. It was shown that strong ligands such as water adsorb onto Co(II) sites after dehydration at 350°C and 500°C, but weak ligands such as CO and C_2H_4 only exhibit adsorption after the high temperature dehydration treatment. It is shown here that NO adsorption occurs after both treatments and that strong absorption bands in the UV-VIS spectral region corresponding to charge transfer spectra are characteristic of the formation of NO-Co intrazeolitic complexes.

The Co(II) exchanged zeolites were prepared under acidic conditions by ion exchange, generally from aqueous $Co(NO_3)_2$ solutions with molarities of 0.01 or 0.02 at room temperature. In particular, the detailed conditions employed for the preparations utilized for the Co(II)-ZSM-5 and Co(II)-erionite zeolites were given earlier in this report.

Adsorption of NO on Co-Containing Zeolites

Procedures used for the optical measurements at room temperature were described

previously in this report. Adsorption and desorption of NO with the dehydrated Co-containing zeolites was carried out while simultaneously monitoring the samples by DRS in the UV-VIS-NIR spectral regions. Typically, after the zeolite was dehydrated at 350 or 525°C, the amount of gas adsorbed by *ca.* 0.8 g of dry sample was regulated by adsorption of gas at pressures of 0.5-700 Torr from 40, 180, and 1400 ml volumes at atmospheric pressure. Nitric oxide (98.5%, Aldrich Chemical Company, Inc.) was purified by freezing it in a glass tube using liquid nitrogen, evacuation, and then thawing. After adsorption of NO at room temperature, desorption was studied at temperatures ranging from room temperature to 440°C. Samples were evacuated from 30 min to 3 h.

Initially, the adsorption/desorption of NO on the following three zeolites was probed:

Co-erionite	Si/Al = 3.5	2.5 wt% Co(II)
Co-ZSM-5	Si/Al = 10	4.4 wt% Co(II)
Co-ZSM-5	Si/Al = 22.5	0.75 wt% Co(II).

After dehydration of the zeolites under vacuum at 350°C, the samples were exposed to excess NO at atmospheric pressure for 30 min. As shown in Figures 39-41, the adsorption of NO strongly influenced the optical absorption of the zeolites in the 12,000- 50,000 cm^{-1} spectral range. The characteristic DRS bands centered about 16,000-17,000 cm^{-1} of "bare" Co(II) disappeared, and new bands centered at 13,500, 22,000, 26,000, and 39,000 cm^{-1} appeared after NO adsorption. The latter band is a very intense charge transfer band.

The positions of the new bands are given in Table 9, where the data for the Co-A zeolite were obtained by analysis of spectra reported elsewhere (41). It is evident that the bands of the NO-Co(II) complexes depend on the zeolite matrix. This dependence might be due to different Co(II) siting in the different zeolite structures or by the influence of

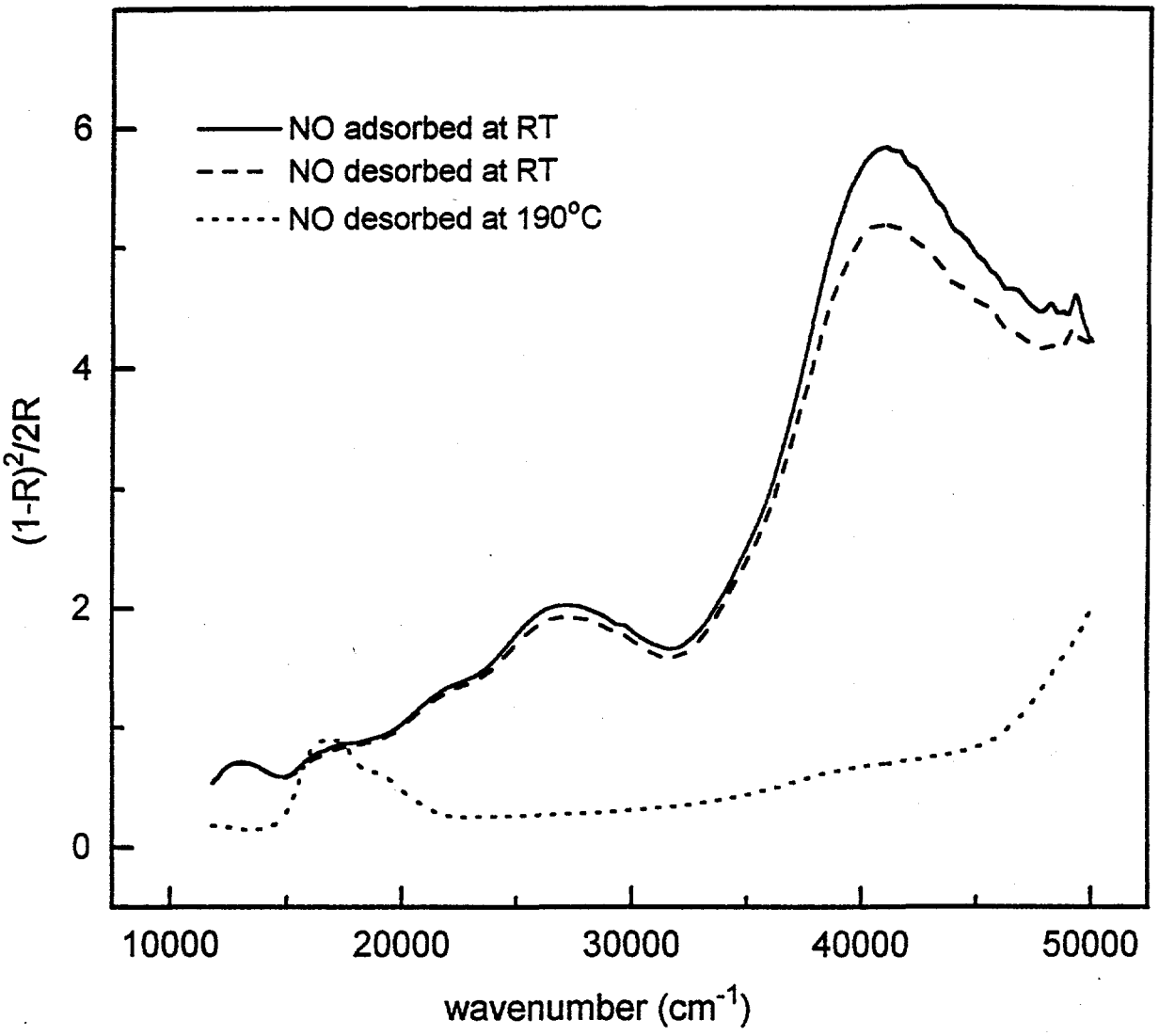

FIGURE 39. The DRS spectrum of Co(II)-erionite (2.5 wt% Co(II)) upon adsorption of excess NO and desorption by evacuation for 30 min at room temperature and at 190°C.

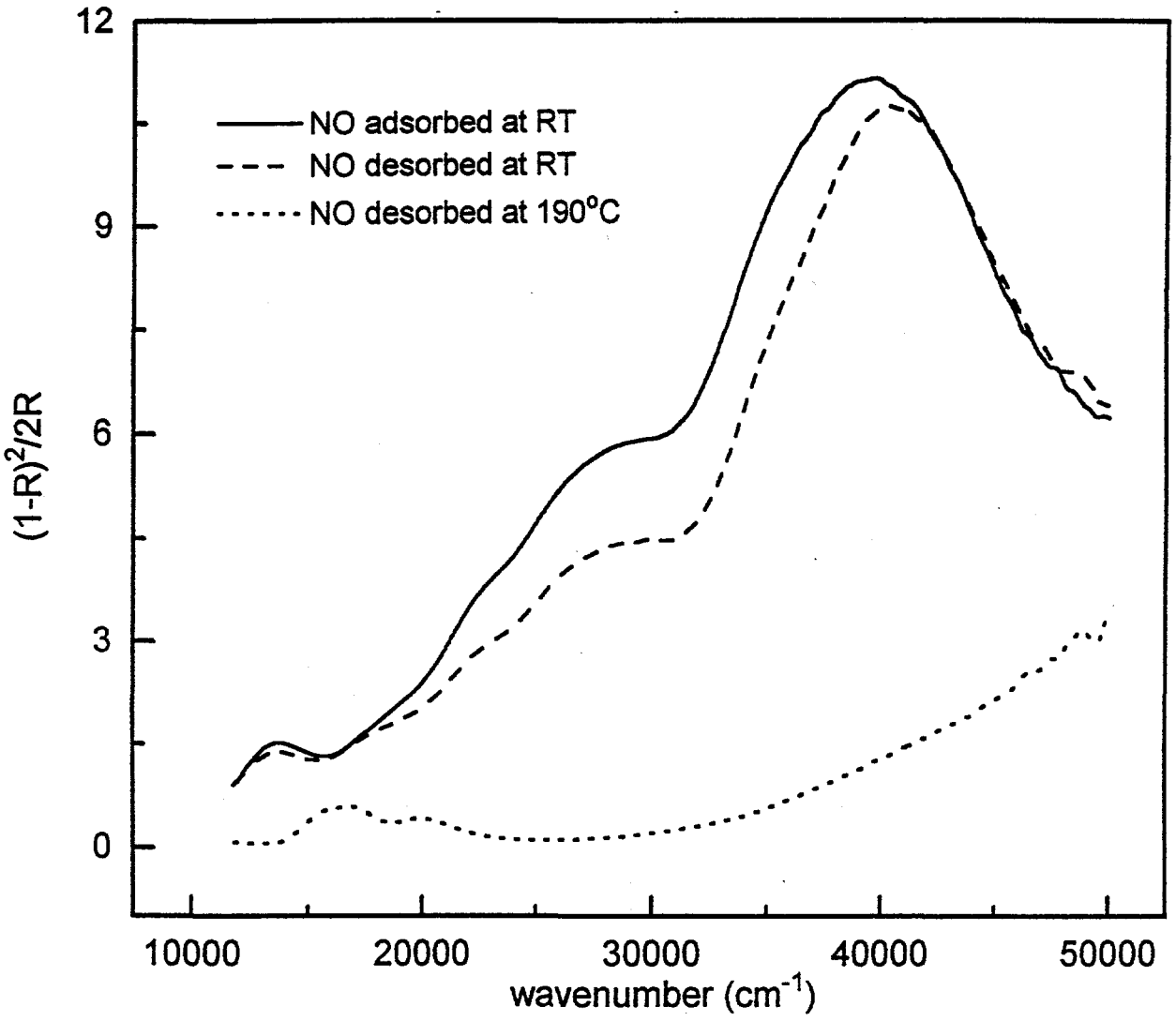

FIGURE 40. The DRS spectrum of Co(II)-ZSM-5 (4.4 wt% Co(II); Si/Al = 10) upon adsorption of excess NO and desorption by evacuation for 30 min at room temperature and at 190°C.

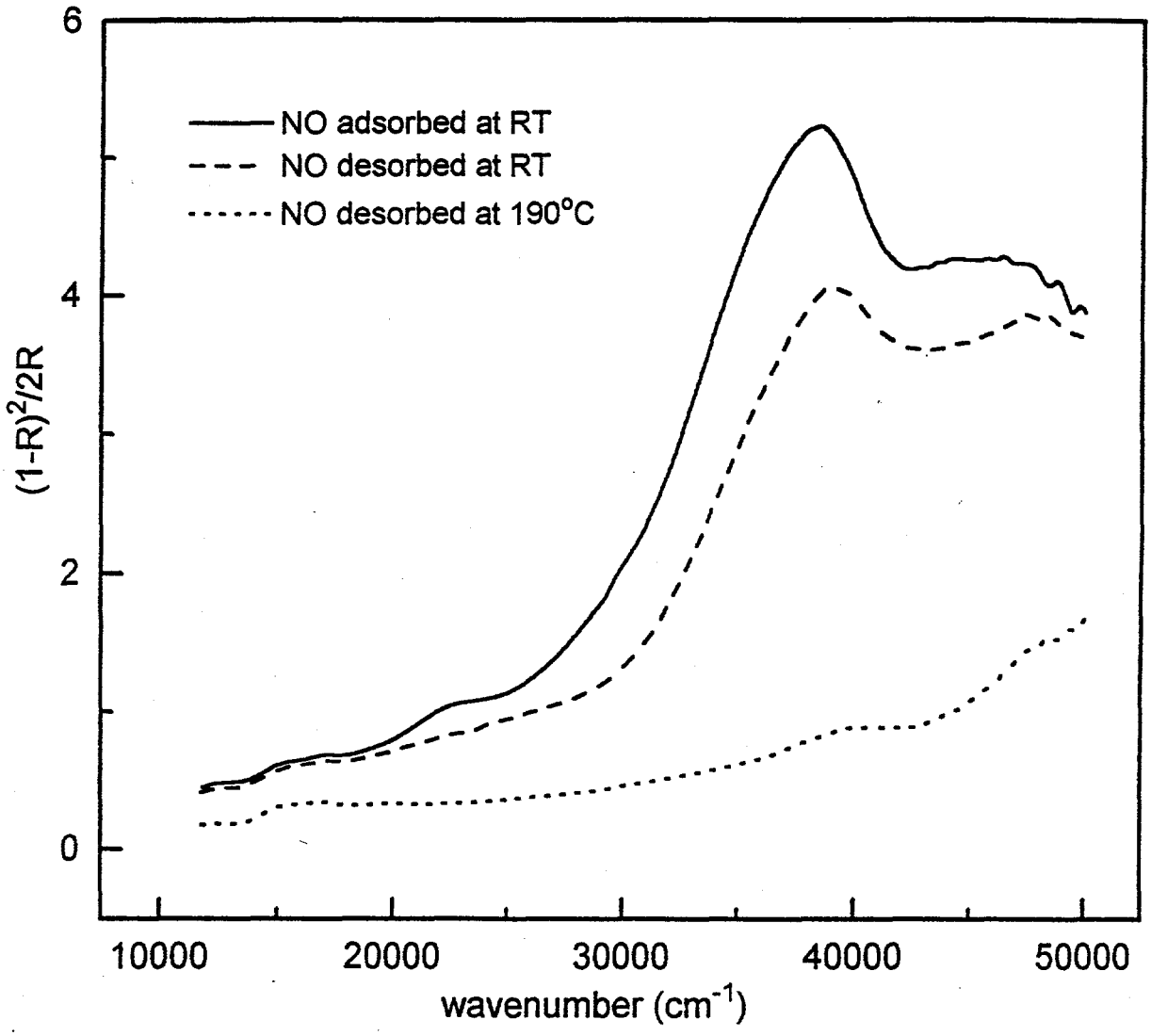

FIGURE 41. The DRS spectrum of Co(II)-ZSM-5 (0.75 wt% Co(II); Si/Al = 22.5) upon adsorption of excess NO and desorption by evacuation for 30 min at room temperature and at 190°C.

framework acidity (different Si/Al ratio) on the charge transfer spectra of the NO-Co-zeolite complex.

TABLE 9. Charge transfer bands of NO-Co(II) complexes in zeolites.

Matrix		CT Bands (cm^{-1})			
Zeolite	Si/Al	ν_1	ν_2	ν_3	ν_4
Co-A	1.0	37,000	24,000	21,000	13,000
Co-erionite	3.6	41,000	26,700	22,000	13,000
Co-ZSM-5	10	40,000	27,500	22,500	13,500
Co-ZSM-5	22.5	39,000	---	23,000	12,500

Desorption was carried out by evacuating at 90, 140, and 190°C. Partial desorption of NO was observed at temperatures ≤ 140°C. Desorption at 190°C resulted in removal of all of the NO and the spectra of the dehydrated zeolites were regenerated, as shown in Figures 39-41. Upon evacuation at ambient temperature, only a slight decrease in the intensity of the spectra was noted, while the spectral features remained the same.

Comparison experiments were carried out with the Co-erionite dehydrated at 350°C and at 525°C, in which the pressure of NO was increased stepwise from 0 to 700 Torr. The resulting spectra are shown in Figures 42 and 43. Distinct differences between the spectra of the two samples are evident. This is clearly seen in Figure 44, which compares the optical spectra for the samples exposed to 700 Torr of NO. The maxima of the DRS bands of the NO-Co complexes in erionite are shifted to lower wavenumbers for the sample dehydrated at 525°C as compared with the sample dehydrated at 350°C. This result indicates that the

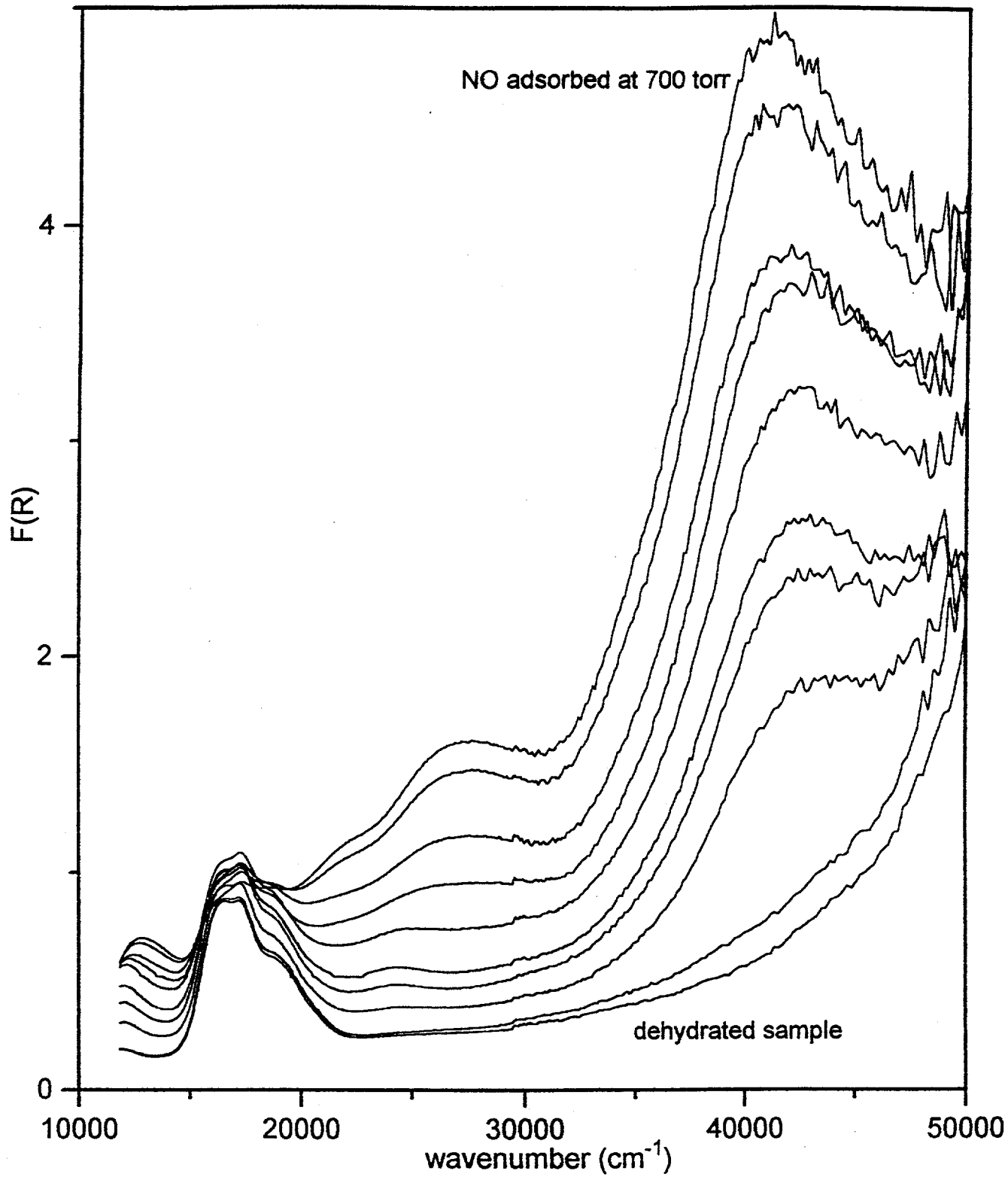

FIGURE 42. Spectral changes observed as increasing pressures of NO were used for adsorption of NO at ambient temperature on a Co(II)-erionite that was dehydrated at 350°C.

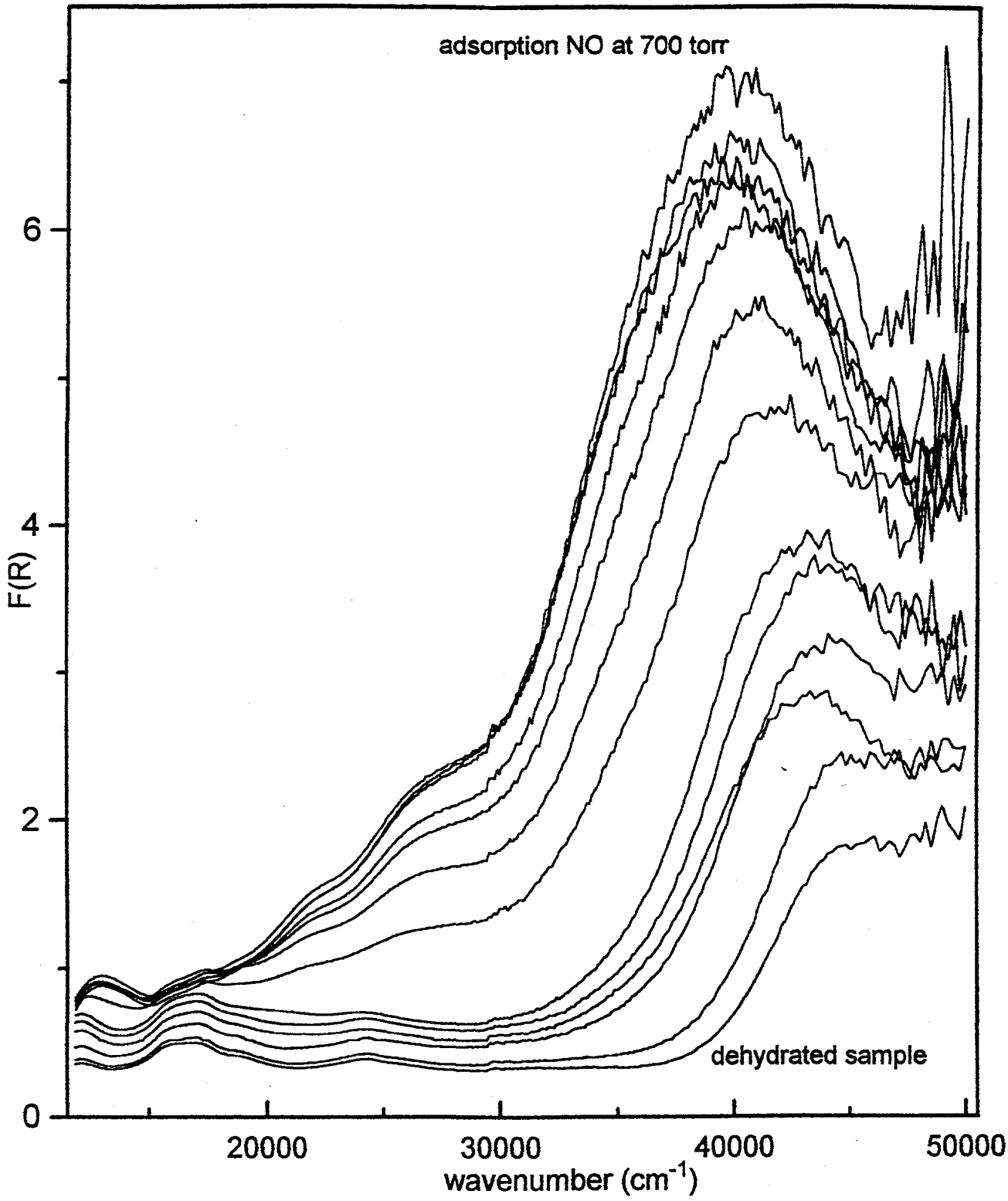

FIGURE 43. Spectral changes observed as increasing pressures of NO were used for adsorption of NO at ambient temperature on a Co(II)-erionite that was dehydrated at 525°C.

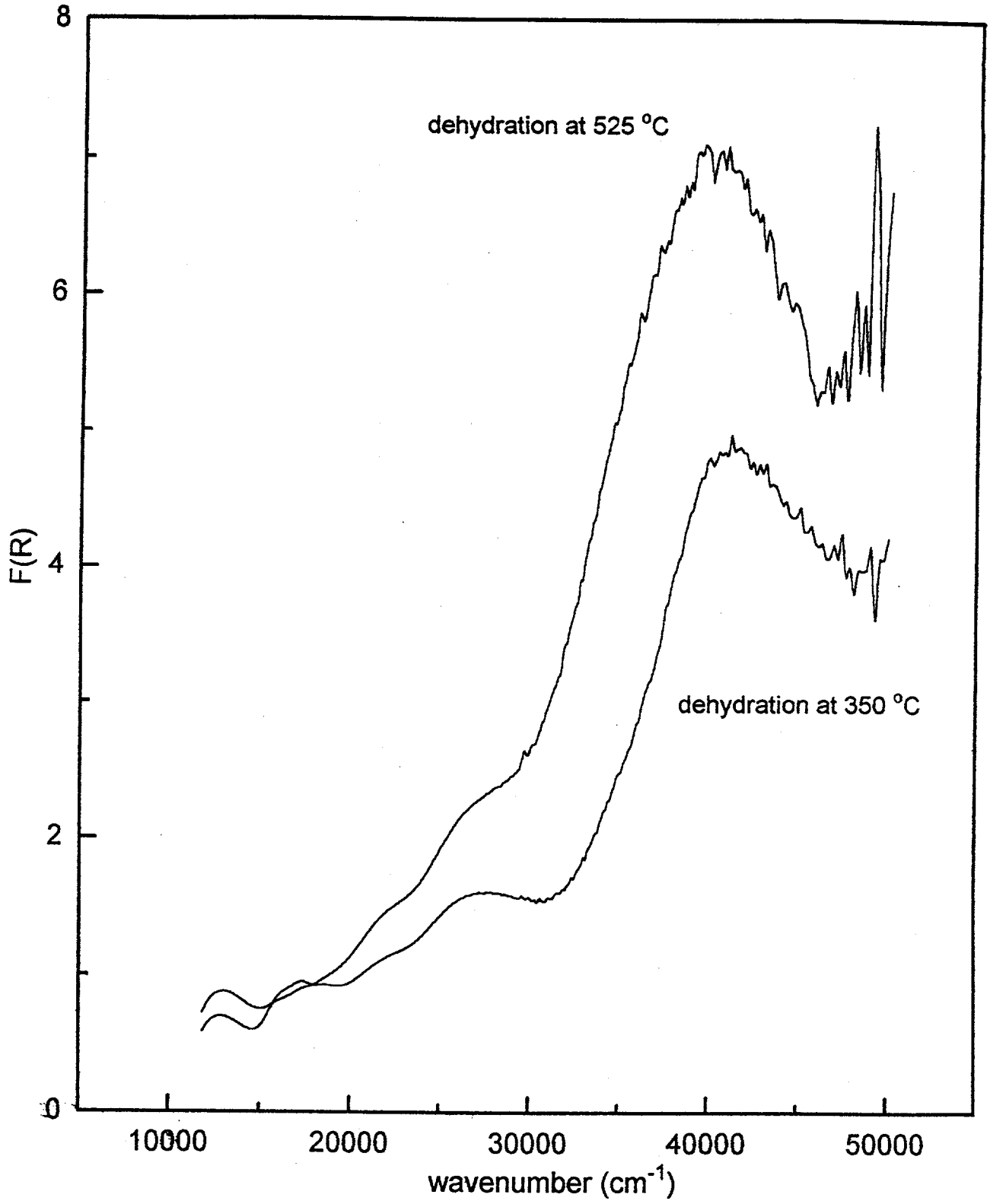

FIGURE 44. Effect of the dehydration temperature upon the spectrum obtained after equilibration of Co(II)-erionite with 700 Torr NO at ambient temperature.

charge transfer complex of Co(II) in erionite is mainly affected by the siting of the cations in the zeolite matrix.

Catalytic Testing of NO Selective Reduction by Methane

Selected Co(II)-containing zeolites were tested for the selective catalytic reduction (SCR) of NO using methane as the reductant. The catalysts tested consisted of the following:

$Co(NH_4)$-erionite	Si/Al = 3.5	3.2 wt% Co
$Co(NH_4)$-ZSM-5	Si/Al = 10	4.4 wt% Co
CoH-mordenite	Si/Al = 8.5	2.1 wt% Co
Co-A zeolite		2.6 wt% Co
Co-ferrierite		5.1 wt% Co.

Samples were dehydrated in a stream of helium using a temperature ramp of 5 °C per min from room temperature to 500 °C, which was then maintained for 1 h. Weights of samples used were 300 mg of Co-A zeolite, 240 mg of Co-erionite, and 360 mg of the other zeolites. SCR of NO by methane in an oxidative atmosphere was carried out at 400 °C using a reaction mixture of 1000 ppm of NO, 1000 ppm of CH_4, and 2.5 vol% of O_2 in helium flowing at a rate of 100 ml/min, corresponding to a gas hourly space velocity (GHSV) of 20,000 ℓ/kg catal/hr in the case of the Co-A zeolite. NO and NO_x were detected by chemiluminescence.

The catalytic activity of cobalt(II)-containing erionite, ferrierite, mordenite, ZSM-5, and A zeolites for the selective reduction of NO in an oxidative atmosphere is given in Table 10. These results were obtained under steady state conditions that were maintained for at least 30 min. All of the Co(II) zeolite catalysts exhibited some activity for the reduction of NO under these reaction conditions.

TABLE 10. Catalytic activity of cobalt(II)-containing zeolites for selective reduction of NO in an oxidative atmosphere at 400°C using a reactant mixture of 1000 ppm NO + 1000 ppm CH_4 + 2.5 vol% O_2 in He flowing at 100 ml/min at ambient pressure.

Zeolite	NO Converted (mol%)	NO Converted to NO_2 (mol%)	Co Content in zeolite (wt%)	Wt of Catalyst in Reactor (g)
Co-A	16	58	2.6	0.30
Co-erionite	25	47	3.2	0.24
Co-mordenite	44	14	2.1	0.36
Co-ferrierite	70	8	5.1	0.36
Co-ZSM-5	39	20	4.4	0.36

Due to varying contents of Co(II) in the catalysts and the different masses of catalysts that were used in the reactor, the conversion of NO was recalculated on the basis of the mass of catalyst and also on the basis of only the cobalt content of the zeolites contained in the reactor. These results are given in Table 11 in terms of rates of NO converted and N_2 formed.

Large differences in conversion of NO relative to the cobalt(II) content in zeolites indicate the presence of different catalytic centers in these zeolite matrices. Very interesting is the high conversion of NO to NO_2 by Co-erionite and Co-A zeolite. This behavior might coorelate with the fact that erionite and A zeolite contain Co(II) ions in a similar site (regular six-ring windows). The high catalytic activity of cobalt(II) ions in Co-mordenite is also of interest, and determination of cobalt sites in this zeolite and population of Co(II) cations in

these sites is of a great importance in optimizing these catalysts for the selective reduction of NO.

TABLE 11. Catalytic activity of cobalt(II)-containing zeolites for selective reduction of NO by methane in an oxidative atmosphere related to the weight of catalyst and to cobalt(II) content.

Zeolite	mol of NO converted /g of zeolite per second	mol of NO converted to N_2/g of zeolite per second	mol of NO converted /mol of Co per second	mol of NO converted to N_2/mol of Co per second
Co-A	$0.44 \cdot 10^{-7}$	$0.18 \cdot 10^{-7}$	$0.27 \cdot 10^{-3}$	$0.11 \cdot 10^{-3}$
Co-erionite	0.87	0.46	0.46	0.24
Co-mordenite	1.00	0.86	0.78	0.67
Co-ferrierite	1.60	1.47	0.52	0.48
Co-ZSM-5	0.90	0.72	0.33	0.26

Summary Conclusions

The optical bands observed upon equilibration of Co(II)-erionite and C(II)-ZSM-5 with excess NO exhibit a strong dependence on the zeolite matrix and upon the temperature utilized for dehydration of the zeolites. The dependence of these on the cobalt siting in erionite indicates that the NO-Co complex is affected mainly by Co(II) siting in zeolites. Among the Co-exchanged zeolites,Co-erionite and Co-ZSM-5 exhibit similar catalytic conversions of NO to products under the reaction conditions employed. However, Co-mordenite and Co-ferrierite exhibited the highest catalytic activities in the selective reduction of NO by methane in the presence of oxygen.

- **XPS and Auger Analyses of Zeolites**

X-ray photoelectron spectroscopy (XPS) was used to monitor the relative concentrations and oxidation states of transition metals in zeolites using the Scienta ESCA-300 spectrometer located in our laboratory. Photoelectrons were excitated by a monochromatic Al K_α X-ray source (1486.7 eV) with a rotating aluminum anode operated at 5.6 kW. A high resolution hemispherical electrostatic analyzer with a diameter of 600 mm was used. The take-off angle of the photoelectrons and Auger electrons was 45°. The background pressure during the experiment was $<10^{-9}$ Torr. To estimate integral intensities of the Auger and core level lines, the Shirley background was subtracted. The spectra were fitted by the Voight function, and the number of Auger lines in the spectrum was estimated from the second derivatives. The C 1s line at 284.4 eV was used as a calibration point. Quantitative analysis of the samples by XPS was carried out using the core level integral intensities of the pertinent elements (Si 2s, O 2s, Na 1s, Na 2p, and Al 2p), corrected for the appropriate values of the sensitivity factors (42).

Samples were measured in the form of self-supporting pellets. Quantitative analysis was carried out with the sodium forms of A zeolite from Linde and X, Y, and mordenite zeolites from PQ Corp. The zeolites were dehydrated in the preparation chamber of the spectrometer at 100°C for 30 min and at 250°C at $\approx 10^{-6}$ Torr. The quantitative results are summarized in Table 12.

Analyses of Co exchanged zeolites were carried out to probe the surface electronic state and surface chemistry of the zeolites. It was observed that substantial changes in intensities of oxygen Auger lines occurred upon ion exchange replacement of Na^+ ions with

Co^{2+} ions. This can be seen by comparing Figures 45 and 46. However, in curve fitting the O K $L_{2,3}$ $L_{2,3}$ spectral line for different zeolites, it was observed that the most intense line at ≈509 eV ($^1D_2$) was influenced primarily by changes in the Si/Al ratio. Plotting the results for the four zeolites listed in Table 12 gives the curves shown in Figure 47. The Auger line intensity of the four Na zeolites could also be related to the oxygen binding energy. The correlation of the intensity of the O K $L_{2,3}$ $L_{2,3}$ Auger line, normalized to the intensity of the O K L_1 L_1 Auger line, with the bind energy (E_b) of the O 1s photoelectron line is shown in Figure 48. The linear relationship shows that both the O $^1D_2$ K $L_{2,3}$ $L_{2,3}$/O K L_1 L_1 ratio and the E_b values increase along the series of zeolites.

It is demonstrated here that chemical effects influence the intensities of Auger lines and core level binding energies of oxygen and sodium in zeolites. It is proposed that the Auger line intensity ratio and the binding energy values are influenced by spatial distributions of charge in the zeolite frameworks, i.e. by structure-induced charge transfer effects. This has been discussed in detail elsewhere (43).

TABLE 12. The Si/Al and Na/Al atomic ratios as determined by XPS line intensities. The estimated error in intensity ratios is ±0.2. Bulk analysis is also given for comparison.

Zeolite	Si/Al (XPS)	Si/Al (Bulk)	Na/Al (XPS)
A	1.0	1.0	1.0
X	1.5	1.4	1.0
Y	4.3	4.2	0.9
Mordenite	12.3	12.4	1.0

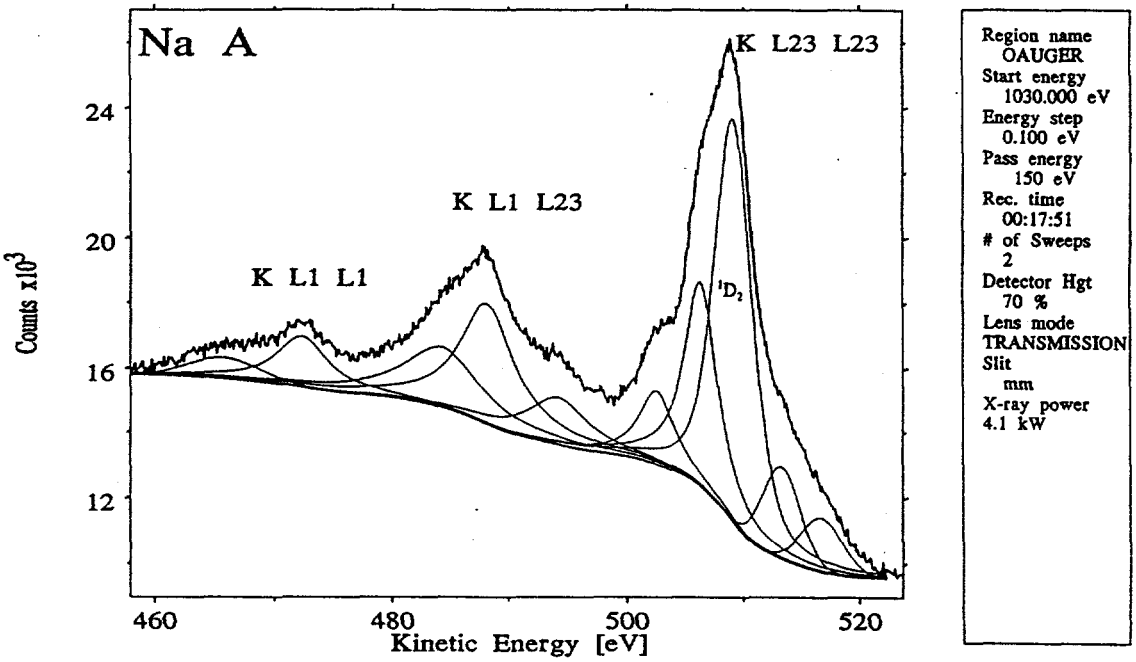

FIGURE 45. Auger spectrum of Na A zeolite in the oxygen 2s region (obtained in ≈18 min), showing the curve resolution and fitting that is typical for Na zeolite samples.

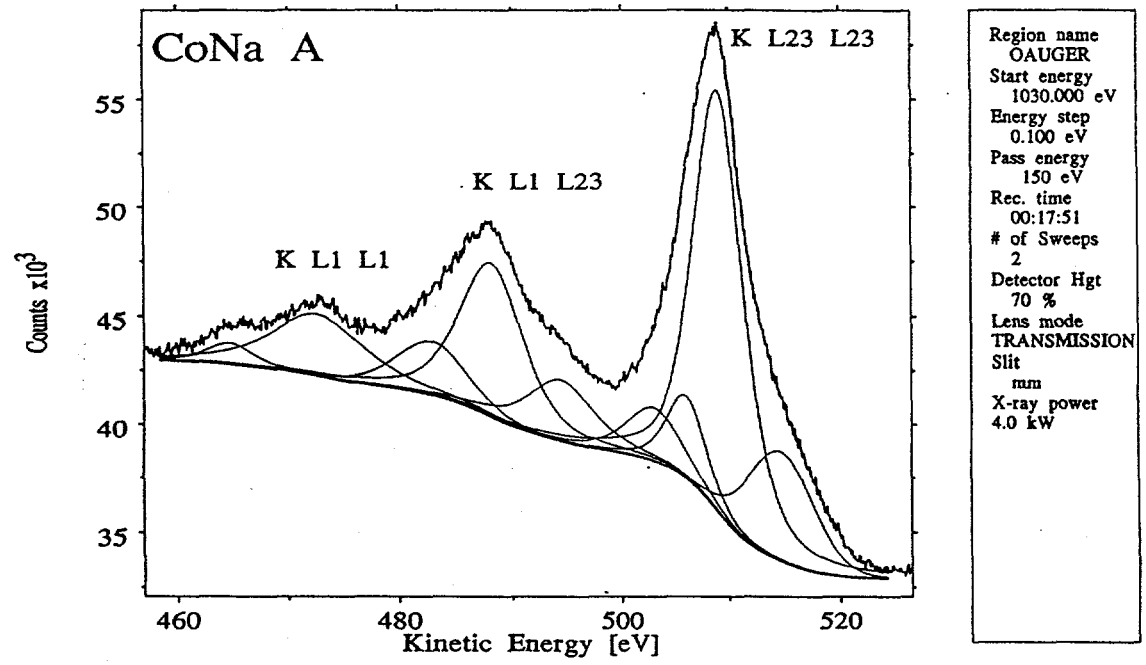

FIGURE 46. Auger spectrum of Co A zeolite in the oxygen 2s region.

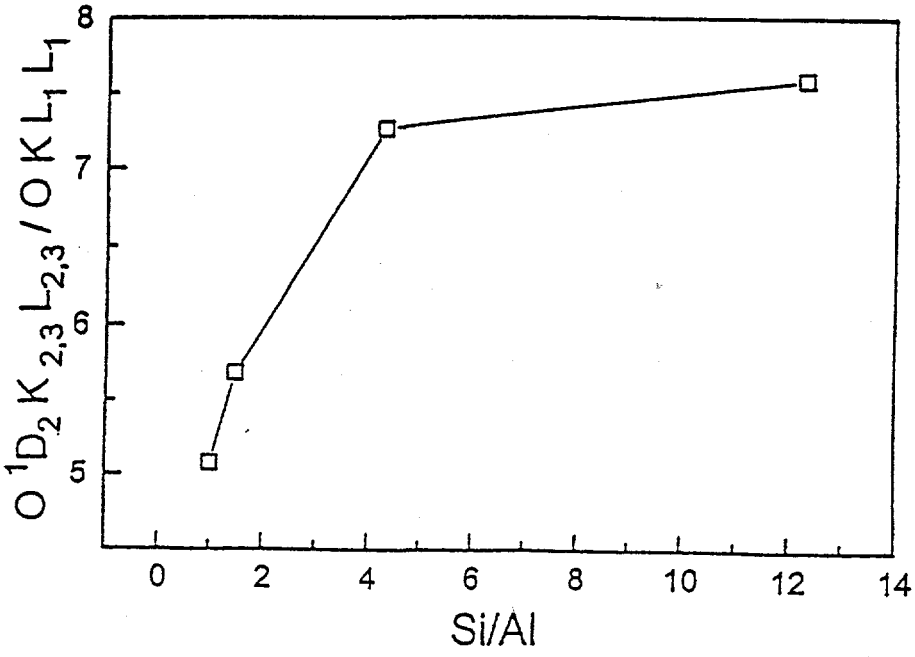

FIGURE 47. The dependence of the O K $L_{2,3}$ $L_{2,3}$ Auger line intensities on the Si/Al intensity ratio of the zeolites utilized here.

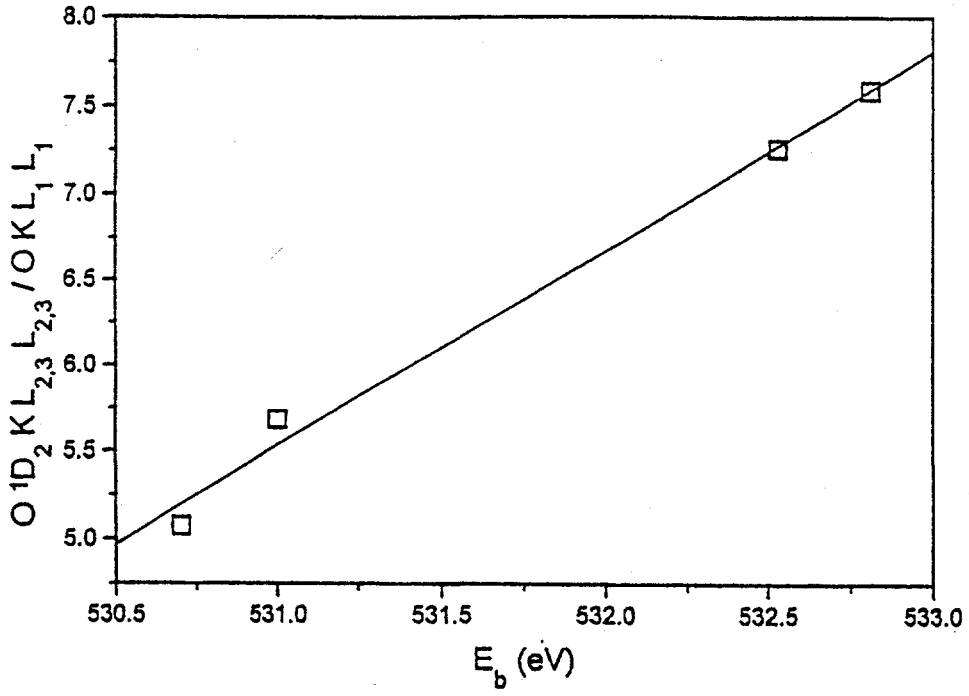

FIGURE 48. Correlation of the binding energy of the O 1s photoelectron line with the relative intensities of the O $^1D_2$ K $L_{2,3}$ $L_{2,3}$ Auger line.

ACKNOWLEDGEMENTS

This research was carried out with collaborative support of the National Science Foundation *via* the international cooperative Project 93050 of the US-CZ Science and Technology Program, supervised by Dr. B. Wichterlová of the J. Heyrovský Institute of Physcial Chemistry at the Academy of Sciences of the Czech Republic in Prague.

LIST OF PUBLICATIONS AND PRESENTATIONS TO-DATE

Articles:

Lange, J.-P. and Klier, K., "UV-Vis-NIR Studies of Fe(II)-A Zeolite," *Zeolites*, **14**, 462-468 (1994).

Klier, K., Herman, R. G., and Hou, S., "Binding and Catalytic Decomposition of NO by Transition Metal Aluminosilicates," in "*Zeolites and Related Microporous Materials: State of the Art 1994*," Studies in Surface Science and Catalysis, Vol. 84, ed. by J. Weitkamp, H. G. Karge, H. Pfeifer, and W. Holderich, Elsevier, Amsterdam, 1507-1514 (1994).

Jirka, I., "Influence of Si/Al Ratio on Auger Line Intensities of Zeolites," *Zeolites*, **17**, 310-313 (1996).

Dědeček, J., Klier, K., and Wichterlová, B., "Identification of Co(II) Ion Sites in Dehydrated Co-Erionite and Their Adsorption Properties: An UV-VIS-NIR Spectroscopy Study," *Zeolites*, submitted.

Presentations:

Herman, R. G., "Preparation of Lehigh University NO Abatement Catalysts," Workshop for Electrical Utility Companies on NO Abatement, Lehigh University, Noveber 30, 1994.

Klier, K., Herman, R. G., and Jirka, I., "NO Decomposition in Non-Reducing Atmospheres," U.S. DOE Fossil Energy Advanced Research Panel Review of Research Project for Treatment of Unwanted Byproducts: Gas Cleanup, Pittsburgh, PA, January 25, 1995.

Herman, R. G., "Recent Catalyst Development for Low Temperature NO Reduction," Workshop on Catalysts for SCR Reactors, Lehigh University, June 27, 1995.

Klier, K., "Electronic, Optical, and Redox Properties of Transition Metal Cations in Zeolites," Invited presentation at the 1995 Intern. Chem. Congr. Of Pacific Basin Societies (PACIFICHEM '95), Honolulu, HI, December 17-22, 1995.

Herman, R. G., "Catalysts for Low Temperature NO Reduction," Workshop on Development of Low Temperature SCR Catalysts, Lehigh University, March 26, 1996.

REFERENCES

1. Li, Y., Armor, J. N., Appl. Catal. B Env., **1**, L31 (1992).

2. Li, Y., Armor, J. N., Appl. Catal. B Env., **2**, 239 (1993).

3. Li, Y., Armor, J. N., J. Catal., **150**, 376 (1994) and U. S. Patent 5,149,512 (Sept. 22, 1992); assigned to Air Products and Chemicals, Inc.

4. Iwamoto, M., Stud. Surf. Sci. Catal., **84**, 1395 (1994); Armor, J. N., Ed.,"*Environmental Catalysis*," ACS Symp. Ser., **552**, 2-88 (1994); Ozkan, U. S., Agarwal, S. K., Marcelin, G, Eds, "*Reduction of Nitrogen Oxide Emissions*," ACS Symp. Ser, **587**, 110-182 (1995).

5. Aylor, A. W., Lohree, I. J., Reiner, J. A., Bell, A. T., in Proc. 11th Intern. Congr. Catal., Baltimore, MD, ed. by J. W. Hightower, W. N. Delgass, E. Iglesia, and A. T. Bell, Stud. Surf. Sci. Catal., **101**, 661 (1996).

6. Cruz, W.,C., Leung, P. W., Seff, K., Inorg. Chem., **83**, 2166 (1979).

7. Gallezot, P., Imelik, B., J. Chim. Phys., **71**, 155 (1974).

8. Klier, K., Langmuir, **4**, 13 (1988).

9. Klier, K., Hutta, P. J., Kellerman, R., Adv. Chem. Ser., **40**, 108 (1977).

10. Kellerman, R., Klier, K., in "*Surface and Defect Properties of Solids*," (Chem. Soc. London), **4**, 1 (1975).

11. Klier, K., Adv. Chem. Ser., **101**, 480 (1971).

12. Klier, K., Kellerman, R., Hutta, P. J., J. Chem. Phys., **61**, 4224 (1974).

13. Klier, K., J. Am. Chem. Soc., **91**, 5392 (1969).

14. Lin, J., Ph.D. Dissertation, Lehigh University, Bethlehem, PA, U.S.A. (1988).

15. Wichterlová, B., Jírù, P., Cuøínová, A., Z. Phys. Chem. Neue Folge, **88**, 180 (1974).

16. van Koningsveld, H., Tuinstra, F., Jansen, J.,C., van Bekkum, H., Zeolites, **9**, 253 (1989).

17. Mortier, W. J., Pluth J. J., Smith, J. W., Mat. Res. Bull., **10**, 1037 (1975).

18. Schlenker, J. L., Pluth J. J., Smith, J. W., Mat. Res. Bull., **14**, 751 (1979).

19. Mortier, W. J., Pluth J. J., Smith, J. W., in "*Natural Zeolites: Occurrence, Properties, Use*," ed. by L. B. Sand, F. A. Mumpton, Pergamon Press, 53 (1978).

20. Schlenker, J. L., Pluth J. J., Smith, J. W., Mat. Res. Bull., **13**, 169 (1978).

21. Schlenker, J. L., Pluth, J. J., Smith, J. W., Acta Crystallogr., **B33**, 3265 (1977).

22. Mortier, W. J., "*Compilation of Extra Framework Sites in Zeolites*," Butterworth Scientific, Ltd., London (1982).

23. Jone, K. G., Bobrov, N. N., Boreskov, K. G., Vostrikova, L. A., Dokl. Akad. Nauk. USSR, **280**, 388 (1973).

24. Rao, V. U. S., Gormley, R. J., Shamsi, A., Petrick, T. R., Stencel, J. M., Schehl, R. R., Chi, R. D. H., Obermyer, R. T., J. Mol. Catal., **29**, 271 (1985).

25. Gard, J. A., Tait, M. J., ACS Symp. Ser., **101**, 230 (1971).

26. Klier, K., Rálek M., J. Phys. Chem. Solids, **29**, 951 (1968).

27. Moore, W. J., "*Physical Chemistry*," Prentice Hall, Inc., New York (1972).

28. Cotton, F. A., Wilkinson, G., "*Advanced Inorganic Chemistry*," John Wiley & Sons Inc., New York, 541 (1972).

29. Busch, D. H., in "*Cobalt: Chemistry, Metallurgy and Uses*," ed. by R. S. Young, ACS Monogr. Ser., **149**, 130 (1960).

30. Herzberg, G., "*Molecular spectra and Molecular Structure II. Infrared and Raman Spectra of Polyatomic Molecules*," Van Nostrand, Boston (1945).

31. Klier, K., Shen, J. H., Zettlemoyer, A. C., Preprints, Div. Pet. Chem., ACS, **18**, 53 (1973).

32. Shen, J. H., Zettlemoyer, A.C., Klier, K., J. Phys. Chem., **84**, 1453 (1980).

33. Lever, A. B. P., "*Inorganic Electronic Spectroscopy*," Elsevier, Amsterdam, 319-321 (1968).

34. Engel, S., Kynast, U., Unger, K. K., Schuth, F., Stud. Surf. Sci. Catal, **84A**, 477 (1994).

35. Eberley, Jr., P. E., Am. Mineralogist, **49**, 30 (1964).

36. Peterson, D. L., Helfferich, F., Blytus, G. C., J. Phys. Chem. Solids, **26**, 835 (1965).

37. Kawahara, A., Curien, H., Bull. Soc. Fr. Miner. Cristallogr., **92**, 250 (1969).

38. Calligaris, M., Nardin, G., Randaccio, L., Zeolites, **4**, 251 (1984).

39. Iwamoto, M., Furukawa, H., Kagawa, S., in "*New Developments in Zeolite Science Technology*," ed. by Y. Murakami, Elsevier, Amsterdam, 943 (1986).

40. Iwamoto, M., Yahiro, H., Tanda, K., in "*Successful Design of Catalysts*," ed. by R. Inui, Elsevier, Amsterdam, 219 (1988).

41. Klier, K., Herman, R.G., Hou, S., "Binding and Catalytic Reduction of NO by Transition Metal Aluminosilicates," Final Technical Report DOE/PC/89784-F, 109 pp (February 1993).

42. Briggs, D., Seah, M. P., "*Practical Surface Analysis*," Vol. 1, 2nd Ed., John Wiley & Sons, New York (1990).

43. Jirka, I., Zeolites, **17**, 310 (1996).